The Dissertation Committee for Charles Brent Chesson Certifies that this is the approved version of the following dissertation:

Supramolecular Peptide Nanofiber Vaccines for Eliciting CD8+ T-cell Responses

Committee:

Jai S. Rudra, PhD
Chair

Gustavo Valbuena, MD, PhD

Janice J Endsley, PhD

Andrew Zloza, MD, PhD

Richard E Rupp, MD

Dean, Graduate School

Supramolecular Peptide Nanofiber Vaccines for Eliciting CD8+ T-cell Responses

by

Charles Brent Chesson, MPH

Supramolecular Peptide Nanofiber Vaccines for Eliciting CD8+ T-cell Responses

Presented to the Faculty of the Graduate School of

The University of Texas Medical Branch

in Partial Fulfillment

of the Requirements

for the Degree of

Doctor of Philosophy

The University of Texas Medical Branch

May, 2016

Dedication

This dissertation work is dedicated to Dr. Joanna K. Kreuger who pushed me to challenge myself and achieve more.

Acknowledgements

This work would not be possible without the dedication of my many people. I would like to thank all of the members of my dissertation committee for their suggestions, comments, and direction over the years with my dissertation project. Thank you to my committee chair and dissertation mentor, Dr. Jai Rudra. The training in your lab was a great experience and I am honored to be among your first students. I would like to thank Dr. Andrew Zloza for his support and training before and after Chicago. Your dedication to going 'all in' at Rush was the reason we published our Vaccine paper. I would like to extend a special thank you to Dr. Janice Endsley and her laboratory students Matt Huante and Rebecca Nusbaum. I always felt like an honorary member in your lab and I truly appreciate the hard work and long hours that went into to training me in bacteriology and containment work from Dr. Endsley and Matt and Rebecca.

I feel lucky to have been a part of the first cohort of students in the HPTM graduate program. The educational curriculum and remarkable faculty provided an exceptional scientific training program that constantly challenged us. Warmest regards to our faculty, Mark Hellmich, Gustavo Valbuena, and Judy Aronson for creating such fantastic entity to train new scientists.

The Sealy Center for Vaccine Development supported my graduate education and research project for a number of years in addition to selecting me for various travel awards including an internship at the World Health Organization to study vaccine policy.

I would like to extend my deepest thanks to the SCVD and the director, Dr. Alan Barrett for the numerous awards and funding.

Finally, I would like to thank my family for their constant support during my training. It is because of you that I kept pushing.

Supramolecular Peptide Nanofiber Vaccines for Eliciting CD8+ T-cell Responses

Publication No._____

Charles Brent Chesson, Ph.D, MPH

The University of Texas Medical Branch, 2016

Supervisor: Jai S Rudra

Abstract

CD8+ T cells play a central role in immunity against intracellular pathogens and cancer.Vaccines that elicit robust CD8+ T cell responses are desirable for protection against such infectious diseases and cancers. Subunit vaccines using whole protein or peptide epitopes are becoming increasingly favored due to their superior safety profile compared with live-attenuated or inactive pathogen formulations. The immunogenicity of subunit vaccines often depend heavily on adjuvants. Currently approved clinical adjuvants are chemically heterogeneous mixtures of plant- or pathogen-derived byproducts or formulations of mineral salts, which suffer from toxic side effects. The widely used systemic adjuvant alum is a heterogeneous mixture of aluminum salts whose mechanism of action is still being debated after 80 years of use. These current adjuvants elicit robust humoral responses but fail to elicit robust CD8+ T cell responses.

We recently reported that self-assembling peptides that assemble into β-sheet rich nanofibers in physiological buffers could act as self-adjuvanting vaccine carriers. Nanofibers bearing an antigenic peptide epitope from chicken egg ovalbumin ($OVA_{323-339}$) elicited strong CD4+ T cell-dependent antibody responses, which were detectable for a year. Our report begins with the investigation into whether self-assembling peptide adjuvants can activate CD8+ T cells and elicit protective CTL responses. We conjugated the CD8+ T cell epitope from chicken egg ovalbumin ($OVA_{257-264}$) via a short linker to a peptide self-assembling domain and investigated immune responses in mice. Our results indicate that $OVA_{257-264}$-bearing nanofibers can activate CD8+ T cells leading to the production of cytokines, cytolytic markers, and robust antigen-specific CTL responses in vivo. We found that CD8+ specific T-cells populations are significantly higher when

immunized with the nanofiber adjuvants compared to clinical adjuvants. Also, CD8+ memory recall responses were enhanced and provided superior protection against an OVA-expressing influenza challenge.

Mycobacterium *tuberculosis* (M*tb*) is an opportunistic pathogen that causes nearly 1.4 million deaths and over 8 million new or reactivated infections each year worldwide. It is known that CD4+ and CD8+ T cells are required to mount an effective immune response and IFN-γ and TNF-α are key cytokines in fighting Mtb infection. While IFN-γ is crucial in the protective immune response to Mtb, it is not sufficient on its own. Multifunctional CD8+ T cells that produce IFN-γ/ TNF-α/IL-2 have been associated with lower risk of reactivation of latent infection and enhanced control of active infection. Building on our report that self-assembling nanofibers bearing a model antigen OVA can stimulate robust CD8+ T cell effector and memory responses, we investigated whether self-assembling peptide (KFE8) nanofibers displaying multiple Mtb epitopes (TB10.4 and AG85B) or toll-like receptor (TLR) agonists (MALP, a TLR-2 agonist) can be co-assembled to generate vaccines capable of eliciting higher levels of IFN-γ^+ CD8+ T cells and multifunctional CD8+ T cells that produce IFN-γ/TNF-α/IL-2. Our data indicates that co-assembled peptide nanofiber vaccines bearing TB10.4 and AG85B elicit significantly higher levels of IFN-γ^+ CD8+ T cells compared to single epitopes. Inclusion of MALP or a CD4+ epitope leads to 8-fold increase in the production of multifunctional CD8+ T cells that produce IFN-γ/TNF-α/IL-2 in mouse models. Mice primed with BCG and then inoculated with a booster dose of peptide nanofiber vaccines had decreased bacterial loads in the lungs. Our data suggests that peptide based nanofibers exhibit desirable qualities as a vaccine carrier and show promising potential as adjuvants for prophylactic vaccines for infectious diseases.

Table of Contents

List of Figures

List of Tables

List of Abbreviations

AG85B	Antigen 85 complex B
APC	Antigen presenting cell
BCG	Bacille Calmette–Guérin vaccine
BMDC	Bone marrow derived dendritic cell
CMI	Cell mediated immunity
CTB	Cholera toxin B
CD4+/CD8+	Cluster of differentiation 4 & 8
DC	Dendritic cell
ECM	Extracellular matrix
ELISA	Enzyme linked immuno-absorbent assay
FRET	Fluorescence resonance energy transfer
GALT	Gut associated lymphoid tissue
HLA	Human leukocyte antigen
HPLC	High pressure liquid chromatography
HPV	Human papillomavirus
IEDB	Immune epitope database
IFN-γ	Interferon gamma
IFA	Incomplete Freund's adjuvant
IL-2	Interleukin-2
LPS	Lipopolysaccharide
KFE8	Self-assembling peptide domain [FKFEFKFE]
MALDI-TOF	Matrix assisted laser desorption/ionization-time of flight
MALT	Mucosal associated lymphoid tissue
MHC	Major histocompatibility complex
MTB	Mycobacterium tuberculosis
MP	Microparticle
OVA	Chicken ovalbumin protein
PPD	Purified protein derivative
TB	Tuberculosis
TCR	T-cell receptor
TEM	Transmission electron microscopy
TLR	Toll-like receptor
TNF-α	Tumor necrosis factor-alpha
SEM	Scanning electron microscopy

Chapter 1 : REVIEW OF MATERIALS-BASED STRATEGIES FOR T-CELL BASED VACCINES

INTRODUCTION

Biomaterials are an attractive route for the development of vaccine delivery or immunomodulatory platforms. Although biomaterials has typically referred to materials used in medical applications such as titanium and ceramic implants, advances in the past two decades have shifted the focus of biomaterial science to biological based materials. Biological materials have biological origin and can be designed or fabricated at the molecular level to design new materials for specific purposes. Biological materials are often designed specifically to interact with the extracellular environment and trigger a biological stimulus as opposed to simply restoring a basic function. Novel engineered biomaterials are now being widely used in the field of vaccine design including nanogels, virus-like particles, multilayer particles, artificial antigen presenting cells, implants and biofilms.

Intracellular pathogens as well as malignant cancer cells are eliminated through cytotoxic T- lymphocytes which are the basis of cell mediated protection. A major hurdle for biomaterial based vaccine design is the ability to elicit a functional cell mediated immune response. Nearly all vaccines are evaluated and licensed on antibody mediated protection although cell mediated immunity is required for many pathogens for which we currently lack any effective vaccines or have none at all. The purpose of this review is to encompass the current state of materials science focused eliciting cell mediated protection in the form of vaccines or immunotherapies.

PEPTIDE-BASED MATERIALS AND HYDROGELS

Peptide based supramolecular assemblies, specifically nanofibers and nanofiberous hydrogels provide an ideal environment for the delivery of antigens, immunomodulatory compounds or other biologically functional molecules that can interact with cells or the local microenvironment. Our lab as well as several others are exploring short peptides that spontaneously self-assemble into beta-sheet rich fibrils as a vaccine platform. Peptide self-assembly mostly occurs through non-covalent hydrophobic and electrostatic interactions from self-complementary amino acid side chains. Linear chain epitopes can be synthesized in chain but separated by a short linker to provide flexibility and freedom for peptide epitopes or immunostimulatory ligands to interact with the cell surface or extracellular matrix (ECM). Peptide epitopes displayed on the surface on the fibrils can stimulate both humoral and cell mediated immune responses depending on the nature of the epitope [1, 2]. Employing a model antigen from chicken ovalbumin, we have shown that short peptides conjugated to a nanofiber self-assembling domain can induce expansion and activation of antigen specific CD8+ T-lymphocytes [3]. Further, self-assembling peptide nanofibers act as a self-adjuvanting platform precluding the need for additional extraneous adjuvants that can result in overt inflammation. Many recombinant protein or peptide subunit vaccines rely on adjuvants and this is a major barrier for clinical licensure. Adjuvants function to enhance the immune response to the antigens with which they are co-delivered. Typical adjuvants are compositions of mineral salts or oil emulsions which suffer from poor chemical definition, suboptimal protection, and increasing toxicity. Currently only several adjuvants are in clinically use, Alum, MF59 and AS04. These adjuvants elicit strong

humoral responses but have recently been shown to promote immune T cell tolerance, dysfunction, and prolonged inflammatory conditions at the site of inoculation.

The modular nature of self-assembling peptides along with their inherent biocompatibility are distinct advantages. Multiple peptide epitopes or immunomodulatory compounds that possess a common self-assembling domain can yield multi-valent or multifunctional nanofibers by simple mixing [4]. This allows for the design of highly specific vaccine formulations and the ability to combine broader antigenic and HLA diversity with a tunable immune response.

Supramolecular structures may interact strongly with water to produce hydrogels that contain over 99% water content (w/v) [5]. Peptide based nanofibrous hydrogels have been shown to be effective vectors for DNA based vaccines. In a recent study from Tian et al. Nap-GFFY-NMe hydrogels loaded with HIV-Env DNA were able to induce cellular immune responses through multiple routes of administration [6]. The hydrogels were hypothesized to protect DNA from extracellular degradation and thus promote uptake of the plasmid. Cholesteryl pullulan (CHP) is a modified lipopolysaccharide that self-assembles into cross-linked nanoparticles in water to form a hydrogel. The particles readily associate with polypeptide or whole protein antigens making them attractive for subunit vaccine design. CHP nanogels have been effective antigen delivery vehicles for tumor associated antigens MART-A4 and mERK2, resulting in tumor volume reduction or growth inhibition in mouse models as a result of potent antitumor CD8+ mediated response [7].

LIPID-BASED MATERIALS

Liposomes and Cationic Liposomes

Liposomes are a useful platform for sustained and targeted release of antigen as well as delivery of immunomodulatory molecules through surface conjugation or intra-vesicle encapsulation. The choice of lipids used in liposome synthesis significantly affects their physical properties and biological activity. Cationic lipids are becoming increasingly favored over neutral and anionic lipid compounds as a vaccine platform especially when CMI is desired. Cationic lipids are efficiently taken up by antigen presenting cells and can induce cross-presentation of antigen payload through MHC-I pathway. Synthetic lipids that have been investigated for their ability to induce CMI are listed in **Table I**.

Dimethyldioctadecylammonium (DDA) is a synthetic cationic amphiphilic lipid used as the primary lipid component in a number of cationic adjuvant formulations (CAF01-CAF09) in preclinical and clinical development as vaccine platforms. These formulations combine DDA with an immunomodulatory ligand or stabilization component, usually α,α'- trehalose 6,6'dibehenate (TDB). TDB is an analogue of a mycobacterium cord factor found in the membranes of mycobacterium species and potentiates both cellular and humoral immune responses [8]. The earliest formulation, CAF01, was found to be efficacious in inducing a cell mediated immune response to Mycobacterium *tuberculosis* antigens ESAT-6 and AG85B in humans [9]. Later formulations have replaced TDB with MMG-1, a synthetic analogue of a mycobacterial cell wall lipid that has been shown to enhance the activation of human DCs, as well as incorporated additional innate immune agonists or toll-like receptor ligands such as unmethylated CpG dsDNA and or Poly(I:C). These later formulations generated robust cell mediated immune responses as assessed through both cellular assays and tumor

reduction studies in vivo [10]. A clear advantage of liposomal formulations is ability to induce both humoral and cellular immunity to protein antigens from exogenous pathogens as well as altered host proteins.

A number of other cationic liposomal and lipid-polymer hybrid particles have been shown to induce potent cell-mediated immunity with associated protection from viral or bacterial challenge or therapeutic reduction or elimination of tumor mass. Lipofectamine, a liposomal mixture of 3:1 polycationic to neutral lipids, DO-SPA:DOPE, was used initially to increase transfection efficacy but has also been utilized to deliver respiratory syncytial viral protein antigens in mice, leading to CD8+ and CD4+ T-cell expansion and activation [11]. Octadecnolyoxy[ethyl-2-heptadecenyl-3 hydroxyethyl]imidazolinium, in conjunction with cholesterol and nucleic acid TLR agonists, form the liposomal complex LANAC. This cationic lipid complexed to either TLR9 agonist CpG nucleic acid generated therapeutic anti-tumor immunity or prophylactic protective immunity to M. *tuberculosis* challenge through durable CD8+ and CD4+ T-cell responses to protein and peptide antigens [12].

Polymer coated liposomes are used to stabilize the liposomal particle and increase its solubility and bioavailability. Fan *et al*. reported on a liposome-hyaluronic acid (HA) hybrid nanoparticle which incorporates cationic lipids 1,2-dioleoyl-3-trimethylammonium propane (DOTAP) and 1,2-dioleoyl-sn-glycero-3-phosphoethanolamine (DOPE) with the anionic HA polymer and surface conjugated PEG [13]. Following encapsulation and immunization with OVA, a balanced Th1/Th2 response was reported along with significant OVA-specific CD8+ T-cell expansion.

Lipid implants

Implantable materials that provide sustained release of antigen or drug payload have broad applicability particularly in the field of cancer therapeutics. Even *et al.* prepared lipid implants derived from cholesterol, soybean lecithin, and Dynasan 114 which encapsulated preformed OVA-antigen loaded liposomes and Quil-A adjuvant. The lipid implants with OVA antigen and adjuvant were shown to expand antigen-specific CD8+ T-cells in mice but this was not dependent on antigen encapsulation into preformed liposomes [14]. In a separate study, lipid implants prepared from cholesterol and phosphatidyl-choline and also utilizing the model antigen OVA and Quil-A adjuvant were able to induce OVA-specific CD8+ T-cell expansion and may also have utility as an injectable solution [15].

Virosomes

Viral liposomes mimic native viral structure through the inclusion of purified viral envelope proteins into a lipid bilayer lacking any viral genomic material of the native virus. For example, Influenza virosomes can be formed from purified hemagglutinin (HA), neuraminidase (NA) envelope proteins incorporated into a mixture of synthetic, phosphatidylcholine (PC) and phosphatidylethanolamine (PE), as well as natural viral lipids [16]. Immunopotentiating reconstituted influenza virosomes (IRIV) are the most extensively studied viral liposomes and can serve as carriers for multiple antigens. Encapsulation of peptide antigens inside the liposomal vectors has been shown to be effective strategies to elicit cellular immune responses directed against infectious pathogens [17] or oncogenic transformation [18, 19].

Cubosomes

Cubosome nanoparticles are composed of a highly ordered lipid bilayer with non-intersecting water channels [20]. These particles are formed through solvent evaporation of Phyantriol, Plurionic F127, and propylene glycol. Rizwan et al. demonstrated cubosomes to be effective as a consistent sustained release vehicle for OVA antigen while activating CD8+ cellular immune responses when combined with MPLA + imiquimod adjuvants [21]. Further investigation into disease specific models will be needed to assess the value of cubosomes for vaccine development or as an immunotherapy.

Bacteriosomes or Bacterial Ghosts

Escherichia coli (E. *coli*) liposomes, or escheriosomes, are a novel unilamellar liposome modality prepared from membrane phospholipids isolated from E. *coli* bacterial membranes [22]. These lipid carriers readily fuse with cell membranes, presumably due to their higher content of anionic phospholipids, to deliver encapsulated antigen which is processed for MHC class I presentation. Esheriosomes were first demonstrated to elicit cellular immunity using encapsulated whole protein OVA [23] but were also shown to be effective in inducing cell mediated immune responses against HIV gp100 peptides [24] as well as the fungal pathogen *Candida albicans* [25]. The liposomes were delivered without the use of an exogenous adjuvant. Bacteriosomes prepared in a similar manner from *Mycobacterium bovis* Bacille Calmette-Guérin (BCG) have also been used as a vaccination platform using whole protein OVA. The BCG liposomes were as effective as a recombinant BCG expressing $OVA_{257-264}$ as measured by cytotoxic CD8+ mediated cell lysis [26].

POLYMER BASED MATERIALS

Synthetic polymers that are assembled into nanoparticle vehicles for the delivery of antigens or peptide epitopes promote cross presentation into MHC-I molecules by antigen presenting cells. Di-block co-polymers self-assemble to form micelle nanoparticles to which protein antigen can be surface conjugated. Stayton and colleagues developed a pH-responsive neutral micelle polymeric nanoparticle carrier from 2-(N,N-diethylamino)ethyl methacrylate (DEAEMA) and butyl methacrylate (BMA) which was elongated with hydrophilic N,N-dimethylacrylamide (DMA) and demonstrated in vivo CMI response to thiol conjugated OVA antigen [27, 28]. Efficient cross-presentation was dependent on the pH-responsiveness of the polymer which began degradation in the endosome. Polymersomes are another type of delivery platform fabricated from poly(ethylene glycol) (PEG)-*bl*-poly(propylene sulfide) (PPS) block copolymer which are designed to degrade in response to the oxidative environment of the endosome [29]. Polymersomes form approximately 100nm hollow spheres with a hydrophilic core which efficiently encapsulates antigens and immunostimulatory ligands. Interestingly, Hubbell and colleagues recently reported that solid core nanoparticles (PPS) with surface conjugated OVA induced a significantly higher cell mediated immune response comparted to antigen encapsulated polymersomes [30, 31]. OVA encapsulated polymersomes induce CD4+ T cells and antibody production and highlight how different antigen delivery systems may be used to tune vaccine induced immunity to the desired response. Protein carrier polymers can also be designed to promote the escape of protein and peptide antigens. Poly(propylacrylic acid) (PPAA) carrier particles in ionic association with cationic poly(dimethylaminoethyl methacrylate) (PDMAEMA) were shown to have increased endosomolytic activity resulting in intracellular accumulation of

antigen and significantly increased antigen specific tetramer positive cells in the spleen with just one dose [32, 33].

DNA vaccination is generally an effective means for inducing CMI but is rapidly degraded in the absence of a carrier. Amphipathic di-block copolymers of polyethyleneoxide/polypropyleneoxide (PEO/PPO) strongly associate electrostatically with DNA forming nanosphere micelles for gene delivery [34, 35]. Magnan and colleagues delivered plasmid DNA using PEO/PPO polymeric nanoparticles encoding dust mite allergen which resulted in CD8+ IFN-γ expression among lung leukocytes while decreasing the Th2 response and IgE secretion [36]. Nanoparticles which mimic the native size of many viruses, combined with DNA based vaccines or DNA based therapies may exert synergistic pressure to drive cell mediated immune responses and Th1 phenotypes. Pelbanski and colleagues demonstrated that poly-L-lysine (PLL) coated poly-styrene (PS) nanoparticles efficiently delivered plasmid DNA with the model antigen OVA to induce potent CTL responses resulting inhibition of tumor growth [ref 118 and internal ref 16]. Particles on the micro-scale size are also suitable carriers for DNA vaccination [37]. Poly(lactic-coglycolide) (PLG) microparticles encapsulating plasmid DNA encoding for human tumor associated antigen CYP1B1 elicited strong CD8+ responses in murine models [38] although this modality was also shown to promote T cell responses to HPV antigens in human trials [39, 40]].

PLGA, poly(lactic-coglycolic acid), is widely used in nanoparticle formulations and as vaccine carriers and is already approved for use by the FDA in humans. Polymer based nanoparticles are readily taken up by dendritic cells although targeting DCs with additional ligands may further promote efficient uptake while

maintaining cross-presentation via MHC-I [41, 42]. PLGA polymers alone, however, are partially dependent on activation of toll like receptors through encapsulation of TLR ligands that fully stimulate DC or macrophage activation [43, 44], which is critical for anti-tumor CD8+ T-cell responses [45]. The dose of encapsulated TLR agonist encapsulated within these particles can be largely reduced through DC receptor specific targeting which controls for extraneous inflammatory conditions while maintaining strong CD8+ T cell activation [46].

PLGA and other polymeric nanoparticles provide a suitable platform for surface conjugation of antibodies and other immunomodulatory ligands. Using this concept, surface conjugation of costimulatory molecules CD28 and peptide loaded MHC-I can act as artificial antigen presenting cells (aAPCs) that present antigen to T cells with appropriate secondary and tertiary signals [47, 48]. Natural DC activation undergoes a carefully controlled sequence where specific co-stimulatory molecules and cytokines are expressed. Additional research is needed to better define the optimal ratio of appropriate co-stimulatory molecules for aAPCs [49]. The tertiary signal is achieved through encapsulation of cytokines such as IL-2 that are released as the particle is naturally biodegraded [48, 50, 51].

PLGA particles can be fabricated with varying size distributions. Nano-scale (<50nm) distributions have been shown to be effective for trafficking to the lymph nodes [52] while micro-scale formulations are better equipped to act as aAPCs. Microsphere sized PLGA particles are also readily taken up by DCs, and co-encapsulating TLR ligands and antigen can provide potent antigen specific CD8+ T-cell expansion with a single dose [53]. PLGA microspheres are readily taken up by DCs however antigen is

slowly released as the capsule degrades leading to an antigen reservoir within the DC. Constant and prolonged MHC-I antigen presentation was shown to last up to 9 days which provides rationale for the robust cellular immune responses seen with only single doses [54].

MULTILAYER PARTICLES

Multilayer particles are a unique class of nanoparticle that allows surface associated antigens and immunomodulatory molecules to also be trapped within additional lipid bilayers. In this respect antigen is both surface associated and encapsulated within the particle. Interbilayer crosslinked multilamellar vesicles are among the first multilayer lipid vesicles and have been shown to be elegant vaccine platforms for cell-mediated immune responses. Further, they are effective platforms for mucosal delivery against pulmonary viral and tumor challenge where CD8+ T-cell immunity was necessary [55, 56]. Vaccines capable of eliciting mucosal immunity are highly favorable against pathogens that initially invade through the mucosa as they provide frontline defense to control infection.

Solid core particles made from whole protein antigen or polymer allow layer by layer deposition of particulate antigen carriers that associate through electrostatic attraction. Oppositely charged polypeptides can be introduced in a controlled manner through successive adsorption steps onto the core with the final layer consisting of an appropriate peptide epitope. Polypeptide layer by layer assembly with surface OVA epitopes was shown to induce CTL activity and subsequent protection from transgenic Listeria *monocytogenes* expressing OVA [57]. Alternatively, layer by layer adsorption of

polymer such as thiol modified poly(methacrylic acid) (PMA) on a solid core allows polymer cross-linking for stability that degrades in the reductive intracellular environment to release an antigen payload. PMA nanocapsules loaded with either OVA peptide or whole protein OVA were highly immunostimulatory and induced robust CD8+ as well as CD4+ T cell activation and expansion [58].

Chitosan Based Materials

Naturally derived polymers such as chitosan and alginate form hydrogels that can act as sustained delivery systems for chemotherapeutics as well as antigen-adjuvant combinations for subunit vaccination [59, 60]. Chitosan is a derivative of the polysaccharide chitin which is a major component of the exoskeleton of crustaceans and one of the most abundant polysaccharides in nature. This natural polymer provides excellent biocompatibility and can be manipulated to form a variety of nanostructures [61, 62]. As a hydrogel they can be designed such that the solutions only gelate at body temperature for ease of delivery enabling the hydrogels in situ to act as antigen depots that control antigen release over time. This was shown with a model antigen/adjuvant combination using OVA/Quil-A embedded in chitosan hydrogels which able to induce potent antitumor CD8+ responses leading to 100% survival in a mouse model of melanoma [63].

CONCLUSION

There is an urgent need to develop vaccines for emerging pathogens and for those without pathogens with no vaccine currently available. Many of these diseases are intracellular and require vaccines that stimulate potent cell mediated immunity.

Biomaterial based strategies provide an innovative and attractive route for novel vaccine design due to their ability to stimulate both humoral and cell mediated immunity often without the currently approved adjuvants leading to improved safety profiles. Self-assembling peptide based vaccines may provide an avenue for rationale based vaccine design to elicit cell-mediated immunity in the absence of overt inflammatory effects that can reduce the impact of any immune response to the vaccine. Supramolecular peptide based vaccines can be easily synthesized and purified with minimal cost. Additionally, they are free of microbial contaminants and are chemically well defined, as opposed to whole protein recombinant antigens that require heterogeneous adjuvants. Self-assembling supramolecular vaccines are also highly modular and can be rapidly adapted to alternate pathogens or personalized for MHC haplotype diversity. Finally, the robust biocompatibility of peptide based vaccines results in a remarkably safer vaccine platform with many advantages and will be the focus of our investigation.

Table 1. Cationic Liposomal Formulations Evaluated for CMI

Name	Cationic Lipid	Immunomodulatory or stabilizing additive	Adjuvant	Disease models
CAF01	Dimethyldioctadecylammonium (DDA)	Trehalose 6,6 dibehenate (TDB)	None	M.tb (ESAT-6) &BCG ; Chlamydia (rMOMP);Malaria
CAF05	Dimethyldioctadecylammonium (DDA)	Trehalose 6,6 dibehenate (TDB)	Poly(I:C)	HIV gag p24; B16-OVA
CAF09	Dimethyldioctadecylammonium (DDA)	MMG-1	Poly(I:C)	Hiv gag p24; HPV16-E7; TB10.3 & H56;
SUV/MLV/DRV	Dimethyldioctadecylammonium (DDA)	Trehalose 6,6 dibehenate (TDB)	Poly(I:C)	OVA
SUV/MLV/DRV	Dimethyldioctadecylammonium (DDA)	Trehalose 6,6 dibehenate (TDB)	CpG	OVA
DDA/TDB/MPL Liposome	Dimethyldioctadecylammonium (DDA)	Trehalose 6,6 dibehenate (TDB)	TLR4 agonist: MPLA	OVA
LANAC [DOTIM]	octadecnolyoxy[ethyl-2-heptadecenyl-3 hydroxyethyl] imidazolinium	Cholesterol	Poly(I:C)	Melanoma trp2 peptide; M.tb ESAT-6 protein
None	Lipofectamine reagent (3:1) of DO-SPA:DOPE			RSV
DC-Chol	3B-[N-(N',N'-dimethylaminoethane)-carbamoyl] cholesterol			
DOTAP	1,2-dioleoyl-3-trimethylammonium-propane			
DOTMA	N-[1-(2,3-dioleyloxy)propyl]-n,n,n-trimethylammonium			
DOTAP-DOPC	1,2-dioleoyl-3-trimethylammonium-propane	1,2-dioleyl-sn-glycero-3-ethylphosphocoline	Poly(I:C)	OVA; anti-tumor
CCS	N-palmitoyl-D-erythrospingosyl-1-Ocarbamoyl			
	phosphatidylcholine (PC); DOTAP-DOPE	α-galactosylceramide		Trp2 self-antigen;anti-tumor
mannose-PEG-cholesterol/lipid A-liposomes (MLLs				
DOTAP/HA core-PEG	1,2-dioleoyl-3-trimethylammonium-propane	hyaluronic acid (HA)	MPLA	i.n. Y. pesits (F1-V); OVA

REFERENCES

1. Rudra, J.S., et al., *A self-assembling peptide acting as an immune adjuvant.* Proc Natl Acad Sci U S A, 2010. **107**(2): p. 622-7.
2. Rudra, J.S., et al., *Modulating adaptive immune responses to peptide self-assemblies.* ACS Nano, 2012. **6**(2): p. 1557-64.
3. Chesson, C.B., et al., *Antigenic peptide nanofibers elicit adjuvant-free CD8+⁺ T cell responses.* Vaccine, 2014. **32**(10): p. 1174-80.
4. Rudra, J.S., et al., *Self-assembled peptide nanofibers raising durable antibody responses against a malaria epitope.* Biomaterials, 2012. **33**(27): p. 6476-84.
5. Hauser, C.A. and S. Zhang, *Designer self-assembling peptide nanofiber biological materials.* Chem Soc Rev, 2010. **39**(8): p. 2780-90.
6. Tian, Y., et al., *A peptide-based nanofibrous hydrogel as a promising DNA nanovector for optimizing the efficacy of HIV vaccine.* Nano Lett, 2014. **14**(3): p. 1439-45.
7. Muraoka, D., et al., *Nanogel-based immunologically stealth vaccine targets macrophages in the medulla of lymph node and induces potent antitumor immunity.* ACS Nano, 2014. **8**(9): p. 9209-18.
8. Christensen, D., et al., *Liposome-based cationic adjuvant formulations (CAF): past, present, and future.* J Liposome Res, 2009. **19**(1): p. 2-11.
9. van Dissel, J.T., et al., *A novel liposomal adjuvant system, CAF01, promotes long-lived Mycobacterium tuberculosis-specific T-cell responses in human.* Vaccine, 2014. **32**(52): p. 7098-107.
10. Korsholm, K.S., et al., *Induction of CD8+ T-cell responses against subunit antigens by the novel cationic liposomal CAF09 adjuvant.* Vaccine, 2014. **32**(31): p. 3927-35.
11. Mbawuike, I.N., et al., *Cationic liposome-mediated enhanced generation of human HLA-restricted RSV-specific CD8+ CTL+.* J Clin Immunol, 2002. **22**(3): p. 164-75.
12. Zaks, K., et al., *Efficient immunization and cross-priming by vaccine adjuvants containing TLR3 or TLR9 agonists complexed to cationic liposomes.* J Immunol, 2006. **176**(12): p. 7335-45.
13. Fan, Y., et al., *Cationic liposome-hyaluronic acid hybrid nanoparticles for intranasal vaccination with subunit antigens.* J Control Release, 2015. **208**: p. 121-9.

14. Even, M.P., et al., *In vivo investigation of twin-screw extruded lipid implants for vaccine delivery.* Eur J Pharm Biopharm, 2014. **87**(2): p. 338-46.
15. Myschik, J., et al., *Immunostimulatory lipid implants containing Quil-A and DC-cholesterol.* Int J Pharm, 2008. **363**(1-2): p. 91-8.
16. Huckriede, A., et al., *The virosome concept for influenza vaccines.* Vaccine, 2005. **23 Suppl 1**: p. S26-38.
17. Hunziker, I.P., et al., *In vitro studies of core peptide-bearing immunopotentiating reconstituted influenza virosomes as a non-live prototype vaccine against hepatitis C virus.* Int Immunol, 2002. **14**(6): p. 615-26.
18. Angel, J., et al., *Virosome-mediated delivery of tumor antigen to plasmacytoid dendritic cells.* Vaccine, 2007. **25**(19): p. 3913-21.
19. Schumacher, R., et al., *Efficient induction of tumoricidal cytotoxic T lymphocytes by HLA-A0201 restricted, melanoma associated, L(27)Melan-A/MART-1(26-35) peptide encapsulated into virosomes in vitro.* Vaccine, 2005. **23**(48-49): p. 5572-82.
20. Rizwan, S.B., et al., *Preparation of phytantriol cubosomes by solvent precursor dilution for the delivery of protein vaccines.* Eur J Pharm Biopharm, 2011. **79**(1): p. 15-22.
21. Rizwan, S.B., et al., *Cubosomes containing the adjuvants imiquimod and monophosphoryl lipid A stimulate robust cellular and humoral immune responses.* J Control Release, 2013. **165**(1): p. 16-21.
22. Ahmad, N., A.K. Masood, and M. Owais, *Fusogenic potential of prokaryotic membrane lipids. Implication in vaccine development.* Eur J Biochem, 2001. **268**(22): p. 5667-75.
23. Syed, F.M., et al., *Antigen entrapped in the escheriosomes leads to the generation of CD4+(+) helper and CD8+(+) cytotoxic T cell response.* Vaccine, 2003. **21**(19-20): p. 2383-93.
24. Ahmad, N., M.A. Khan, and M. Owais, *Liposome mediated antigen delivery leads to induction of CD8+ T lymphocyte and antibody responses against the V3 loop region of HIV gp120.* Cell Immunol, 2001. **210**(1): p. 49-55.
25. Chauhan, A., et al., *Escheriosome mediated cytosolic delivery of Candida albicans cytosolic proteins induces enhanced cytotoxic T lymphocyte response and protective immunity.* Vaccine, 2011. **29**(33): p. 5424-33.

26. Sprott, G.D., et al., *Activation of dendritic cells by liposomes prepared from phosphatidylinositol mannosides from Mycobacterium bovis bacillus Calmette-Guerin and adjuvant activity in vivo.* Infect Immun, 2004. **72**(9): p. 5235-46.
27. Keller, S., et al., *Neutral polymer micelle carriers with pH-responsive, endosome-releasing activity modulate antigen trafficking to enhance CD8+(+) T cell responses.* J Control Release, 2014. **191**: p. 24-33.
28. Wilson, J.T., et al., *pH-Responsive nanoparticle vaccines for dual-delivery of antigens and immunostimulatory oligonucleotides.* ACS Nano, 2013. **7**(5): p. 3912-25.
29. Scott, E.A., et al., *Dendritic cell activation and T cell priming with adjuvant- and antigen-loaded oxidation-sensitive polymersomes.* Biomaterials, 2012. **33**(26): p. 6211-9.
30. Stano, A., et al., *Tunable T cell immunity towards a protein antigen using polymersomes vs. solid-core nanoparticles.* Biomaterials, 2013. **34**(17): p. 4339-46.
31. Nembrini, C., et al., *Nanoparticle conjugation of antigen enhances cytotoxic T-cell responses in pulmonary vaccination.* Proc Natl Acad Sci U S A, 2011. **108**(44): p. E989-97.
32. Foster, S., et al., *Intracellular delivery of a protein antigen with an endosomal-releasing polymer enhances CD8+ T-cell production and prophylactic vaccine efficacy.* Bioconjug Chem, 2010. **21**(12): p. 2205-12.
33. Flanary, S., A.S. Hoffman, and P.S. Stayton, *Antigen delivery with poly(propylacrylic acid) conjugation enhances MHC-1 presentation and T-cell activation.* Bioconjug Chem, 2009. **20**(2): p. 241-8.
34. McIlroy, D., et al., *DNA/amphiphilic block copolymer nanospheres promote low-dose DNA vaccination.* Mol Ther, 2009. **17**(8): p. 1473-81.
35. Pitard, B., et al., *Negatively charged self-assembling DNA/poloxamine nanospheres for in vivo gene transfer.* Nucleic Acids Res, 2004. **32**(20): p. e159.
36. Rolland-Debord, C., et al., *Block copolymer/DNA vaccination induces a strong allergen-specific local response in a mouse model of house dust mite asthma.* PLoS One, 2014. **9**(1): p. e85976.
37. McKeever, U., et al., *Protective immune responses elicited in mice by immunization with formulations of poly(lactide-co-glycolide) microparticles.* Vaccine, 2002. **20**(11-12): p. 1524-31.
38. Luby, T.M., et al., *Repeated immunization with plasmid DNA formulated in poly(lactide-co-glycolide) microparticles is well tolerated and stimulates durable T cell responses to*

the tumor-associated antigen cytochrome P450 1B1. Clin Immunol, 2004. **112**(1): p. 45-53.

39. Sheets, E.E., et al., *Immunotherapy of human cervical high-grade cervical intraepithelial neoplasia with microparticle-delivered human papillomavirus 16 E7 plasmid DNA.* American Journal of Obstetrics and Gynecology, 2003. **188**(4): p. 916-926.
40. Klencke, B., et al., *Encapsulated plasmid DNA treatment for human papillomavirus 16-associated anal dysplasia: a Phase I study of ZYC101.* Clin Cancer Res, 2002. **8**(5): p. 1028-37.
41. Tel, J., et al., *Targeting uptake receptors on human plasmacytoid dendritic cells triggers antigen cross-presentation and robust type I IFN secretion.* J Immunol, 2013. **191**(10): p. 5005-12.
42. Hamdy, S., et al., *Activation of antigen-specific T cell-responses by mannan-decorated PLGA nanoparticles.* Pharm Res, 2011. **28**(9): p. 2288-301.
43. Kasturi, S.P., et al., *Programming the magnitude and persistence of antibody responses with innate immunity.* Nature, 2011. **470**(7335): p. 543-7.
44. Hamdy, S., et al., *Enhanced antigen-specific primary CD4+ and CD8+ responses by codelivery of ovalbumin and toll-like receptor ligand monophosphoryl lipid A in poly(D,L-lactic-co-glycolic acid) nanoparticles.* J Biomed Mater Res A, 2007. **81**(3): p. 652-62.
45. Zhang, Z., et al., *Induction of anti-tumor cytotoxic T cell responses through PLGA-nanoparticle mediated antigen delivery.* Biomaterials, 2011. **32**(14): p. 3666-78.
46. Tacken, P.J., et al., *Targeted delivery of TLR ligands to human and mouse dendritic cells strongly enhances adjuvanticity.* Blood, 2011. **118**(26): p. 6836-44.
47. Han, H., et al., *A novel system of artificial antigen-presenting cells efficiently stimulates Flu peptide-specific cytotoxic T cells in vitro.* Biochem Biophys Res Commun, 2011. **411**(3): p. 530-5.
48. Steenblock, E.R. and T.M. Fahmy, *A comprehensive platform for ex vivo T-cell expansion based on biodegradable polymeric artificial antigen-presenting cells.* Mol Ther, 2008. **16**(4): p. 765-72.
49. Rudolf, D., et al., *Potent costimulation of human CD8+ T cells by anti-4-1BB and anti-CD28 on synthetic artificial antigen presenting cells.* Cancer Immunol Immunother, 2008. **57**(2): p. 175-83.

50. Prakken, B., et al., *Artificial antigen-presenting cells as a tool to exploit the immune 'synapse'.* Nat Med, 2000. **6**(12): p. 1406-10.
51. Yu, X., et al., *Artificial antigen-presenting cells plus IL-15 and IL-21 efficiently induce melanoma-specific cytotoxic CD8+ CD28+ T lymphocyte responses.* Asian Pac J Trop Med, 2013. **6**(6): p. 467-72.
52. Hirosue, S., et al., *Antigen delivery to dendritic cells by poly(propylene sulfide) nanoparticles with disulfide conjugated peptides: Cross-presentation and T cell activation.* Vaccine, 2010. **28**(50): p. 7897-906.
53. Schlosser, E., et al., *TLR ligands and antigen need to be coencapsulated into the same biodegradable microsphere for the generation of potent cytotoxic T lymphocyte responses.* Vaccine, 2008. **26**(13): p. 1626-37.
54. Audran, R., et al., *Encapsulation of peptides in biodegradable microspheres prolongs their MHC class-I presentation by dendritic cells and macrophages in vitro.* Vaccine, 2003. **21**(11-12): p. 1250-5.
55. Li, A.V., et al., *Generation of effector memory T cell-based mucosal and systemic immunity with pulmonary nanoparticle vaccination.* Sci Transl Med, 2013. **5**(204): p. 204ra130.
56. Moon, J.J., et al., *Interbilayer-crosslinked multilamellar vesicles as synthetic vaccines for potent humoral and cellular immune responses.* Nat Mater, 2011. **10**(3): p. 243-51.
57. Powell, T.J., et al., *Synthetic nanoparticle vaccines produced by layer-by-layer assembly of artificial biofilms induce potent protective T-cell and antibody responses in vivo.* Vaccine, 2011. **29**(3): p. 558-69.
58. Sexton, A., et al., *A protective vaccine delivery system for in vivo T cell stimulation using nanoengineered polymer hydrogel capsules.* ACS Nano, 2009. **3**(11): p. 3391-400.
59. Han, H.D., et al., *A chitosan hydrogel-based cancer drug delivery system exhibits synergistic antitumor effects by combining with a vaccinia viral vaccine.* Int J Pharm, 2008. **350**(1-2): p. 27-34.
60. Seo, S.H., et al., *Chitosan hydrogel containing GMCSF and a cancer drug exerts synergistic anti-tumor effects via the induction of CD8+ T cell-mediated anti-tumor immunity.* Clin Exp Metastasis, 2009. **26**(3): p. 179-87.
61. Borges, O., et al., *Preparation of coated nanoparticles for a new mucosal vaccine delivery system.* Int J Pharm, 2005. **299**(1-2): p. 155-66.

62. Borges, O., et al., *Evaluation of the immune response following a short oral vaccination schedule with hepatitis B antigen encapsulated into alginate-coated chitosan nanoparticles.* Eur J Pharm Sci, 2007. **32**(4-5): p. 278-90.
63. Highton, A.J., et al., *Chitosan hydrogel vaccine generates protective CD8+ T cell memory against mouse melanoma.* Immunol Cell Biol, 2015. **93**(7): p. 634-40.

Chapter 2 : PROTECTIVE ADJUVANT-FREE CD8+ T CELL RESPONSES INDUCED BY SELF-ASSEMBLING PEPTIDE NANOFIBERS

Reprinted with permission from Elsevier from the article Reprinted from "Antigenic peptide nanofibers elicit adjuvant-free CD8+ T cell responses", Charles B. Chesson, Erica J. Huelsmann, Andrew T. Lacek, Frederick J. Kohlhapp, Matthew F. Webb, Arman Nabatiyan, Andrew Zloza, Jai S. Rudra, 2014 Feb 26;32(10):1174-80 with permission from Elsevier

Introduction

Subunit vaccines that incorporate defined CD8+ T cell epitopes that are known to play a role in protective immunity have great potential in terms of antigen specificity and safety (1, 2). However, co-administration of subunit antigens with adjuvants is a prerequisite to enhance, maintain, and direct the adaptive immune response (3). In clinical trials, administration of CD8+ T cell epitopes in combination with incomplete Freund's adjuvant (IFA) has been shown to enhance CD8+ T cell responses in the periphery but not necessarily provide protection (4, 5). Additionally, vaccination with IFA elicits a transient response and sometimes inhibits CD8+ T cell responses (6, 7). IFA is thought to exert its adjuvant effect by forming a local antigen depot, leading to sustained antigen presentation and inflammation at the injection site although the exact mechanism of its adjuvanticity remains poorly understood (8). Recently, Overwijk and colleagues have reported that persisting IFA vaccine depots can induce T cell

sequestration, dysfunction, and deletion in a mouse model of melanoma (9). Here, we report a nanofiber platform based on molecular self-assembly that can induce adjuvant-free CD8+ T cell primary and memory recall responses while overcoming the limitations of depot-forming adjuvants like IFA.

Recently, we reported that short synthetic peptides that assemble into β-sheet-rich nanofibers in physiological buffers act as effective immune adjuvants in mice (10). We have previously shown that linking the OT-II peptide epitope (chicken egg ovalbumin aa 323-339, $OVA_{323-339}$) to the self-assembling peptide domain Q11 (QQKFQFQFEQQ), will assemble into nanofibers with the antigen present on the surface of the fibers (10, 11). When administered subcutaneously to mice, these antigenic nanofibers elicited strong, persistent, and CD4+ T cell-dependent $OVA_{323-339}$-specific antibodies comparable to $OVA_{323-339}$ administered in complete Freund's adjuvant (CFA) (11). When nanofibers bearing peptide epitopes from the malaria parasite *P. falciparum* or the cell surface associated Mucin 1 (MUC1) protein overexpressed in epithelial tumors were injected into mice, protective serum antibodies were generated (12, 13). Significantly, Q11 itself was found to be non-immunogenic even when administered in CFA. Moreover, simple mixing of $OVA_{323-339}$ and Q11 completely abrogated the antibody response suggesting that physical conjugation of the epitope to Q11 was required for adjuvant activity (10).

However, it is unknown if Q11 nanofibers likewise can elicit strong CD8+ T cell responses, which are an integral requirement for vaccines to prevent viral infections and cancer. Thus, we have investigated the ability of Q11 to promote robust primary and recall CD8+ T cell responses. The H-$2k^b$-restricted OT-I peptide epitope (chicken egg ovalbumin aa 257-264, hereafter referred to as OVA) was conjugated to Q11 via the

amino acid linker GGAAY (AAY is a preferred proteasome cleavage site) (14). Mice were immunized with nanofibers of Q11-OVA, or with OVA in IFA, or OVA in saline as controls. CD8+ T cell effector responses, recall responses, and antigen persistence at the immunization site were investigated. Further, as a model, protection was evaluated after a prime/boost regimen with the nanofibers against challenge with an influenza virus expressing OVA protein. In this report, we show that Q11 nanofibers acts as effective adjuvants for eliciting robust primary and memory recall CD8+ T cell responses and protects against an influenza pathogenic challenge.

Materials and Methods

PEPTIDES

Peptides QQKFQFQFEQQ-GGAAY-SIINFEKL (Q11-OVA) and SIINFEKL (OVA) were purchased from CS Bio (Menlo Park, CA) at >95% purity. Peptide solutions for transmission electron microscopy (TEM) and circular dichroism spectroscopy (CD) studies were prepared, and the experiments were conducted as described previously (10). TEM studies were conducted on a JEOL JEM-1400 electron microscope (Tokyo, Japan) and CD studies were conducted on a Jasco J-815 CD spectrometer (Easton, MD). Endotoxin levels of peptide formulations were tested using a limulus amebocyte lysate assay kit (Lonza, USA) and found to be < 0.1 EU/mL.

ANIMALS AND IMMUNIZATIONS

C57BL6/J (B6) and OT-I transgenic (B6 background) male mice, 6-8 weeks old, were purchased from The Jackson Laboratory (Bar Harbor, ME). For all animal work, strict guidelines were followed according to protocols approved by Institutional Animal Care and Use Committees. Peptide solutions for immunizations (2 mM working concentration) were prepared as described previously (10-12). Mice were primed in the right footpad with 50 nmol of antigen in saline or IFA, or as nanofibers and boosted with 25 nmol of the same 24 days later for each experiment. Control groups were primed and boosted with equimolar amounts of antigen in IFA or saline from Sigma Aldrich (St. Louis, MO).

LYMPHOCYTE ISOLATION

Lymphocytes were harvested from the ipsilateral inguinal and popliteal draining lymph nodes for primary response studies. For recall responses, axillary lymph nodes were also included. Pooled lymph nodes were pressed through a BD Biosciences (San Jose, CA) 70-μm cell strainer and washed twice with 1640 RPMI containing 1% penicillin/streptomycin, 2% L-glutamine, and 10% FBS. To measure interferon gamma (IFN-γ) production, cells were stimulated on OVA- or Q11-OVA nanofiber-coated plates (20 μg/ml) for 6 hours at 37°C with brefeldin A (1μl/ml; BD Biosciences).

SURFACE MARKER AND INTRACELLULAR CYTOKINE STAINING

SIINFEKL MHC class I tetramer, cell surface marker, and intracellular staining was performed according to standard protocols described previously (15-17). Live/dead stain (AmCyan) and CD3 (PE-Cy7), CD8+ (APC-Cy7), CD69 (APC), CD25 (Pacific Blue),

CD4+4 (PerCP-Cy5.5) CD62L (FITC), IFN-γ (PE-Cy7), CD11c (Pacific Blue), and H2k-OVA (PerCP-Cy5.5) antibodies were purchased from BD Biosciences (San Jose, CA). OVA tetramer (PE) was purchased from Beckman Coulter (Indianapolis, IN). Flow cytometry was performed using a BD FACS Canto II flow cytometer and data were analyzed using FlowJo software (Tree Star, OR).

INFLUENZA CHALLENGE STUDIES

Influenza (PR8-OVA strain expressing the OVA peptide in the neuraminidase stalk) was a kind gift from Dr. Paul Thomas (St. Jude's Children Research Hospital) and Dr. Amanda Marzo (Rush University Medical Center), and has been described in detail elsewhere (18-20). Mice were primed intranasally with 50 nmol of peptide and boosted with 25 nmol on day 24. Four days later mice were challenged intranasally with 20 μl of PR8-OVA at a dose of 80,000 EID_{50}. Mice were monitored and weighed daily.

STATISTICAL ANALYSIS

Statistical analysis was performed by either student's t-test or one-way ANOVA with Tukey's or Bonferroni post-hoc test for comparison between groups. Group mean differences were considered statistically significant according to a p-value < 0.05. All data are presented as mean ± SEM.

Results and Discussion

Q11-OVA NANOFIBERS DISPLAY OVA AND ACTIVATE OT-I CELLS IN VITRO

We have previously shown that self-assembling peptide Q11 retains its ability to assemble when other active ligands such as peptides or chemical groups are covalently attached to either terminus, resulting in nanofibers that present the pendant ligands on their surface (10-13). In this study, self-assembly of the OVA epitope in tandem with Q11 was confirmed using TEM, and the nanofibers of Q11-OVA were similar in morphology to the nanofibers of Q11 (Fig. 1*A*). Secondary structure analysis of Q11-OVA indicated a transition from a random coiled structure for OVA (minimal ellipticity at 200 nm) to a β-sheet rich structure similar to Q11 with a minimal ellipticity at 220 nm (Fig. 1*B*). In previous studies, similar fibril morphology and secondary structure were observed when the OT-II peptide epitope ($OVA_{323-339}$) was conjugated to Q11 (10). Lymphocytes from the spleens and lymph nodes of OT-I transgenic mice were stimulated in wells coated with Q11-OVA nanofibers to determine whether or not the OVA peptide was displayed on the surface of the nanofibers and available for antigen processing. Wells coated with Q11 only, free OVA peptide, or PBS were used as controls. Activation of OT-I cells was measured by IFN-γ production by OVA-specific CD8+ T cells. Flow cytometry analysis showed antigen-specific CD8+ T cells producing IFN-γ in wells coated with Q11-OVA nanofibers, suggesting that OVA epitope was present on the surface of the nanofibers (Fig. 1*C* and 1*D*). Control wells coated with Q11 nanofibers alone (without OVA) did not result in any non-specific activation of CD8+ T cells. Thus, conjugating OVA to Q11 resulted in nanofibers (Q11-OVA) capable of activating OT-I cells *in vitro*.

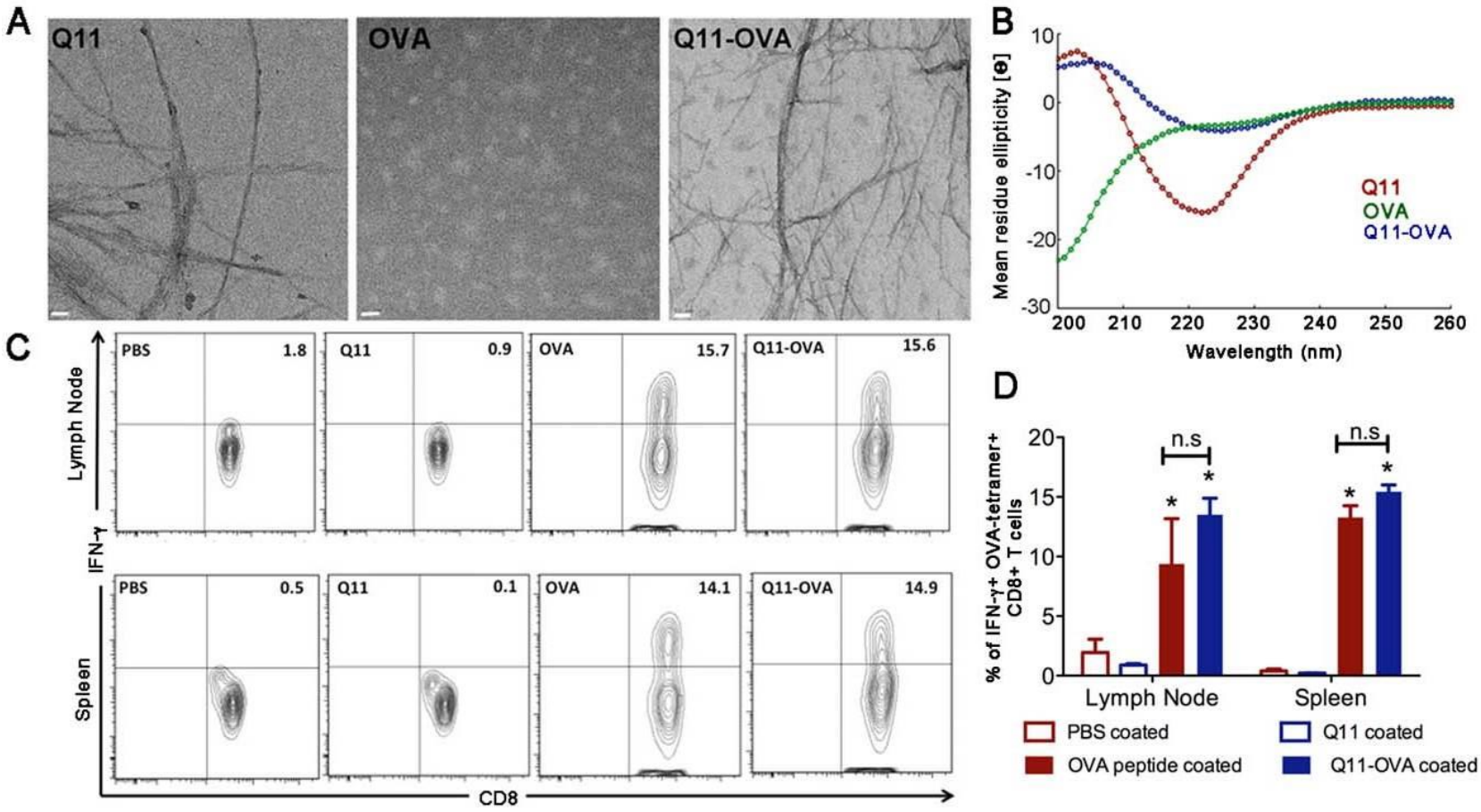
A
Q11
OVA
Q11-OVA
B
Mean residue ellipticity [θ]
10
0
-10
-20
-30
200
210
220
230
240
250
260
Wavelength (nm)
Q11
OVA
Q11-OVA
C
Lymph Node
Spleen
IFN-γ
CD8
PBS
1.8
Q11
0.9
OVA
15.7
Q11-OVA
15.6
PBS
0.5
Q11
0.1
OVA
14.1
Q11-OVA
14.9
D
% of IFN-γ+ OVA-tetramer+ CD8+ T cells
20
15
10
5
0
n.s
n.s
*
*
*
*
Lymph Node
Spleen
PBS coated
Q11 coated
OVA peptide coated
Q11-OVA coated

Figure 2.1. Characterization and *in vitro* function of antigenic peptide nanofibers.

(A) Q11 and Q11-OVA nanofibers as observed by TEM (scale bar = 50 nm). OVA peptide does not form fibers by itself but undergoes self-assembly into nanofibers after conjugating to Q11. (B) CD spectroscopy of Q11, OVA, and Q11-OVA nanofibers indicates that after conjugation to Q11, OVA transits from unstructured (minima at 200 nm) to a beta-sheet rich structure (minima at 220 nm) similar to Q11. (C) Flow cytometry plots showing INF-γ production by OT-I (OVA-specific) CD8+ T cells after 6-hr stimulation on plates coated with PBS (Control), Q11 nanofibers, OVA peptide, or Q11-OVA nanofibers. (D) Cumulative bar graph from (C) showing the percentage of OT-I CD8+ T cells producing INF-γ from one experiment of three conducted with similar results (n = 3 mice per group per experiment). n.s. = not significant. * $p < 0.05$ by ANOVA using Tukey post-hoc comparison.

Q11-OVA NANOFIBERS ELICIT ROBUST IN VIVO PRIMARY CD8+ T CELL RESPONSES

To assess the ability of Q11-OVA nanofibers to elicit *in vivo* effector CD8+ T cell responses, B6 mice were primed, boosted on day 5, and sacrificed on day 8 (Fig. 2*A*). Lymphocytes were obtained from draining popliteal and inguinal lymph nodes, and tetramer flow cytometry analysis showed the percentage of OVA antigen-specific CD8+ T cells was significantly enhanced in mice immunized with Q11-OVA compared with the other groups (Fig. 2*B and 2C*). We determined the efficiency of Q11-OVA nanofibers to elicit robust effector phenotypes by measuring expression of the very early-stage activation marker CD69 and early-stage activation marker CD25 on the surface of OVA-specific CD8+ T cells, the expression of which serves as a useful method of identifying a temporal continuum of antigen-specific activation of T cells (21). Q11-OVA immunized mice had significantly higher numbers of antigen-specific cells co-expressing CD69 and CD25 compared to soluble OVA or IFA-OVA (Fig. 2*D* and 2*E)*. Since CD69 has been identified as the earliest T cell activation marker and CD25, the high-affinity interleukin-2 (IL-2) receptor α chain, is rapidly up regulated by antigen-specific CD8+ T cells after

T cell receptor, these results demonstrate that Q11-OVA nanofibers elicit higher frequencies of CD8+ T cells with enhanced activation phenotype than soluble antigen or antigen in IFA.

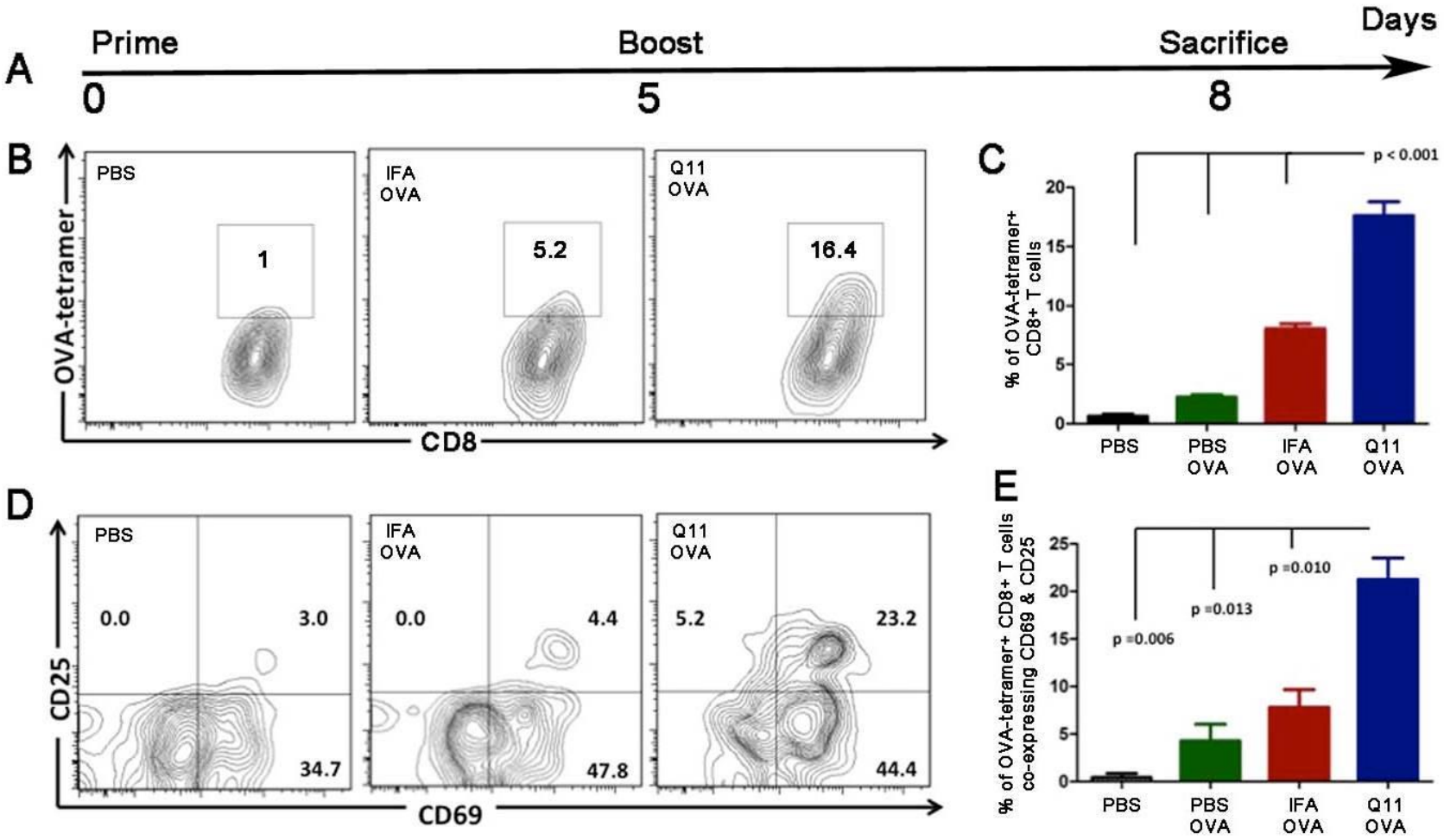
A
Prime
Boost
Sacrifice
Days
0
5
8
B
PBS
IFA OVA
Q11 OVA
1
5.2
16.4
OVA-tetramer
CD8
C
p < 0.001
% of OVA-tetramer+ CD8+ T cells
PBS
PBS OVA
IFA OVA
Q11 OVA
D
PBS
IFA OVA
Q11 OVA
0.0
3.0
34.7
0.0
4.4
47.8
5.2
23.2
44.4
CD25
CD69
E
p =0.006
p =0.013
p =0.010
% of OVA-tetramer+ CD8+ T cells co-expressing CD69 & CD25
PBS
PBS OVA
IFA OVA
Q11 OVA

Figure 2.2. Q11-OVA nanofibers elicit robust *in vivo* primary CD8+ T cell responses.

(A) Immunization schedule for assessing effector CD8+ T cell responses. (B, C) Flow cytometry plots (B) and cumulative bar graph (C) showing a greater percentage of OVA tetramer+ T cells produced with Q11-OVA immunization compared to IFA-OVA and PBS-OVA. (D, E) Flow cytometry plots (D) and cumulative bar graph (E) showing significantly higher levels of CD69 (very early stage marker of activation) and CD25 (early stage marker of activation) co-expression on OVA tetramer+ CD8+ T cells generated in response to Q11-OVA compared to IFA-OVA. Cumulative figures are from one experiment of three conducted with similar results. (n = 3-5 mice per group per experiment). * $p < 0.05$ by ANOVA using Tukey post-hoc comparison.

Q11-OVA NANOFIBERS ELICIT ROBUST IN VIVO RECALL RESPONSES

Formation of potent recall responses is an important goal of CD8+ T cell vaccine development. Thus, we investigated whether peptide nanofibers can elicit robust recall responses as a number of studies have demonstrated that the protective capacity of CD8+ T cells is dependent on their absolute number and phenotype (22). Mice were primed on day 0, boosted on day 24 and sacrificed on day 29 (Fig. 3*A*). The lymphocytes from draining popliteal, inguinal, and axillary lymph nodes were stimulated *in vitro* for 6 h, and flow cytometry analysis indicated significantly higher percentage of OVA antigen-specific cells in mice immunized with Q11-OVA compared to controls (Fig. 3*B* and 3*C*). The percentage of IFN-γ-producing CD8+ T cells (after re-stimulation *in vitro* for 6 h) was found to be higher in mice immunized with Q11-OVA nanofibers compared to soluble OVA and IFA-OVA (Fig. 3*D* and 3*E*). Thus, the quality and quantity of the recall CD8+ T cell pool was enhanced with Q11-OVA nanofibers compared to soluble OVA or IFA-OVA.

Recently, IFA has been shown to result in CD8+ T cell dysfunction and deletion at the injection site presumably due to sequestration of T-cells at the site of inoculation (9). Thus, to establish that Q11-OVA does not form a persistent antigen depot, we determined the presence of OVA antigen-specific CD8+ T cells and antigen presenting cells displaying OVA in the lymph nodes of mice prior to and after Q11-OVA boost. Such assessment indicated that a higher percentage of OVA antigen-specific CD8+ T cells were generated in response to a boost in Q11-OVA-immunized mice compared to IFA-OVA (Fig. S1*A*). Although the total number of OVA antigen-presenting cells was lower prior to boosting in Q11-OVA-immunized mice (compared to IFA-OVA), the numbers of antigen-presenting cells displaying OVA (cells expressing OVA antigen in the context of MHC) after the boost were higher in the lymph nodes of Q11-OVA mice compared to IFA-OVA mice (Fig. S1*B*). Also, the footpads from mice immunized with IFA-OVA grossly showed signs of local inflammation and were enlarged prior to boost, whereas footpads of mice immunized with Q11-OVA did not show any signs of inflammation and were similar to footpads of mice that had received soluble OVA or saline (Fig. S2). These data demonstrate that Q11-OVA nanofibers are capable of eliciting better recall responses than soluble OVA without resulting in a persistent antigen depot at the injection site compared to IFA-OVA.

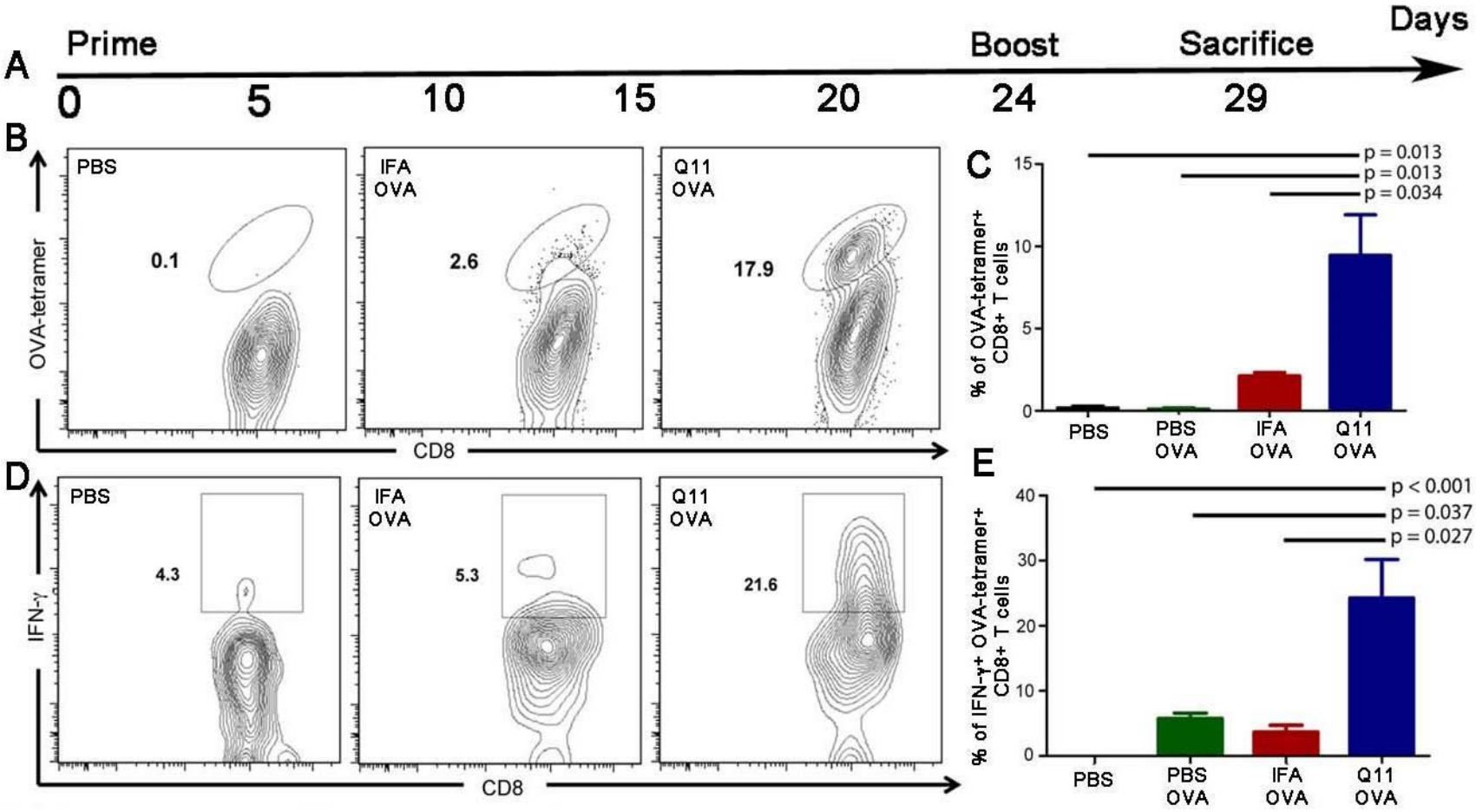
A
Prime
Boost
Sacrifice
Days
0
5
10
15
20
24
29
B
PBS
IFA
OVA
Q11
OVA
0.1
2.6
17.9
OVA-tetramer
CD8
C
p = 0.013
p = 0.013
p = 0.034
% of OVA-tetramer+
CD8+ T cells
15
10
5
0
PBS
PBS
OVA
IFA
OVA
Q11
OVA
D
PBS
IFA
OVA
Q11
OVA
4.3
5.3
21.6
IFN-γ
CD8
E
p < 0.001
p = 0.037
p = 0.027
% of IFN-γ+ OVA-tetramer+
CD8+ T cells
40
30
20
10
0
PBS
PBS
OVA
IFA
OVA
Q11
OVA

Figure 2.3. Q11-OVA nanofibers elicit robust in vivo recall responses.

(A) Immunization schedule for assessing *in vivo* recall CD8+ T cell responses. (B, C) Flow cytometry plot (B) and cumulative bar graph (C) showing a greater percentage of OVA tetramer+ CD8+ cells in the Q11-OVA group after recall boost. (D, E) Flow cytometry plot (D) and cumulative bar graph (E) showing greater percentage of IFN-γ production in the Q11-OVA group after restimulation in vitro for 6 hrs on OVA-coated plates. Cumulative figures are from one experiment of three conducted with similar results (n = 3-5 mice per group per experiment). p values listed were derived by ANOVA using Tukey post-hoc comparison.

Q11-OVA NANOFIBER VACCINATION PROTECTS MICE FROM INFLUENZA CHALLENGE

To test whether CD8+ T cells primed with Q11-OVA nanofibers could provide protection to an infectious challenge, mice were immunized intranasally with 50nM Q11-OVA nanofibers or controls, boosted on day 24 with 25nM Q11-OVA, and challenged with PR8-OVA at a sub lethal dose of 80,000 EID_{50} on day 29 (Fig. 4*A*). Mice immunized with soluble OVA or with IFA-OVA lost a significant amount of weight in contrast to mice immunized with Q11-OVA nanofibers, which did not lose any weight over the course of the challenge (Fig. 4*B*). This indicates that immunization with Q11-OVA nanofibers protected mice from an infectious challenge better than soluble OVA or IFA-OVA. In conclusion, protection from PR8-OVA challenge demonstrates that CD8+ T cells primed with Q11-OVA were able to mount an augmented antigen-specific recall CTL response.

Our findings report for the first time that self-assembling peptide nanofiber adjuvants elicit robust effector and recall CD8+ T cell responses. The data presented above demonstrate that self-assembling peptide nanofibers can elicit robust CD8+ T cell

primary and recall responses that protect from infections. Peptide nanofibers are totally synthetic and do not require bacterial expression systems for production, thereby decreasing contamination risk and enhancing safety. We have previously found nanofibers of Q11 and other self-assembling peptides to be completely non-immunogenic (10, 11), which minimizes the "carrier effect" induced by most microbial or toxin-based vaccine delivery systems (23). Significantly, the nanofibers can be stored at ambient temperatures after freeze-drying, eliminating the need for cold storage chains. Also, previous studies have demonstrated that Q11 peptides bearing two different antigens can be simply mixed to generate nanofibers displaying both antigens and eliciting dual antibody responses (12) and the nanofibers are also amenable to whole protein conjugation (24). This modularity and chemical versatility could possibly enable the production of candidate vaccines that can incorporate multiple CD8+ epitopes for a targeting a wide spectrum of pathogen antigens or a broad population distribution. Future studies will investigate incorporation of CD4+ T helper epitopes and toll-like receptor agonists linked to the nanofibers for enhanced effector responses and long-term memory. While immunologically effective and non-inflammatory, the *in vivo* processing, persistence in the periphery, and toxicity of the peptide nanofiber formulations needs to be investigated for their effective clinical translation. The ability of self-assembling nanofiber adjuvants to mount antigen-specific CTL responses makes them attractive in vaccines and immunotherapies for cancer and infectious diseases where CD8+ T cell-mediated protection is necessary.

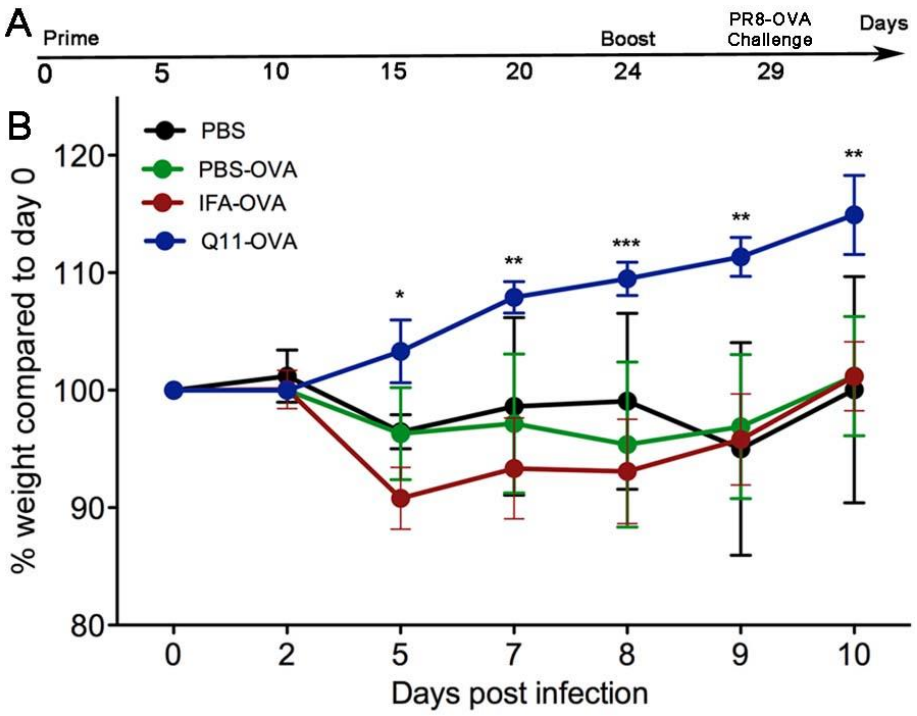

Figure 2.4 Q11-OVA nanofiber vaccination protects mice from influenza challenge.

(A) Immunization schedule for assessing protection from influenza challenge after immunization with PBS-OVA, IFA-OVA, or Q11-OVA nanofibers. (B) Cumulative figure showing that mice immunized with Q11-OVA are better protected against influenza (PR8-OVA) challenge than mice immunized with PBS, PBS-OVA, or IFA-OVA. Figure is cumulative of two experiments conducted with similar results (n = 5-10 mice per group per experiment). * $p<0.05$, ** $p<0.01$, *** $p<0.001$ by ANOVA using Tukey post-hoc comparison.

Conclusion

We have demonstrated in this chapter the clear utility of self-assembling peptides to initiate the expansion of antigen specific CD8+ T cells in vivo. Supramolecular peptide vaccine antigens are cross-presented into MHC-I molecules and are efficiently trafficked to the draining lymph nodes. The resulting CD8+ population was able to protect mice from viral challenge. Our future studies will explore the effect of stereochemistry on the fibril forming domain and how this relates to immunogenicity.

References

1. O'Hagan, D. T., and N. M. Valiante. 2003. Recent advances in the discovery and delivery of vaccine adjuvants. *Nat. Rev. Drug Discov.* 2: 727-735.
2. Black, M., A. Trent, M. Tirrell, and C. Olive. 2010. Advances in the design and delivery of peptide subunit vaccines with a focus on toll-like receptor agonists. *Expert Rev. Vaccines* 9: 157-173.
3. McKee, A.S., M.K. MacLeod, J.W. Kappler, and P. Marrack, 2010. Immune mechanisms of protection: can adjuvants rise to the challenge? *BMC Biol.* 8: 37.
4. Bijker, M.S., S.J.F. van der Eeden, K.L. Franken, C.J.M. Melief, R. Offringa, and S.H. van der Burg. 2007. CD8+ T cell priming by exact peptide epitopes in incomplete Freund's adjuvant induces a vanishing CTL response, whereas long peptides induce sustained CTL reactivity. *J. Immunol.* 179: 5033-5040
5. Rosenberg S.A., J.C. Yang, and N.P. Restifo. 2004. Cancer immunotherapy: moving beyond current vaccines. *Nat. Med.* 10: 909-915.
6. Aichele P., K. Brduscha-Riem, R.M. Zinkernagel, H. Hengartner, and H. Pircher. 1995. T cell priming versus T cell tolerance induced by synthetic peptides. *J. Exp. Med.* 182: 261-266.
7. Toes, R.E.M., R. Offringa, R.J.J. Blom, C.J.M. Melief, and W.M. Kast. 1996. Peptide vaccination can lead to enhanced tumor growth through specific T-cell tolerance induction. *Proc. Natl. Acad. Sci. USA* 93: 7855-7860.
8. Reinhardt, R.L., D.C. Bullard, C.T. Weaver, and M.K. Jenkins. 2003. Preferential accumulation of antigen-specific effector CD4+ T cells at an antigen injection site

involves CD62E-dependent migration but not local proliferation. *J. Exp. Med.* 197: 751-762.

9. Hailemichael, Y., Z. Dai, N. Jaffarzad, Y. Ye, M.A. Medina, X.F. Huang, S.M. Dorta-Estremera, N.R. Greeley, G. Nitti, W. Peng et al. 2013. Persistent antigen at vaccination sites induces tumor-specific CD8+ T cell sequestration, dysfunction and deletion. *Nat. Med*. 19: 465-472.

10. Rudra J.S., Y.F. Tian, J.P. Jung, and J.H. Collier. 2010. A self-assembling peptide acting as an immune adjuvant. *Proc. Natl. Acad. Sci. U S A* 107 :622-627.

11. Rudra J.S., T. Sun, K.C. Bird, M.D. Daniels, J.Z. Gasiorowski, A.S. Chong, and J.H. Collier. 2012. Modulating adaptive immune responses to peptide self-assemblies. *ACS Nano* 6 :1557-1564.

12. Rudra J.S., S. Mishra, A.S. Chong, R.A. Mitchell, E.H. Nardin, V. Nussenzweig, and J.H. Collier. 2012. Self-assembled peptide nanofibers raising durable antibody responses against a malaria epitope. *Biomaterials* 33 :6476-6484.

13. Huang, Z.H., L. Shi, J.W. Ma, Z. Y. Sun, H. Cai, Y.X. Chen, Y.F. Zhao, and Y.M. Li. 2012. A totally synthetic, self-assembling, adjuvant-free MUC1 glycopeptide vaccine for cancer therapy. *J. Am. Chem. Soc.*134 :8730-8733.

14. Huebener, N., B. Lange, C. Lemmel, H.G. Rammensee, A. Strandsby, J. Wenkel, J. Jikai, Y. Zeng, G. Gaedicke, and H.N. Lode. 2003. Vaccination with minigenes encoding for novel 'self' antigens are effective in DNA-vaccination against neuroblastoma. *Cancer Lett.* 197: 211-217.

15. Kohlhapp, F.J., A. Zloza, J.A. O'Sullivan, T.V. Moore, A.T. Lacek, M.C. Jagoda, J. McCracken, D.J. Cole, and J.A. Guevara-Patino. 2012. CD8+(+) T cells

sabotage their own memory potential through IFN-γ-dependent modification of the IL-12/IL-15 receptor α axis on dendritic cells. *J. Immunol.* 188 :3639-3647.

16. Zloza, A., G.E. Lyons, L.K. Chlewicki, F.J. Kohlhapp, J.A. O'Sullivan, A. T. Lacek, T.V. Moore, M.C. Jagoda, V. Kumar, and J.A. Guevara-Patino. 2011. Engagement of NK receptor NKG2D, but not 2B4, results in self-reactive CD8+ T cells and autoimmune vitiligo. *Autoimmunity* 44 :599-606.

17. Zloza, A., F.J. Kohlhapp, G.E. Lyons, J.M. Schenkel, T.V. Moore, A.T. Lacek, J.A. O'Sullivan, V. Varanasi, J.W. Williams, J.C. Jagoda, et al. 2012. NKG2D signaling on CD8^{+} T cells represses T-bet and rescues CD4+-unhelped CD8^{+} T cell memory recall but not effector responses. *Nat. Med.* 18 :422-428.

18. Garulli, B., G. Di Mario, E. Sciaraffia, Y. Kawaoka, and M.R. Castrucci. 2011. Immunogenicity of a recombinant influenza virus bearing both the CD4+ and CD8+ T cell epitopes of ovalbumin. *J. Biomed. Biotechnol.* 2011: 497364.

19. Chapman, T.J., M.R. Castrucci, R.C. Padrick, L.M.T Bradley, and D.J. Topham. 2005. Antigen-specific and non-specific CD4+ T cell recruitment and proliferation during influenza infection. *Virology* 340 :296-306.

20. Jenkins, M.R., R. Webby, P.C. Doherty, and S.J. Turner. 2006. Addition of a prominent epitope affects influenza A virus-specific CD8+ T cell immunodominance hierarchies when antigen is limiting. *J. Immunol.* 177 :2917-2925.

21. Nickoloff, B.J. and T. Wrone-Smith. 1999. Injection of pre-psoriatic skin with CD4+ T cells induces psoriasis. *Am. J. Pathol.* 155 :145-158.

22. Zaiss, D.M., C.J. Boog, W. van Eden and A.J. Sijts. 2010. Considerations in the design of vaccines that induce CD8+ T cell mediated immunity. *Vaccine* 28 :7716-7722.

23. Knuf, M., F. Kowalzik, and D. Kieninger. 2011. Comparative effects of carrier proteins on vaccine-induced immune response. *Vaccine* 29 :4881-4890.

24. Hudalla, G.A., J.A. Modica, Y.F. Tian, J.S. Rudra, A.S. Chong, T. Sun, M. Mrksich, and J.H. Collier. 2013. A self-adjuvanting supramolecular vaccine carrying a folded protein antigen. *Adv. Healthc. Mater.* doi: 10.1002/adhm.201200435. [Epub ahead of print].

APPENDIX

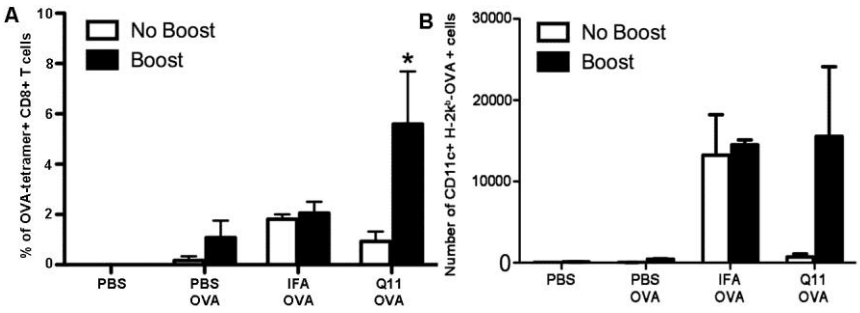

Figure 2.5. Q11-OVA nanofibers elicit robust in vivo recall responses after a boost.

(A) Cumulative bar graphs showing OVA tetramer+ CD8+ T cells from draining lymph nodes on day 29 from mice which received or did not receive a boost on day 24. (B) Cumulative bar graphs showing the percentage of CD11c+ (CD3- B220-) antigen-presenting cells displaying OVA from draining lymph nodes. * $p < 0.05$ by ANOVA using Bonferroni post-hoc comparison. Cumulative figures are from one experiment of two conducted with similar results. (n = 2 mice per group per experiment).

Figure 2.6. Q11-OVA does not form a persistent antigen depot or cause inflammation at the injection site.

Gross images of footpads of mice indicating significant swelling in the IFA-OVA group compared to Q11-OVA group.

Chapter 3 : ENANTIOMERS OF SELF-ASSEMBLING PEPTIDES ELICIT INVERSE ANTIBODY AND CD8+ T CELL RESPONSES

Reprinted with permission from the article, "Enhancing the Magnitude of Antibody Responses through Biomaterial Stereochemistry" Rajagopal Appavu†, Charles B. Chesson‡§, Alexey Y. Koyfman†, Joshua D. Snook†, Frederick J. Kohlhapp‖,Andrew Zloza‖, and Jai S. Rudra*†§ *ACS Biomater. Sci. Eng.*, 2015, *1* (7), pp 601–609 from the American Chemical Society.

INTRODUCTION

Most vaccine adjuvants are limited in their ability at inducing strong immune responses without associated toxicity and there is an ever-growing need for effective and safe adjuvants (1). Self-assembling peptides that form β-sheet rich nanofibers have been reported to elicit strong immune responses in mice when linked to peptide or protein antigens (2-4). This adjuvanting capability was not restricted to primary sequence of the self-assembling domain, position of the epitope, linker sequence, mouse strains, or the route of immunization (5-7). Immunization with peptide nanofibers bearing disease-relevant epitopes has been shown to be protective in murine models of malaria and cancer (6, 7). Interestingly, strong immune responses have not been detected against self-assembling peptides in the absence of antigen, even when co-administered with strong exogenous adjuvants, which makes them ideal for applications in vaccine development and immunotherapy (2, 5). While both L- and D- amino acids are chemically possible, naturally occurring proteins utilize only the L-form. Therefore it is not surprising that

most self-assembling peptides designed to date have utilized naturally occurring L amino acids (8-10). However, D amino acid self-assembling peptides have recently gained considerable attention due to their complementary chemical nature and reduced proteolytic sensitivity for a variety of biomedical applications (11).

Zhang and co-workers first reported the assembly and behavior of D-form self-assembling peptides using the peptide enantiomers L-EAK16 and D-EAK16 (11, 12). While both peptides assembled into well-ordered nanofibers with mirror image secondary structures, significant differences were observed in responses to external stimuli like pH, temperature, and the presence of denaturing agents or proteases. Interestingly, hybrid self-assembling peptides composed of alternating L and D amino acids did not self-assemble (13, 14). The effects of stereochemistry on the mechanical properties of self-assembling peptide biomaterials were first reported by Schneider and Pochan who observed that racemic hydrogels of the β-hairpin peptide MAX1 and its enantiomer DMAX1, exhibited maximum rigidity compared to the individual peptides or any other ratio of the enantiomers (15). Using a FRET pair coupled to the enantiomers of KFE8(L) and KFE8(D), Nilsson and co-workers demonstrated that equimolar mixtures of enantiomers packed into “rippled β-sheet” nanofibers composed of alternating L- and D-peptides (16). This alternate packing had an enthalpic advantage over all-L or all-D nanofibers, which explained the enhanced rigidity of the MAX1 and DMAX1 racemic hydrogels. Scaffolds of D amino acid self-assembling peptides have also been reported to be effective at supporting *in vitro* cell cultures, homeostasis and wound healing in animal models, (14, 17) and resistant to proteolytic degradation by a number of proteases (12)

making them attractive for applications in tissue engineering, regenerative medicine, and drug delivery.

Although D amino acids very rarely participate in protein synthesis they are vital to all living organisms including bacteria (D-alanine is a component of the cell wall) and mammals (D-serine is involved in glutamatergic neurotransmission in the central nervous system) (18, 19). In humans, physiological fluids such as plasma, cerebrospinal fluid, and amniotic fluid have been reported to contain high levels of D amino acids (20) and peptides containing D amino acids are useful in many applications in microbiology, physiology and medicine (21-23). While a few studies have investigated the immunological properties of D amino acid peptide antigens (24, 25), the influence of adjuvant chirality on immune responses is not known. In this study, we investigated the effect of D amino acids on the adjuvanting potential of the self-assembling peptide KFE8. Peptide epitopes from chicken egg ovalbumin known to elicit either antibody or CD8+ T cell responses were coupled to KFE8 or its enantiomer via short amino acid linkers and adaptive immune responses were investigated. Our results indicate that enantiomers of self-assembling peptides elicit inverse antibody and CD8+ T cell responses and suggest that chirality can be used as a design tool to modulate the strength of adaptive immune responses.

MATERIALS AND METHODS

PEPTIDE SYNTHESIS AND PURIFICATION

All peptides (sequences in Table 1) were synthesized using standard Fmoc Chemistry on a CS Bio-CS336X solid phase peptide synthesizer. Rink Amide MBHA or Wang resin was swelled in dry DMF for 1hr, and peptides were double coupled using HBTU (O-(Benzotriazol-1-yl)-N,N,N′,N′-tetramethyluronium hexafluorophosphate) and HOBt (1-Hydroxybenzotriazole) chemistries. Peptides were cleaved from the resin using 95% TFA / 2.5% H_20 / 2.5% triisopropyl silane cocktail and washed in diethyl ether. The crude product was purified by reverse-phase HPLC (C18 column) using Acetonitrile/H_2O gradients to > 90% purity and peptide mass was confirmed by MALDI using α-cyano-4-hydroxycinnamic acid matrix (Bruker Daltonics, MA). All peptides were lyophilized and stored at 4°C. Endotoxin levels of all peptides were tested using a limulus amebocyte lystae (LAL) chromogenic end point assay (Lonza, USA) at the same volume and peptide concentration used for immunizations and were found to be less than 0.11 EU/mL and within acceptable limits[26]. To account for batch-to-batch variability three different sets of peptides were synthesized for immunizing mice.

TRANSMISSION ELECTRON MICROSCOPY (TEM)

Stock solutions of 1 mM peptides were allowed to fibrillize in water overnight at 4°C, diluted in PBS to 0.3 mM and applied to 400 mesh copper grids with carbon support film. The grids were negatively stained with 2% uranyl acetate, and imaged on a JEOL EM1400 TEM equipped with LaB_6 electron gun and digital cameras. Images were viewed and recorded with an Orius Ultrascan 1000 camera. Scale bar is 50 nm.

CIRCULAR DICHROISM SPECTROSCOPY (CD)

CD experiments were carried out on a JASCO J-815 CD Spectrometer. 1 mM peptide stock solutions were made in ultra pure water and diluted to working concentrations before use. CD wavelength range was from 260 nm to 195 nm with a scanning speed of 0.3 nm/s and a bandwidth of 0.5nm. CD spectra were recorded at room temperature with a fixed-path-length (1 mm) cell. The solvent background contribution was subtracted and resultant CD signal was converted to mean residue ellipticity.

CYTOTOXICITY ASSAY

A standard MTS assay was utilized to determine peptide cytotoxicity (Promega, Madison, WI, cat# G3582). Mouse lymphocytes (B6 mice, 100,000 cells/well) were seeded in 96-well plates in culture media (1640 RPMI containing 1% penicillin/streptomycin, 2% L-glutamine, and 10% FBS) containing 0.01, 0.1 or 1 mg/mL of KFE8(L) or KFE8(D) peptide. The cells were incubated for 24h and the medium was replaced. MTS reagent was applied for 4 h and absorbance at 490 nm was measured using a microplate reader. Controls included cultures fixed with absolute ethanol or treated with 5 μg/ml anti-CD3 and 1 μg/ml CD28 antibodies. All groups contained 3 replicates.

ANIMALS AND IMMUNIZATIONS

Peptides were dissolved in sterile water to 8 mM stock solutions, stored overnight at 4°C, and diluted to working concentration of 2 mM using sterile PBS. Female mice (C57BL/6, 6-8 weeks old) were purchased from Taconic Farms. To investigate antibody responses, 50 μl of OVA-KFE8(L) or OVA-KFE8(D) peptide solution (100 nm of

antigen) were injected subcutaneously in the flank at two different sites. Mice were boosted on day 28 with two 25 μl injections of peptide solution or controls (50 nmol of antigen) and sacrificed on day 42. Blood was collected weekly via the submandibular vein and sera stored at -80°C. To investigate CD8+ T cell responses, mice we immunized in the footpad with 20 μl of SIN-KFE8(L) or SIN-KFE8(D) peptide solution, boosted on day 5, and sacrificed on day 8 (for effector responses) or boosted on day 28 and sacrificed on day 32 (for memory responses). Mice immunized with OVA or SIN peptides in PBS or ISA-720 adjuvant were used as controls. ISA-720 emulsion was prepared by mixing equal volumes of peptide solution and adjuvant immediately prior to immunization. All experiments were conducted under approved protocols by the University of Texas Medical Branch Institutional Animal Care and Use Committee and repeated independently 3 times with 3-5 mice per group per experiment.

ANTIBODY RESPONSES

High-binding ELISA plates (eBioscience) were coated with 20 μg/mL of antigen in PBS overnight at 4 °C and blocked with 200 μL of 1% BSA in PBST (0.5% Tween-20 in PBS) for 1 h. Serum dilutions were applied ($1:10^{-2}$ to $1:10^{-9}$, 100 μL/well) for 1 h at room temperature followed by peroxidase-conjugated goat anti-mouse IgG (H+L) (Jackson Immuno Research) (1:5000 in 1 % BSA-PBST, 100 μL/well). Plates were developed using TMB substrate (100 μL/well, eBioscience), the reaction stopped using 50μl of 1 M phosphoric acid, and absorbance measured at 450 nm. Absorbance values of PBS (no antigen) coated wells were subtracted to account for background. Antibody

isotypes were determined using a mouse monoclonal antibody kit (Sigma, MO) with secondary goat anti-mouse IgG1, IgG2a, IgG2b, IgG3, IgM, and IgA.

CD8+ T CELL FREQUENCY

Lymphocytes were harvested from the ipsilateral inguinal and popliteal draining lymph nodes for effector and memory response studies. Pooled lymph nodes were pressed through a 70 μm cell strainer (BD Biosciences, CA) and washed twice with 1640 RPMI containing 1% penicillin/streptomycin, 2% L-glutamine, and 10% FBS. SIINFEKL MHC class I tetramer and cell surface marker staining was performed according to standard protocols described previously (4). $H2K^b$-OVA tetramer (PE) was purchased from Medical Biological Laboratories (Woburn, MA). Live/dead stain (eF506), CD3 (Pacific Blue), CD8+ (APC-Cy7), CD4+4 (PerCPCy5.5) and CD62L (FITC) were purchased from BD Biosciences (San Jose, CA). Flow cytometry was performed using a BD FACS Canto II flow cytometer and data were analyzed using FlowJo software (Tree Star, OR).

STATISTICAL ANALYSIS

All the experimental data were plotted using Prism software and represented as mean±SEM, and statistical analysis was performed by ANOVA with Tukey's post hoc test. Statistical significance was assigned at p values <0.05.

RESULTS

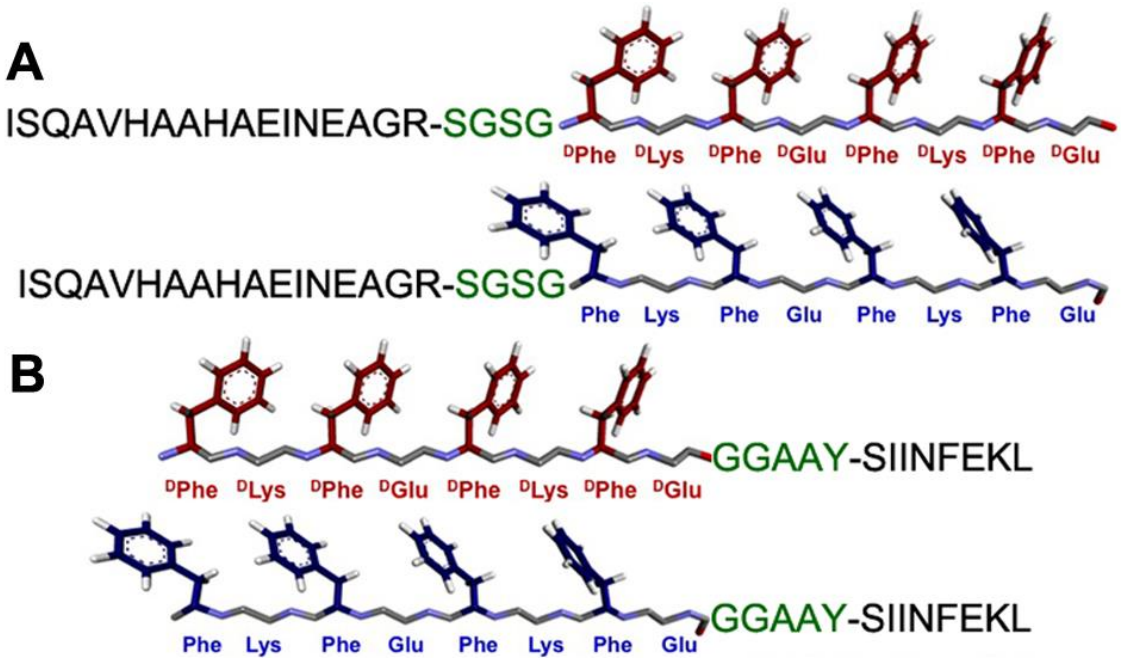

Figure 3.1.Schematic of self-assembling peptide enantiomers KFE8(L) and KFE8(D) showing the position of the epitopes and linker sequences.
(A) OVA epitope was linked to the N-terminus of the enantiomers using -SGSG- linker and (B) SIN epitope was linked to the C-terminus through -GGAAY- linker.

PEPTIDE DESIGN AND ASSEMBLY

OVA (aa 323-339 of chicken egg ovalbumin) is a MHC-Class II (I-A^b)-restricted epitope with a B cell determinant and antibody responses to self-assembling peptide nanofibers bearing OVA have been shown to be entirely CD4+ T cell dependent[5]. The CD8+ T cell epitope, SIN (aa 257-264 of chicken egg ovalbumin) is a MHC-Class I (H-2K^b)-restricted epitope and known to elicit strong effector and memory CD8+ T cell responses in mice when coupled to self-assembling peptides[4]. The OVA epitope was conjugated to the N-terminus of the enantiomers via a SGSG linker (Fig 3.1*A*) and the SIN epitope was conjugated to the C-terminus of the enantiomers via a GGAAY linker (Fig. 3.1*B*) (4, 5). By TEM, it was observed that KFE8(L) and KFE8(D) assembled into nanofibers (Fig 3.2*A* and 3.2*B*) and retained their ability to assemble when functionalized with OVA or

SIN peptide epitopes on their N- or C-terminus (Fig. S3.1*A* to Fig. S3.1*D*). Secondary structure analysis of the enantiomers indicated equal and opposite optical rotations, reflecting their molecular chirality with signals at 218 nm (β-sheet secondary structure) and 205 nm (from π-π effects of Phe aromatic groups) (Fig. 3.2*C*) (16). Optical rotations of OVA and SIN functionalized enantiomers were also found to be equal and opposite suggesting that the addition of unstructured L amino acid epitopes on either termini did not significantly affect self-assembly (Fig. S3.1*E*). L amino acid self-assembling peptides have been found to be non-cytotoxic in cultures of primary cells (27) whereas D amino acids like D-Ala and D-Asp have been reported to be cytotoxic and inhibit cell proliferation (28). To facilitate the interpretation of the immunological outcomes without significant concerns for cytotoxicity, peptides KFE8(L) and KFE8(D) were added to primary mouse lymph node cell cultures at three different concentrations of 0.01, 0.1, or 1 mg/mL and incubated for 24 h. Cells fixed with absolute ethanol or stimulated with anti-CD3 and CD28 antibodies were used as negative and positive controls respectively. No significant differences in cytotoxicity were found between the enantiomers at any concentrations tested (Fig. 3.2*D*).

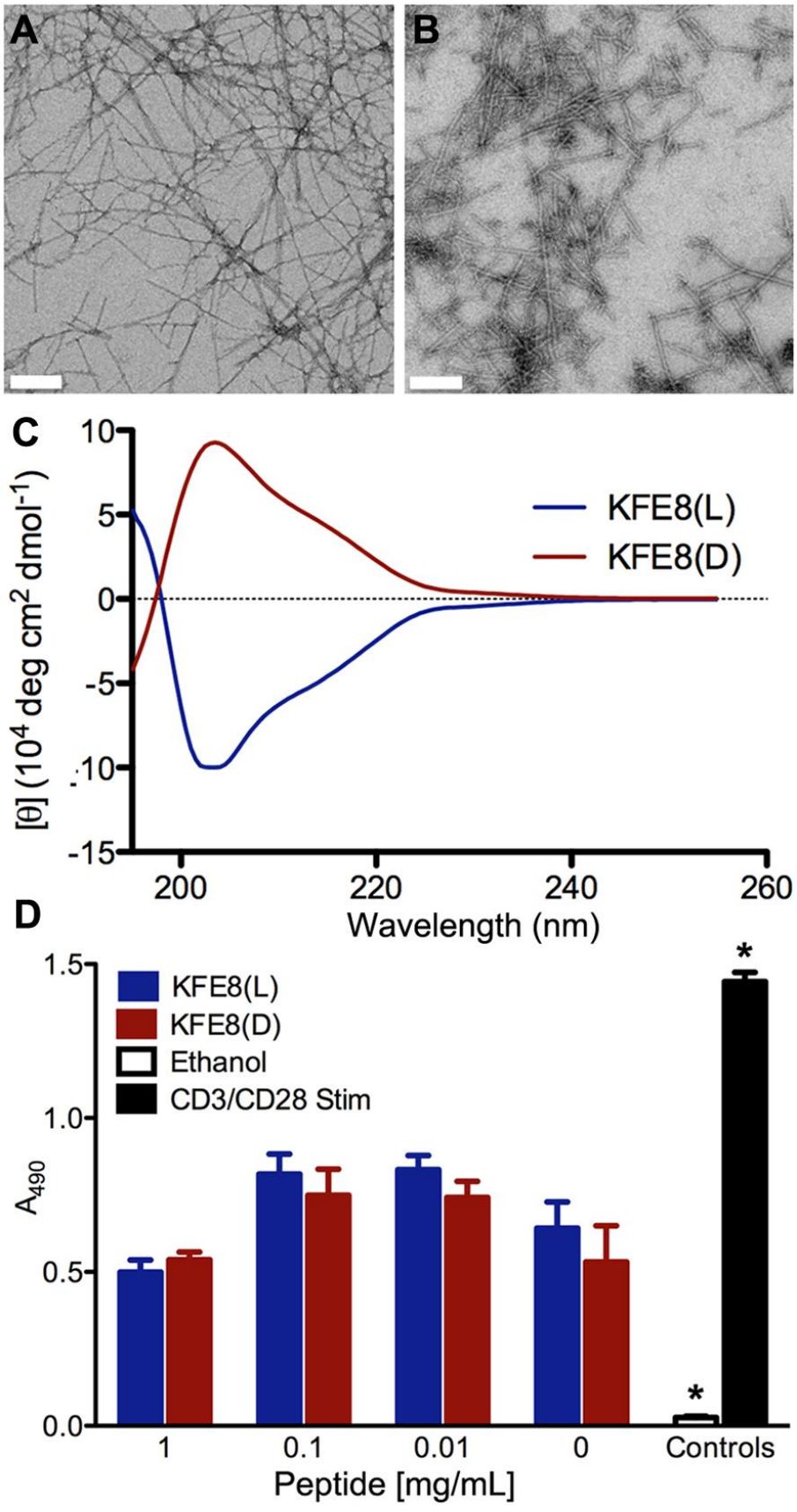
A
B
C
10
5
0
-5
-10
-15
[θ] (10^4 deg cm^2 dmol^-1)
KFE8(L)
KFE8(D)
200
220
240
260
Wavelength (nm)
D
1.5
1.0
0.5
0.0
A490
KFE8(L)
KFE8(D)
Ethanol
CD3/CD28 Stim
*
*
1
0.1
0.01
0
Controls
Peptide [mg/mL]

Figure 3.2. Electron micrographs, secondary structures, and cytotoxicity of KFE8(L) and KFE8(D) nanofibers.

TEM images of (A) KFE8(L) and (B) KFE8(D). Scale bar is 50 nm. (C) CD spectra of KFE8(L) and KFE8(D) in water at 0.5 mM indicating beta-sheet rich structures and the spectra are mirror images reflecting molecular chirality. (D) MTS assay data showing non-cytotoxicity of KFE8(D) nanofibers mouse lymph node cell cultures at different concentrations. Cultures fixed with absolute ethanol or stimulated with anti-CD3 and CD28 antibodies are shown as controls. *$p<0.05$ by ANOVA using Tukey post-hoc test.

D-FORM SELF-ASSEMBLING PEPTIDES ELICIT STRONGER ANTIBODY RESPONSES

Mice were immunized and boosted subcutaneously with OVA-KFE8(L) or OVA-KFE8(D) nanofibers and antibody responses were evaluated by ELISA (5, 7, 8). Sera from mice immunized with OVA-KFE8(L) or OVA-KFE8(D) were applied to plates coated with the antigenic enantiomers and sera from control groups were applied to plates coated with the free OVA-peptide. OVA-KFE8(D) nanofibers raised robust antibody responses demonstrating that self-assembling peptide domains composed of all D amino acids can adjuvant effectively (Fig. 3.3*A*). Interestingly, antibody levels in mice immunized with OVA-KFE8(D) nanofibers were significantly higher in a series of serum dilutions compared to OVA-KFE8(L) nanofibers or OVA in ISA-720 adjuvant and OVA delivered in PBS did not raise any detectable IgG, as expected (Fig. 3.3*A*). This suggests that D amino acid peptide nanofibers elicit stronger antibody responses compared to L amino acid peptide nanofibers. To preclude the effects of the linker-fiber regions, ELISA's were conducted with wells coated with the antigenic enantiomers and control wells coated with nanofibers of SGSG-KFE8(L or D). The background signal from the control wells was subtracted from wells coated with the antigenic enantiomers to ascertain the levels of antigen-specific antibodies. Data indicated significantly higher

levels of antibodies in the sera of mice immunized with OVA-KFE8(D) nanofibers compared to OVA-KFE8(L) nanofibers (Fig. 3.3*B*). Also, when serum from mice immunized with the enantiomers was applied to plates coated with the free OVA peptide, higher levels of anti-OVA antibodies were observed in the sera of mice vaccinated with OVA-KFE8(D) nanofibers compared to OVA-KFE8(L) (Fig. S3.2*A*). To confirm that higher antibody levels observed with OVA-KFE8(D) nanofibers were not due to strong recall responses following the booster shot, we compared antibody levels between the antigenic enantiomers pre-boost. Data indicated significantly higher levels of antibodies pre-boost in mice vaccinated with OVA-KFE8(D) compared with OVA-KFE8(L) (Fig. S2*B*). Taken together, the data indicate that D amino acid peptide nanofibers elicit significantly stronger antibody responses in mice compared to L amino acid peptide nanofibers.

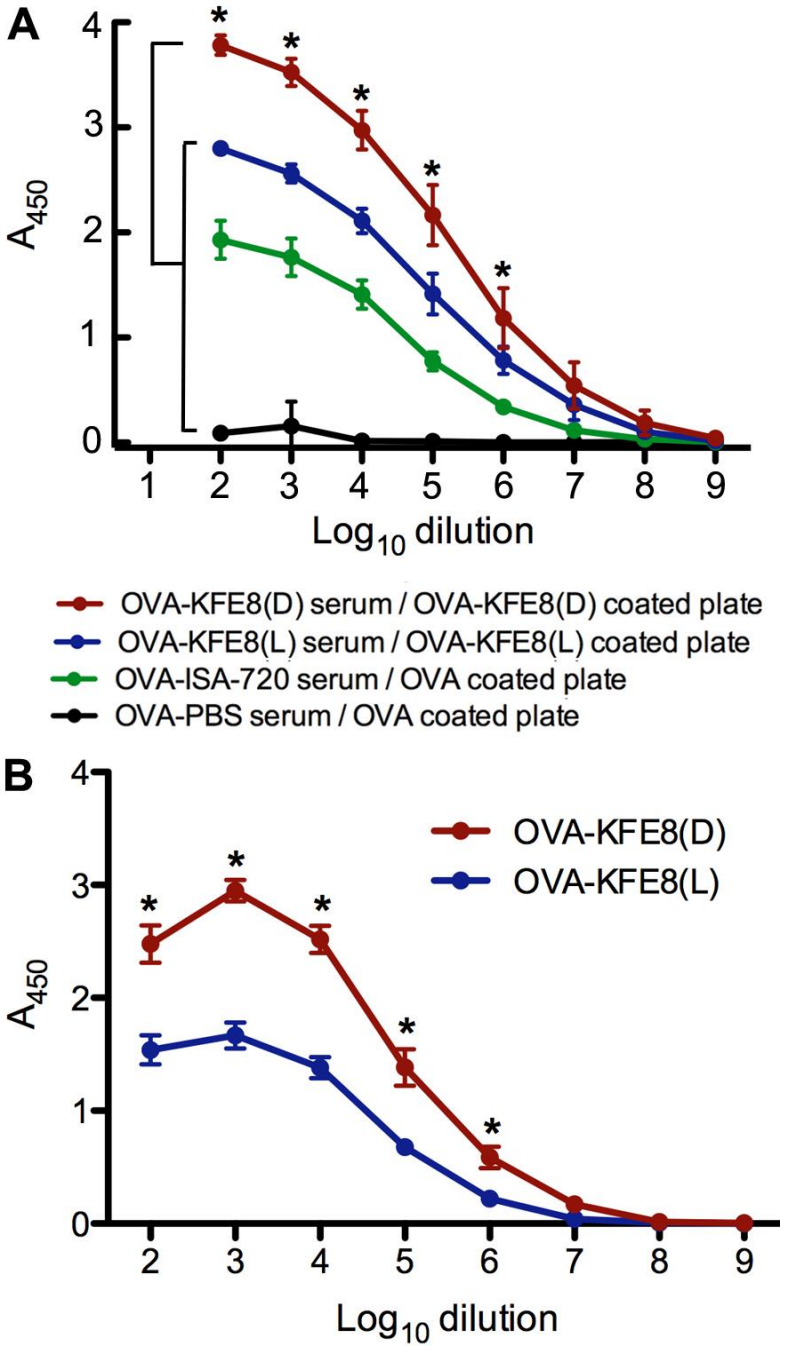

Figure 3.3. Self-assembling D amino acid peptide nanofibers act as immune adjuvants and elicit strong antibody responses.

(A) Significantly higher levels of total IgG were detected in the sera of mice immunized with OVA-KFE8(D) nanofibers compared to OVA-KFE8(L) nanofibers or controls. (B) Data showing significantly higher levels of OVA-specific antibodies in the sera of mice immunized with OVA-KFE8(D) nanofibers compared to OVA-KFE8(L) nanofibers where absorbance from control wells coated with SGSG-KFE8(L) or SGSG-KFE8(D) was subtracted to account for contribution from the linker-fiber region. Data is cumulative of three independent experiments (n = 3-5 mice per group per experiment). *$p<0.05$ by ANOVA using Tukey post-hoc test.

D-FORM SELF-ASSEMBLING PEPTIDES DO NOT AFFECT THE NATURE OF THE ANTIBODY RESPONSE

To determine the nature of the immune response elicited by the enantiomers, antibody isotypes were evaluated. All isotypes were evaluated by coating the plates with the free OVA peptide to preclude fiber and linker contributions and enable a direct comparison of isotype levels. For both L and D nanofibers the dominant isotype found was IgG1, consistent with previous findings (2). Isotypes IgG2a, IgG2b, IgG3, IgM, and IgA were also produced by both enantiomers and all isotypes were significantly higher in the OVA-KFE8(D) group compared to OVA-KFE8(L) (Fig. 4). The production of IgG2a, IgM, and IgA was also significantly higher in the OVA-KFE8(D) group compared to OVA in ISA-720 adjuvant (Fig. 4*E*). Taken, together these results indicate that D-amino acid peptide nanofibers do not affect the nature of the immune response.

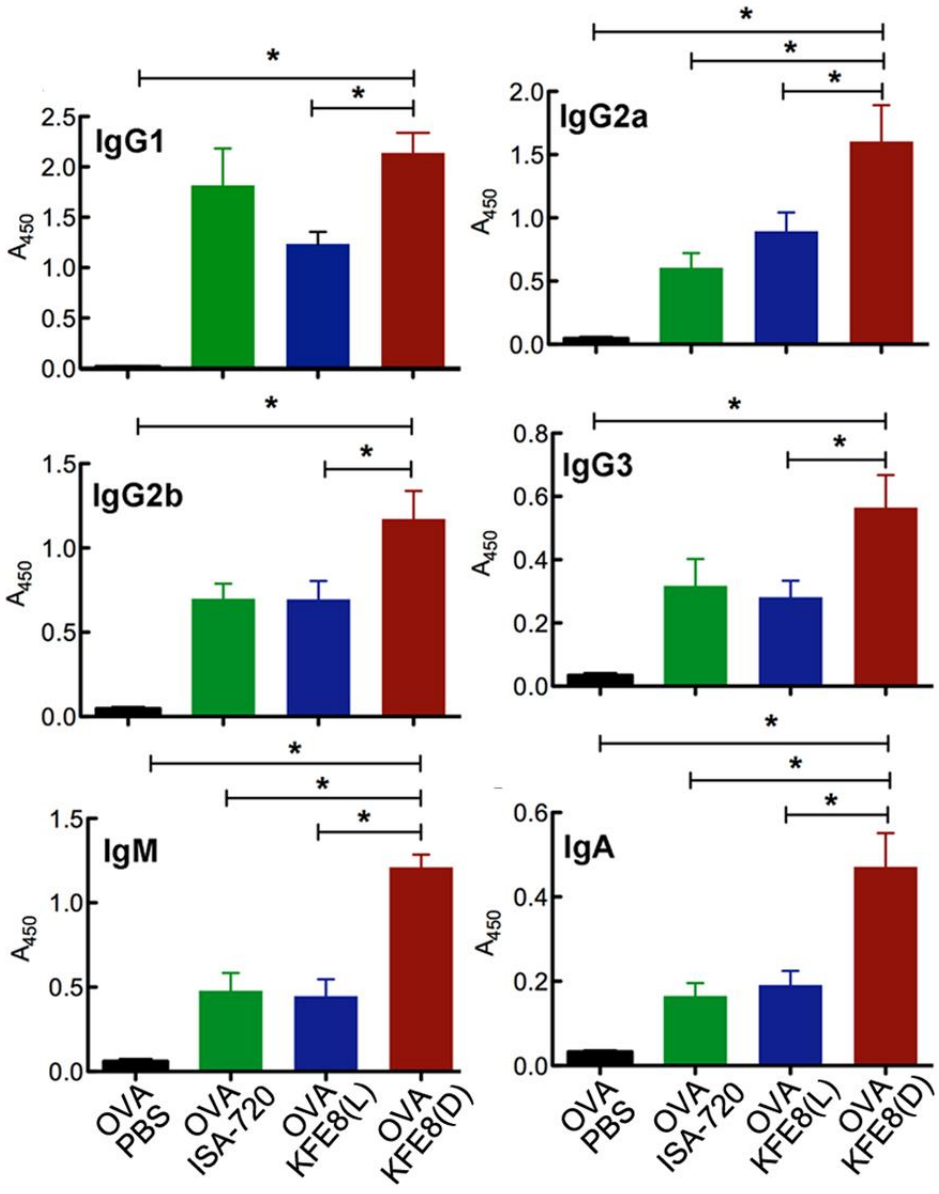

Figure 3.4. Antibody isotypes in sera from mice immunized with the enantiomers.

Significantly higher levels of all antibody isotypes are detected in the sera of mice immunized with OVA-KFE8(D) nanofibers compared to OVA-KFE8(L) nanofibers. Data is cumulative of three independent experiments (n = 3-5 mice per group per experiment). *$p < 0.05$ by ANOVA using Tukey post-hoc test.

D-FORM SELF-ASSEMBLING PEPTIDES ELICIT WEAKER CD8+ T CELL RESPONSES

CD8+ T cell responses were investigated by immunizing mice in the footpad with nanofibers of SIN-KFE8(L) or SIN-KFE8(D) and determining the numbers of antigen-specific T cells in the draining lymph nodes. For effector CD8+ T cell responses, mice were immunized and boosted on day 5, and the numbers of antigen-specific T cells in the draining lymph nodes were evaluated on day 8. We hypothesized that nanofibers composed of D amino acids would also enhance CD8+ T cell responses but surprisingly, mice immunized with SIN-KFE8(D) nanofibers had significantly lower numbers of antigen-specific T cells in their draining lymph nodes compared to mice immunized with SIN-KFE8(L) nanofibers (Fig. 3.5*A* and Fig. 3.5*B*). To investigate whether the poor CD8+ T cell effector responses were transient, long-term memory responses were investigated by priming mice with the enantiomers followed by a boost at day 28. On day 32 significantly higher numbers of antigen-specific T cells were again observed in the lymph nodes of mice immunized with SIN-KFE8(L) nanofibers, confirming that nanofibers composed of D amino acids elicit weaker CD8+ T cell responses compared to nanofibers of L amino acids (Fig. 3.5*B* and Fig. 3.5*D*).

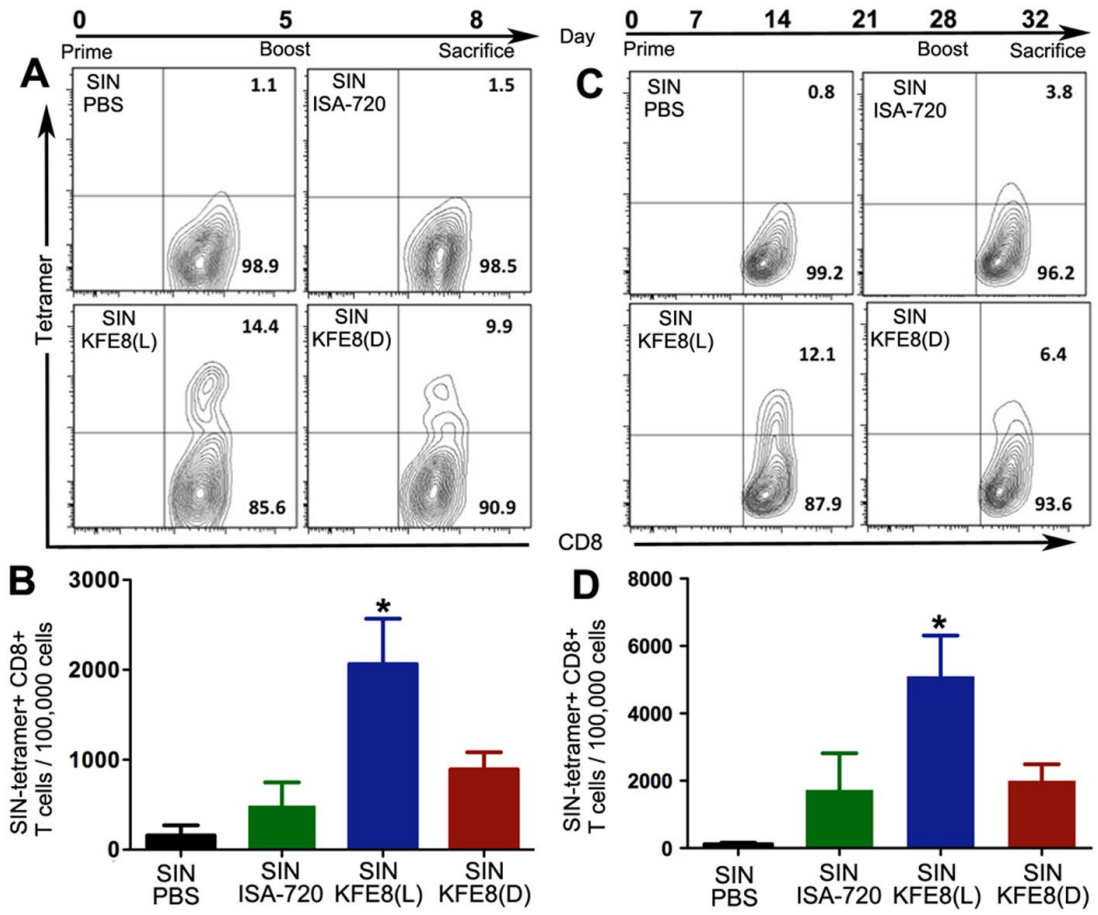

Figure 3.5. Self-assembling peptides composed of D amino acids result in lower frequencies of CD8+T cells compared to L amino acids.

(A, C) Flow cytometry plots and (B, D) cumulative bar graphs showing that SIN-KFE8(L) nanofibers elicit robust effector and memory CD8+ T cell responses and generate higher numbers of tetramer+ CD8+ T cells compared to SIN-KFE8(D) nanofibers. Data is cumulative of three independent experiments (n = 3 mice per group per experiment). *$p<0.05$ by ANOVA using Tukey post-hoc test.

DISCUSSION

The epitope-bearing enantiomer pairs used in this study differ only in the amino acid composition of the self-assembling domain, which allows for direct comparison of the effect of chirality on antibody and CD8+ T cell responses. Our results indicate that

simply changing the chirality of a self-assembling peptide domain can enhance or suppress antibody or CD8+ T cell responses suggesting that stereochemistry can be used as a design tool to modulate the adjuvanting properties of self-assembling peptides. Although no studies have reported conjugating biofunctional molecules to D amino acid self-assembling peptides, it is likely that there are no significant differences in the numbers of OVA or SIN epitopes displayed on the fibril surface when coupled to KFE8(L) or KFE8(D). While previous studies have shown that immune responses to self-assembling peptides are affected by immunogenicity of the attached ligand or epitope (5), here we demonstrate that immune responses can also be modulated by the stereochemistry of the self-assembling peptide domain.

Among the factors known to affect the strength and duration of an immune response, persistence of the antigen in an appropriate location is considered to play an important role (29). Robust and long-term antibody responses lasting up to a year have been observed in response to a single prime/boost regimen with self-assembling peptide adjuvants previously (5). Recent studies by Chen and Pompano *et al*. demonstrated that self-assembling peptide nanofibers are internalized by dendritic cells at the injection site and elicit differentiation of CD4+ T cells into T follicular helper (Tfh) cells and B cells into germinal center cells (30). This resulted in the production of higher-titer, higher-affinity IgG responses to a peptide antigen compared to the clinically approved adjuvant alum (30). Using adoptive transfer studies of transgenic T cells, Baumjohann *et al*. have established that sustained antigen presentation is required for the maintenance of Tfh cells and that germinal center B cell numbers strongly correlate with the amount of available antigen (29). Taken together, our data showing significantly higher levels of

antibodies, particularly the IgM isotype, suggest that the strong antibody responses observed against OVA-KFE8(D) could be a result of sustained antigen persistence and reduced susceptibility to proteolysis compared to OVA-KFE8(L). On the other end of the immune spectrum, antigen persistence has been shown to result in CD8+ T cell dysfunction and deletion (31). Using a melanoma tumor model and incomplete Freund's adjuvant (IFA), Overwijk and co-workers demonstrated that persisting antigen shifts CD8+ T cell localization away from the tumor, induces poor antitumor immunity, increases systemic T cell dysfunction, and leads to poor memory formation (31). Adjuvants such as alum and IFA are thought to influence immune responses by forming a local antigen depot leading to sustained antigen presentation. Our recent investigations have shown that L-amino acid peptide nanofibers are effectively cleared from the footpads of mice as early as 10 days after vaccination and induce robust effector and memory CD8+ T cell responses compared to a persisting IFA depot (4). Footpads from mice immunized with IFA also showed signs of inflammation and higher numbers of antigen-specific T cells localized to the immunization site (4). Although we did not notice gross differences in the footpads of mice vaccinated with L or D nanofibers, persistence of SIN-KFE8(D) nanofibers could be one of the causes for the suppressed CD8+ T cell responses observed here. Also, while it is likely that SIN-KFE8(D) nanofibers are cleared at the immunization site, their persistence in the peripheral lymphoid tissues could also contribute to CD8+ T cell dysfunction.

While antigen persistence in the context of B cells and T cells seems to be a plausible explanation, other factors may contribute to the inverse antibody and CD8+ T cell responses observed here. Immune responses to the self-assembling peptide domain

Q11 have been reported to be dependent on the universal adaptor protein MyD88, which is down-stream of a number of toll-like receptor (TLR) agonists and studies in knock out mice indicated that TLR-2, TLR-4, or TLR-5 were not involved (6, 30). Also, self-assembling peptide nanofibers are structurally similar to the fibrillar peptide amyloid-β, and also particulate in nature similar to alum, both of which activate the NALP3 inflammasome pathway (32, 33). Studies in NALP3 knockout mice have shown that nanofibers of the self-assembling peptide Q11 do not activate the inflammasome (6). Further studies are required to clarify the mechanism of innate immune responses elicited by other self-assembling peptides and the impact of chirality on innate immunity. Sentinel cells of the innate immune system like macrophages and neutrophils and some epithelial cells have been shown to exhibit differential attachment behavior on chiral surfaces (34). It is possible that there could be differences in the engagement of antigen-presenting cells like dendritic cells by the enantiomers. Therefore the inverse modulation of antibody and CD8+ T cell responses by the enantiomers could be due to a combination of differential activation of innate immune responses, interaction with antigen-presenting cells, and the also longer persistence of the D-form nanofibers compared to the L-form nanofibers. While self-assembling peptide nanofibers composed of L amino acids have been found to be effectively non-immunogenic even in the presence of exogenous adjuvants, the immunogenic potential of D amino acid nanofibers is not fully known. In addition, whether the inverse antibody and CD8+ T cell responses elicited by KFE8 enantiomers are global phenomena of all self-assembling peptides remains to be investigated.

For applications in vaccine development and immunotherapy the synthetic nature of self-assembling peptide adjuvants allows for high purity and unambiguous identification of the final construct through mass spectroscopy; a major advantage for their evaluation and approval for clinical use by regulatory agencies. Most vaccine adjuvants currently used are chemically heterogeneous mixtures of plant- or pathogen-derived products, formulations of mineral salts, or emulsions, and have some associated toxicity making it extremely difficult to understand their mechanism of action (35). The chemical definition of self-assembling peptides enables the design of adjuvants with desired physicochemical and biological characteristics through the addition of modifications, which is made impossible by the compositional heterogeneity of emulsion-based adjuvants. Like most biochemical interactions, immune recognition and response is inherently chiral and antibodies generated against L amino acid epitopes do not cross-react with their D enantiomers[24]. However, a few antibody isotypes produced against a D-form peptide antigens have been shown to cross-react with its L form homolog and also the native protein (25). This allows us to further enhance antibody responses using D-form self-assembling peptide nanofibers linked to D-form peptide epitopes while reducing antigen dose and booster shots. Also, different epitopes linked to self-assembling peptide enantiomers can be precisely co-assembled owing to the 'rippled packing' of the enantiomers for generating multi-antigenic vaccines for a wide variety of pathogen strains or covering a broad population distribution. Additionally, controlling the degree of the antibody and CD8+ T cell responses through adjuvant stereochemistry will open the doors for the development of designer vaccines with tunable properties that might elicit the best immune response, i.e. Th1, Th2 or Th17, for the given pathogen. The

complementary chemical nature of D-form self-assembling peptides might also be useful for uncovering the fundamental immunology of peptide-based nanomaterials, which are currently being developed for a variety of *in vivo* applications including coatings for prosthetic grafts, injectable tissue repair scaffolds, and sustained drug delivery vehicles (9, 10).

CONCLUSIONS

In this study, we demonstrate that self-assembling peptides composed of D amino acids are non-cytotoxic and act as effective immune adjuvants in mice similar to their enantiomeric counterparts. D-form peptide nanofibers elicit stronger antigen-specific antibody responses but poor effector and memory CD8+ T cell responses compared to L-form peptide nanofibers, which elicit the inverse. These findings suggest that adaptive immune responses to self-assembling peptide adjuvants can be modulated by their stereochemistry. Inclusion of D amino acids may be advantageous for developing synthetic vaccines against infectious and non-infectious diseases where antibody mediated protection is desirable yet L amino acids elicit stronger cell mediated responses. Our future studies will investigate prophylactic vaccination using disease specific models of Tuberculosis that requires strong cell mediated immunity for protection.

ACKNOWLEDGEMENTS

This study was supported by funds from the Sealy Center for Vaccine Development and the Department of Pharmacology and Toxicology UTMB (to J.S.R). TEM studies were

conducted at the Sealy Center for Structural Biology Cryo-electron Microscopy core and we thank Dr. Misha Sherman and Michael Woodson for assistance. Flow cytometry was conducted at the Flow Cytometry and Cell Sorting Facility at UTMB. We thank Whitney Yin, Andrew Zloza, and Rebecca Pompano for helpful discussions and Heather Lander for assistance with editing the manuscript.

REFERENCES

1. O'Hagan, D. T.; De Gregorio, E. The path to a successful vaccine adjuvant-'the long and winding road'. *Drug discovery today* **2009**,14(11-12):541-551. doi: 10.1016/j.drudis.2009.02.009.

2. Rudra, J. S.; Tian, Y. F.; Jung, J. P.; Collier, J. H. A self-assembling peptide acting as an immune adjuvant. *Proceedings of the National Academy of Sciences of the United States of America* **2010**,107(2):622-627. doi: 10.1073/pnas.0912124107.

3. Hudalla, G. A*.;* Modica, J. A.; Tian, Y. F.; Rudra, J. S.; Chong, A. S.; Sun, T.; Mrksich, M.; Collier, J. H. A self-adjuvanting supramolecular vaccine carrying a folded protein antigen. *Advanced healthcare materials* **2013**, 2(8):1114-1119.

4. Chesson, C. B.; Huelsmann, E. J.; Lacek, A. T.; Kohlhapp, F. J.; Webb, M. F.; Nabatiyan, A.; Zloza, A.; Rudra, J. S. Antigenic peptide nanofibers elicit adjuvant-free CD8+ T cell responses. *Vaccine* **2013**, 329(10):1174-80. doi: 10.1016/j.vaccine.2013.11.047.

5. Rudra, J. S*.;* Sun, T.; Bird, K. C.; Daniels, M. D.; Gasiorowski, J. Z.; Chong, A. S.; Collier, J. H. Modulating Adaptive Immune Responses to Peptide Self-Assemblies. *ACS nano* **2012**, 6(2):1557-1564. doi: 10.1021/nn204530r.

6. Rudra, J. S*.;* Mishra, S.; Chong, A. S.; Mitchell, R. A.; Nardin, E. H.; Nussenzweig, V.; Collier, J. H. Self-assembled peptide nanofibers raising durable antibody responses against a malaria epitope. *Biomaterials* **2012**, 33(27):6476-6484. doi: 10.1016/j.biomaterials.2012.05.041.

7. Huang, Z. H.; Shi, L.; Ma, J. W.; Sun, Z. Y.; Cai, H.; Chen, Y. X.; Zhao, Y. F.; Li, Y. M. A Totally Synthetic, Self-Assembling, Adjuvant-Free MUC1 Glycopeptide Vaccine for Cancer Therapy. *Journal of the American Chemical Society* **2012**, 134(21):8730-8733. doi: 10.1021/ja211725s.

8. Bowerman, C. J.; Nilsson, B. L. Self-assembly of amphipathic beta-sheet peptides: insights and applications. *Biopolymers* **2012**, 98(3):169-184. doi: 10.1002/bip.22058.

9. Collier, J. H.; Rudra, J. S.; Gasiorowski, J. Z.; Jung, J. P. Multi-component extracellular matrices based on peptide self-assembly. *Chemical Society reviews* **2010**, 39(9):3413-3424. doi: 10.1039/b914337h.

10. Maude, S.; Ingham, E.; Aggeli, A. Biomimetic self-assembling peptides as scaffolds for soft tissue engineering. *Nanomedicine-Uk* **2013**, 8(5):823-847. doi: 10.2217/nnm.13.65.

11. Luo, Z.; Zhang, S. Designer nanomaterials using chiral self-assembling peptide systems and their emerging benefit for society. *Chemical Society reviews* **2012**, 41(13):4736-4754. doi: 10.1039/c2cs15360b.

12. Luo, Z.; Zhao, X.; Zhang, S. Self-organization of a chiral D-EAK16 designer peptide into a 3D nanofiber scaffold. *Macromolecular bioscience* **2008**, 8(8):785-791. doi: 10.1002/mabi.200800003.

13. Luo, Z.; Zhao, X.; Zhang, S. Structural dynamic of a self-assembling peptide d-EAK16 made of only D-amino acids. *PloS one* 3(5):e2364. **2008**, doi: 10.1371/journal.pone.0002364.

14. Luo, Z.; Wang, S.; Zhang, S. Fabrication of self-assembling D-form peptide nanofiber scaffold d-EAK16 for rapid hemostasis. *Biomaterials* **2011**, 32(8):2013-2020. doi: 10.1016/j.biomaterials.2010.11.049.

15. Nagy, K. J.; Giano, M. C.; Jin, A.; Pochan, D. J.; Schneider, J. P. Enhanced mechanical rigidity of hydrogels formed from enantiomeric peptide assemblies. *Journal of the American Chemical Society* **2011**, 133(38):14975-14977. doi: 10.1021/ja206742m.

16. Swanekamp, R. J.; DiMaio, J. T.; Bowerman, C. J.; Nilsson, B. L. Coassembly of enantiomeric amphipathic peptides into amyloid-inspired rippled beta-sheet fibrils. *Journal of the American Chemical Society* **2012**, 134(12):5556-5559. doi: 10.1021/ja301642c.

17. Luo, Z. L.; Yue, Y.; Zhang, Y.; Yuan. X.; Gong, J.; Wang, L.; He. B.; Liu. Z.; Sun. Y.; Liu. J.; Hu. M.; Zheng, J. Designer D-form self-assembling peptide

nanofiber scaffolds for 3-dimensional cell cultures. *Biomaterials* **2013**, 34(21):4902-4913. doi: 10.1016/j.biomaterials.2013.03.081.

18. Zagon, J.; Dehne, L. I.; Bogl, K. W. D-Amino Acids in Organisms and Food. *Nutr Res* **1994**, 14(3):445-463.

19. Billard, J. M. D-Amino acids in brain neurotransmission and synaptic plasticity. *Amino acids* **2012**, 43(5):1851-1860. doi: 10.1007/s00726-012-1346-3.

20. Armstrong, D. W.; Gasper, M.; Lee, S. H.; Zukowski, J.; Ercal, N. D-amino acid levels in human physiological fluids. *Chirality* **1993**, 5(5):375-378.

21. Friedman, M.; Levin, C. E. Nutritional and medicinal aspects of D-amino acids. *Amino acids* **2012**, 42(5):1553-1582. doi: 10.1007/s00726-011-0915-1.

22. Friedman, M. Origin, microbiology, nutrition, and pharmacology of D-amino acids. *Chemistry & biodiversity* **2010**, 7(6):1491-1530.

23. Montero, A.*;* Gastaminza, P.; Law, M.; Cheng, G.; Chisari, F. V.; Ghadiri, M. R. Self-assembling peptide nanotubes with antiviral activity against hepatitis C virus. *Chemistry & biology* **2011**, 18(11):1453-1462. doi: 10.1016/j.chembiol.2011.08.017.

24. Sela, M.; Zisman, E. Different roles of D-amino acids in immune phenomena. *FASEB journal : official publication of the Federation of American Societies for Experimental Biology* **1997**, 11(6):449-456.

25. Benkirane, N.*;* Friede, M.; Guichard, G.; Briand, J. P.; Van Regenmortel, M. H.; Muller, S. Antigenicity and immunogenicity of modified synthetic peptides containing D-amino acid residues. Antibodies to a D-enantiomer do recognize the parent L-hexapeptide and reciprocally. *The Journal of biological chemistry* **1993**, 268(35):26279-26285.

26. Malyala, P.; Singh, M. Endotoxin limits in formulations for preclinical research. *J Pharm Sci-Us* **2008**, 97(6):2041-2044.

27. Jung, J. P.*;* Nagaraj, A. K.; Fox, E. K.; Rudra, J. S.; Devgun, J. M.; Collier, J. H. Co-assembling peptides as defined matrices for endothelial cells. *Biomaterials* **2009**, 30(12):2400-2410. doi: 10.1016/j.biomaterials.2009.01.033.

28. Fisher, G. H.*;* D'Aniello, A.; Vetere, A.; Padula, L.; Cusano, G. P.; Man, E. H. Free D-aspartate and D-alanine in normal and Alzheimer brain. *Brain research bulletin* **1991**, 26(6):983-985.

29. Baumjohann, D.; Preite, S.; Reboldi, A.; Ronchi, F.; Ansel, K.M.; Lanzavecchia, A.; Sallusto, F. Persistent antigen and germinal center B cells sustain T follicular helper cell responses and phenotype. *Immunity* **2013**, 38(3):596-605. doi: 10.1016/j.immuni.2012.11.020.

30. Chen, J. J.; Pompano, R. R.; Santiago, F.W.; Maillat, L.; Sciammas, R.; Sun, T.; Han, H.; Topham, D. J.; Chong, A.S.; Collier, J. H. The use of self-adjuvanting nanofiber vaccines to elicit high-affinity B cell responses to peptide antigens without inflammation. *Biomaterials* **2013**, 34(34):8776-8785. doi: 10.1016/j.biomaterials.2013.07.063.

31. Hailemichael, Y.; Dai, Z.; Jaffarzad, N.; Ye, Y.; Medina, M. A.; Huang, X. F.; Dorta-Estremera, S. M.; Greeley, N. R.; Nitti, G.; Peng, W.; Liu, C.; Lou, Y.; Wang, Z.; Ma, W.; Rabinovich, B.; Sowell, R. T.; Schluns, K. S.; Davis, R. E.; Hwu, P.; Overwijk, W. W. Persistent antigen at vaccination sites induces tumor-specific CD8+(+) T cell sequestration, dysfunction and deletion. *Nature Medicine* **2013**, 19(4):465-472. doi: 10.1038/nm.3105.

32. Halle, A.; Hornung, V.; Petzold, G. C.; Stewart, C. R.; Monks, B. G.; Reinheckel, T.; Fitzgerald, K. A.; Latz. E.; Moore. K.J.; Golenbock, D. T. The NALP3 inflammasome is involved in the innate immune response to amyloid-beta. *Nat Immunol* **2008**, 9(8):857-865. doi: 10.1038/ni.1636.

33. Eisenbarth, S. C.; Colegio, O.R.; O'Connor, W.; Sutterwala, F. S.; Flavell, R. A. Crucial role for the Nalp3 inflammasome in the immunostimulatory properties of aluminium adjuvants. *Nature* **2008**, 453(7198):1122-U1113. doi: 10.1038/nature06939.

34. Sun, T.; Han, D.; Riehemann, K.; Chi. L.; Fuchs, H. Stereospecific interaction between immune cells and chiral surfaces. *Journal of the American Chemical Society* **2007**, 129(6):1496-1497.

35. McKee, A. S.; Munks, M.W.; Marrack P. How do adjuvants work? Important considerations for new generation adjuvants. *Immunity* **2007**, 27(5):687-690.

Appendix

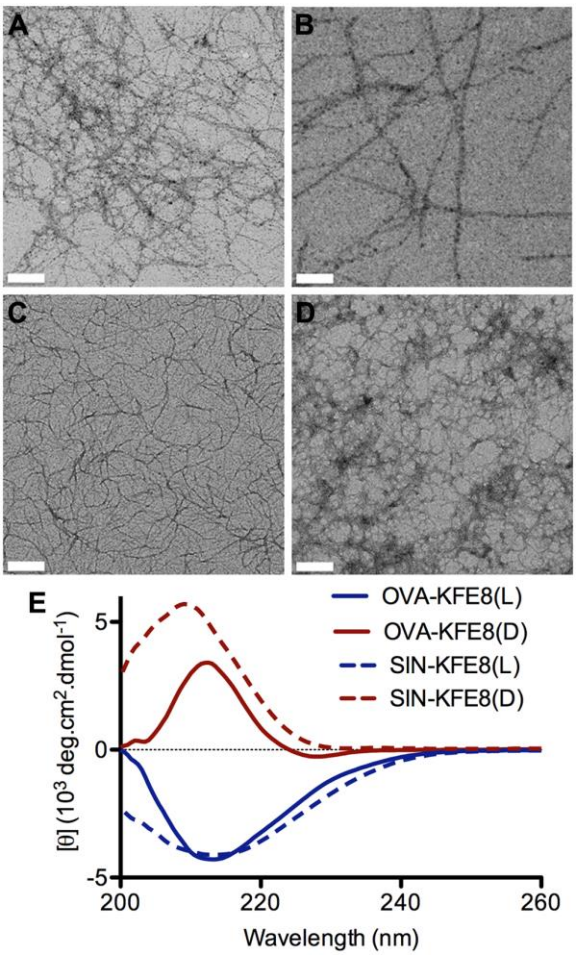

Figure 3.6. Nanofibers and secondary structures of KFE8(L) and KFE8(D) functionalized with OVA and SIN epitopes.

TEM images of (A) SIN-KFE8(L), (B) SIN-KFE8(D), (C) OVA-KFE8(L), and (D) OVA-KFE8(D). Circular dichrosim spectra of epitope-bearing enantiomers showing β-sheet rich secondary structures. Peptide concentration was 0.5 mM in ultrapure water.

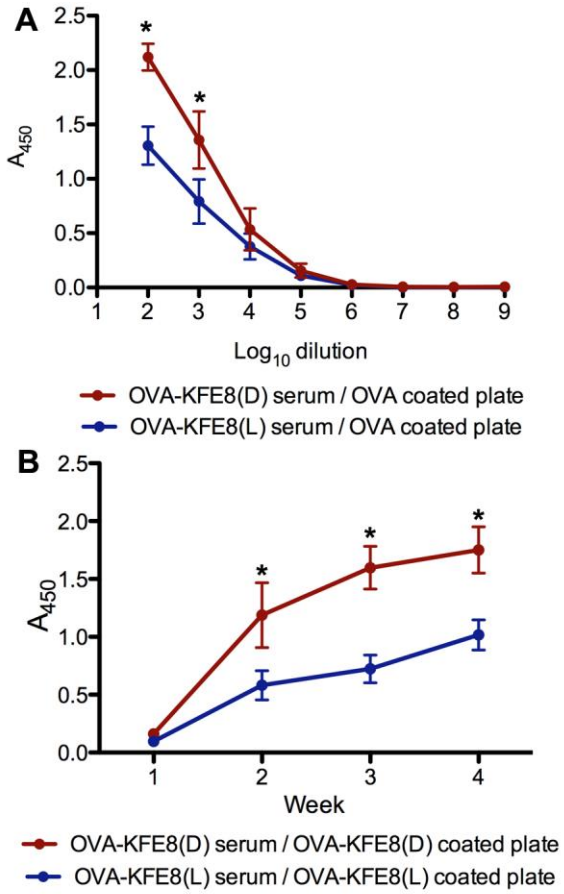

Figure 3.7. D amino acid nanofibers elicit stronger antibody responses compared to L amino acid nanofibers.

(A) Significantly higher levels of antibodies were detected in the sera of mice immunized with OVA-KFE8(D) nanofibers on plates coated with the free OVA peptide. (B) Higher levels of antibodies were detected in the sera of mice immunized with OVA-KFE8(D) nanofibers pre-boost. *$p<0.05$ by ANOVA using Tukey post-hoc test.

Table S1.

Peptide	Sequences	Calc. $[M+H]^+$	Obs. $[M+H]^+$
KFE8(L)	Ac-FKFEFKFE-Am	1161.57	1162.02
KFE8(D)	Ac-^{D}F^{D}K^{D}F^{D}E^{D}F^{D}K^{D}F^{D}E-Am	1161.57	1162.60
OVA	H_2N-ISQAVHAAHAEINEAGR-OH	1773.90	1774.77
SIN	H_2N-SIINFEKL-OH	963.12	964.13
SIN-KFE8(L)	H_2N-FKFEFKFEGGAAYSIINFEKL-Am	2483.27	2508.74
SIN-KFE8(D)	H_2N-^{D}F^{D}K^{D}F^{D}E^{D}F^{D}K^{D}F^{D}EGGAAYSIINFEKL-Am	2483.27	2512.23
OVA-KFE8(L)	H_2N-ISQAVHAAHAEINEAGRSGSGFKFEFKFE-Am	3164.46	3164.58
OVA-KFE8(D)	H_2N-ISQAVHAAHAEINEAGRSGSG^{D}F^{D}K^{D}F^{D}E^{D}F^{D}K^{D}F^{D}E-Am	3164.46	3165.02

Table 2. List of peptides investigated in this study.

The abbreviations, peptide sequences, theoretical mass, and observed mass are shown.

Chapter 4 : MULTIVALENT NANOFIBER SCAFFOLDS BEARING MYCOBACTERIUM *TUBERCULOSIS* EPITOPES

Introduction

Mortality from tuberculosis (TB) continues to rise and is now the leading cause of death worldwide from infectious disease, claiming nearly 1.5 million lives in 2015 [1]. Numerous studies have demonstrated the central role of CD8+ T-cells in the control and elimination of *Mycobacterium tuberculosis* (Mtb) infected host cells and that the Th1 dominant cytokine IFN-γ is critical for driving an appropriate host immune response and determining susceptibility to disease [2-4]. The limited CD8+ T-cell response in the currently approved vaccine BCG is believed to a major factor contributing to lack of sustained immunological memory and inconsistent protective efficacy [5]. Many new current vaccine strategies are therefore focused on driving Mtb antigen specific CD8+ T cell expansion and memory formation along with T cell phenotypes expressing Th1 cytokines.

Previously we have shown that peptide epitopes connected via short linker sequences to a self-assembling nanofibril domain can raise both humoral and cell-mediated immune responses against model antigens [6-8]. In an effort to move into a Tuberculosis (TB) disease model we selected peptide epitopes from Mtb proteins that were previously shown to be immunogenic in humans and that were predicted to bind H-2k MHC class I molecules so that they may be studies in small animal models. Mtb antigens TB10.4 (Rv0288) and Antigen 85 Complex B (AG85B) have been well studied and have also been shown to be immunogenic and contribute to protection in animal

models [9-13]. Of the 8 vaccines for Mtb that are currently undergoing Phase II/III trials, three are subunit protein vaccines containing one of both of these proteins. AG85B, the most abundant protein expressed by Mtb, has been shown to be efficacious as the primary effector molecule in DNA vaccines, fusion protein vaccines and liposomal multi-subunit vaccines. TB10.4 is 6 kDa secretory protein belonging to the early secretory antigenic target gene family known as ESAT-6. Systematic studies using human PBMCs from patients with active pulmonary TB or purified protein derivative+ (PPD+) individuals with previous disease or latent TB infection have identified peptide epitopes from TB10.4 that are MHC class I restricted and induce IFN-γ expression through ELIspot or flow cytometric tetramer staining [14, 15].

Rudra and colleagues previously co-assembled a Malarial TB3 epitope with a CD4+ T cell epitope from chicken ovalbumin (OVA) into a single nanofibril scaffold and were able to elicit dual antibody responses to each epitope [8] . Combining one or more epitopes each connected to a common self-assembling nanofibril domain produces multivalent nanofibers that are appear indistinguishable from their single epitope fibril counterparts. The utility of multivalent fibers not only broadens antigenic coverage for single pathogens but potentially across multiple pathogens as well. For pathogens such as MTB with approximately 4,000 gene products, it is vital to identify essential epitopes involved in a protective immune response and also stimulate the correct type of immune response.

Vaccine induced activation and maturation of dendritic cells (DC) through Toll-like receptors (TLR) has been shown to contribute significantly to the persistence and magnitude of the immune response [16, 17]. Innate immune activators and TLR ligands

are becoming increasingly favored in rational vaccine design due to the ability to activate cytotoxic CD8+ T cells [18] . Natural Mtb infection is recognized by the innate immune system through TLR2 and TLR9, and is a key step to controlling infection [19, 20]. In an effort to mimic the natural response of immune system during infection, we conjugated macrophage activating lipopeptide 2 (MALP-2), a synthetic analogue of a mycobacterial cell wall antigen important for activating TLR2, to our nanofiber self-assembling domain FKFEFKFE (KFE8). Direct conjugation of TLR ligands to peptides or proteins is necessary for downstream activation of antigen presenting cells with peptide or subunit based vaccines, although in our case it is co-presented on a single nanofiber formulation with immunodominant MTB epitopes.

Substantial levels of CD4+ T cells specific for AG85B have been isolated from the lungs post Mtb infection in animals [21]. We therefore selected an MHC class II epitope from AG85B that has previously been well characterized and shown to be immunogenic to CD4+ T cells [22, 23], and then synthesized this epitope with the self-assembling domain FKFEFKFE (KFE8). We also selected MTB MHC class I restricted epitopes from key virulence factors TB10.4 and ESAT-6, shown to be involved in the early pathogenesis of TB infection, and synthesized them to a common self-assembling domain KFE8. Nanofiber vaccines bearing CD8+ epitopes from TB10.4 and ESAT6 were individually immunogenic in mice and when co-assembled together as a single vaccine also initiated antigen specific T-cell expansion to each individual epitope. Multivalent nanofibers targeting CD8+ and CD4+ T cells significantly increased IFN-γ expressing cells and resulted in higher percentages of central memory cells. Inclusion of a TLR2 innate immune agonist likewise produced CD8+ T cells that were polyfunctional,

co-expressing IFN-γ, TNF-α and IL-2. The activation and maturation of dendritic cells is enhanced through interaction with TLR2 conjugated to peptide nanofibers. In a low dose aerosol challenge model, heterologous prime boost with BCG and then TB10.4/TLR2 multivalent nanofibers enhanced protection compared to BCG alone as measured by total bacterial load in the lungs.

Methods

ANIMALS

All animal experiments were conducted under approved protocols from the Institution Animal Care and Use Committee at the University of Texas Medical Branch. C57/Black-6 or BALB/c inbreed mice, 6-8 weeks of age were purchased from Jackson labs and housed using conventional methods under appropriate biosafety level containment areas.

PEPTIDES SYNTHESIS AND PURIFICATION

Solid phase peptide synthesis of peptides TB10.$4_{4\text{-}11}$ (IMYNYPAM-GGAAY-FKFEFKFE), ESAT-$6_{4\text{-}11}$ (QQWNFAGI-GGAAY-FKFEFKFE), and AG85$B_{240\text{-}254}$ (FQDAYNAAGGHNAVF-SGSG-FKFEFKFE) wasperformed on a CEM Blue (Matthews, NC) microwave synthesizer using standard Fmoc chemistry. Briefly, peptides were dissolved in DMF along with coupling reagents DIEA and HBTU and added to wang resin. The solution was heated to 90°C for 2 mins and then washed twice with DMF before removing the Fmoc N-terminal protecting group with 20% Piperidine in DMF. The resulting peptide was dried overnight under vacuum and cleaved in a solution

of 95% TFA containing 2.5% H20, and 2.5% tri-isopropyl silane for 1 hr at room temperature. The peptide was then precipitated in ice cold diethyl ether three times and allowed to dry. Peptide products were then separated by reverse phase HPLC over a 10-80% H20/CAN gradient on a C18 column. Mass and purity were then further characterized by MALDI-TOF mass spectrometry and analytical RP-HPLC. Fmoc-Cys((RS)-2,3-di(palmitoyloxy)-propyl)-OH was purchased from Bachem (Torrance, CA) TLR2 peptide conjugate (2,3di(palmitoyloxy-Cys-FKFEFKFE) was synthesized using the solid phase synthesis methods described above.

IMMUNIZATIONS

Peptides for immunization were first tested for endotoxin using the Lonza LAL QCL-1000™ endotoxin test kit according to the manufacturer's protocol. Any peptides with detectable levels of endotoxin were discarded. Formulations for immunization were prepared 24 hours prior in half the volume of sterile dH_20. Sterile PBS was then added to a final concentration of 2mM and the solutions incubated at RT for 2 hrs prior to inoculation. Injections were given in the left footpad or intranasally in a volume of 25µL.

FLOW CYTOMETRY AND ELISA

5 days after the last booster injection, the draining popliteal and inguinal lymph nodes were excised. For intranasally inoculated animals, the lungs and mediastinal lymph nodes were removed and enzymatically digested with 0.5mg/mL DNase I and 1.0mg/mL collagenase D for 30 mins at 37°C. The cells were then passed through a 70µM filter and

washed twice in sterile cRPMI. The cells were counted and plated onto 96 well plates coated with anti-CD28 at 1μg/mL in cRPMI (background) or cRPMI /w TB10.4$_{(4-11)}$ or AG85B$_{(240-254)}$ peptides at 5μg/mL. Golgiplug™ was added after 1 hour of incubation at 37°C and the cells were incubated an additional 6 hours.Cells were stained for extracellular and intracellular markers as described previously. Briefly, cells were washed twice in cold PBS and stained with a cocktail of anti-CD16/32, anti-CD3 (PerCP-Cy5.5 clone 145-2C11), anti-CD8+ (ef450, clone 53-6.7), anti-CD4+ (APC-ef780, clone 53-6.7) for 30 minutes at 4°C. ICS staining was carried out according BD Biosciences manufacturers recommendations. ICS staining cocktail with anti-TNF-α (FITC, clone MP6-XT22), anti-IL2 (APC, clone JES6-5H4), anti-IFN-γ (PE-Cy7 clone XMG1.2) was added for 30 mins at 4°C. Cells were flowed immediately on a BD Fortessa LSR-II custom cytometer. Flow cytometry analysis was performed on FlowJo™ software, TreeStar (Ashland, OR). Indirect ELISA to evaluate humoral response to peptide antigens was performed as described previously [24]. Briefly, plates were coated with 1μg/mL peptide overnight and washed 3x followed by 1 hour incubation with blocking buffer (eBioscience USA). Sera was collected through intracardiac puncture and diluted serially into PBS. Plates were washed 5x in between adding serum, primary detection antibody and HRP substrate. Antibody titers were positive if the absorbance at 450nm was greater than 3σ from the mean from the control (uncoated) wells.

DENDRITIC CELL ISOLATION AND CYTOKINE ELISA

100μL of 5μg/mL peptide nanofiber solutions of KFE8 and TLR2-KFE8 prepared in sterile PBS were added to 96 well and stored at 4°C overnight. Spleens from 6-8 week

old C57/B6 mice were freshly isolated and pushed through a 70μM filter to create single cell suspensions. RBC Lysis buffer was added and the cells were washed twice in PBS. CD11c+ cells were isolated by positive magnetic selection according to the STEMcell EasySep™ CD11c+ manufacturer's protocol. Cells were seeded at a density of 1E6 cells per well in cRPMI. Cells were then incubated at 37C for 48 hours. After 48 hours the cells were spun down and the supernatant was removed for cytokine ELISA. Supernatant was diluted 1:2 in PBS and cytokines were measured according to the Biorad 23-plex mouse assay manufacturers protocol and measured on a Bio-Plex 200 Multiplex System.

AEROSOL CHALLENGE AND BACTERIAL LOAD

Mice were aerosol challenged with 1.2 x 10^2 CFU of *Mycobacterium tuberculosis* H37Rv. The inoculum was prepared in middlebrook growth media at a concentration of 2.92 x10^5 CFU/mL immediately before challenge and kept at room temperature. Aliquots were taken before and after aerosolization along with samples from the nebulizer and biosampler to ensure accurate bacterial exposure to the animals. Animals were monitered daily for adverse events and weighed weekly. Four weeks post challenge we collected the lungs and liver for bacterial CFU limiting dilution enumeration. For CFU, whole tissue was weighed in PBS, ground and serial diluted before spotting 5μL onto middlebrook 7H11 agar plates supplemented with OADC. The plates were incubated for 4 weeks at 37C.

Results

We screened several immunodominant epitopes from known antigenic MTB secreted proteins. All of our selected sequences were collected from published epitopes found in humans or animal studies, or from MHC class I prediction software (IEDB Analysis Resources, recommended prediction algorithm) using sequences from known immunogenic proteins and clinical trials of subunit MTB vaccines in the pipeline. We ranked peptide candidate epitopes based on strength of evidence supporting their translational applicability. Our candidate peptide epitopes were from proteins CFP10, ESAT6, TB10.4, and AG85B. These sequences were synthesized along with the KFE8 self-assembling domain and inoculated into mice to assess their immunogenicity. We evaluated single epitope immune responses in mice by cytokine ELISA (data not shown) and determined $TB10.4_{(4-11)}$ and $ESAT6_{(4-11)}$ to be our lead candidate epitopes.

MULTIVALENT NANOFIBERS ARE CAPABLE OF ELICITING A DUAL ANTIGEN SPECIFIC CD8+ T CELL RESPONSE

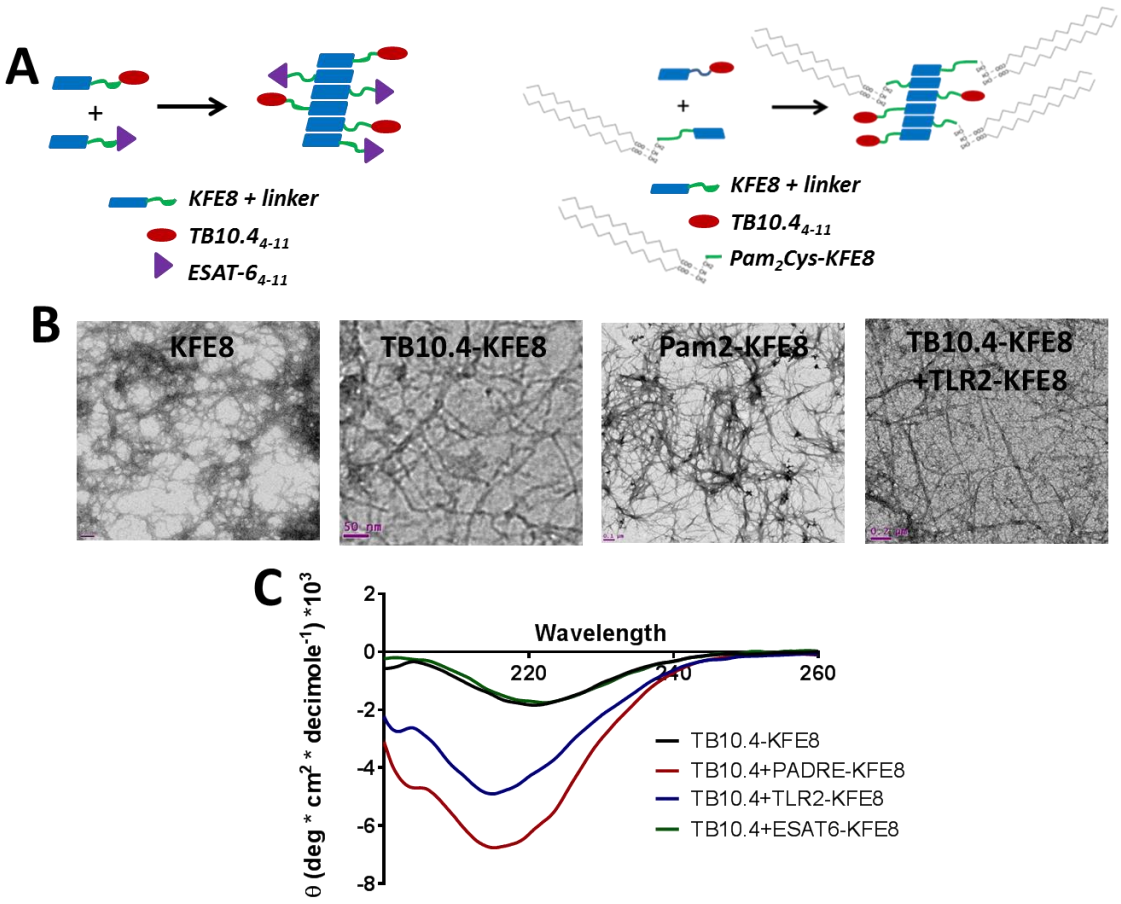

Figure 4.1 Co-assembly of multivalent self-assembling peptide nanofibers resemble single nanofibril formations.

Schematic depicting the mixing of TB epitope peptide monomers sharing a common self-assembling domain and formation of multivalent fibers (A). TEM images of peptide nanofiber solutions at 0.3mM in PBS. Additional sequences from TB10.4 at the C-terminus, Pam2-Cysteiene (TLR2) at the N-terminus, nor mixing of TB10.4/Pam2-Cys (TLR2) fibers resulted in altered molecular self-assembly (B). CD spectra indicates a predominantly beta-sheet rich structure from all four nanofiber solutions (C).

Multivalent nanofibers are formed by mixing equimolar lyophilized dry peptides and results in heterogeneous mixtures of single fibrils decorated with dual epitopes (Figure 4.1A). Representative TEM images of the KFE8 self-assembling domain and KFE8 with the TB10.4 antigen show that the addition of the peptide antigen still results in nanofiber self-assembly (Figure 4.1B). Circular dichroism spectroscopy (CD) data

confirms that the beta-sheet composition of fibrils is unchanged from the individual nanofibers to the multivalent nanofiber solutions (Figure 4.1C). Administration of nanofibers bearing either TB10.4(4-11) or ESAT-6(4-11) into mice produced resulted in antigen specific CD8+ T cell expansion as measured by ex vivo stimulation with the corresponding peptide antigen, although the TB10.4 mice IFN-γ+ CD8+CD3+ cells showed a fold increase as compared to the ESAT-6 mice (Figure 4.2B & 4.2C). Co-assembly of the two epitopes resulted in a marginal drop in the amount of IFN-γ+ cells responding to the TB10.4 antigen, while the percentage of IL-2+ cells was also diminished in the co-assembled group compared to the single TB10.4 epitope group (Figure 4.2D).

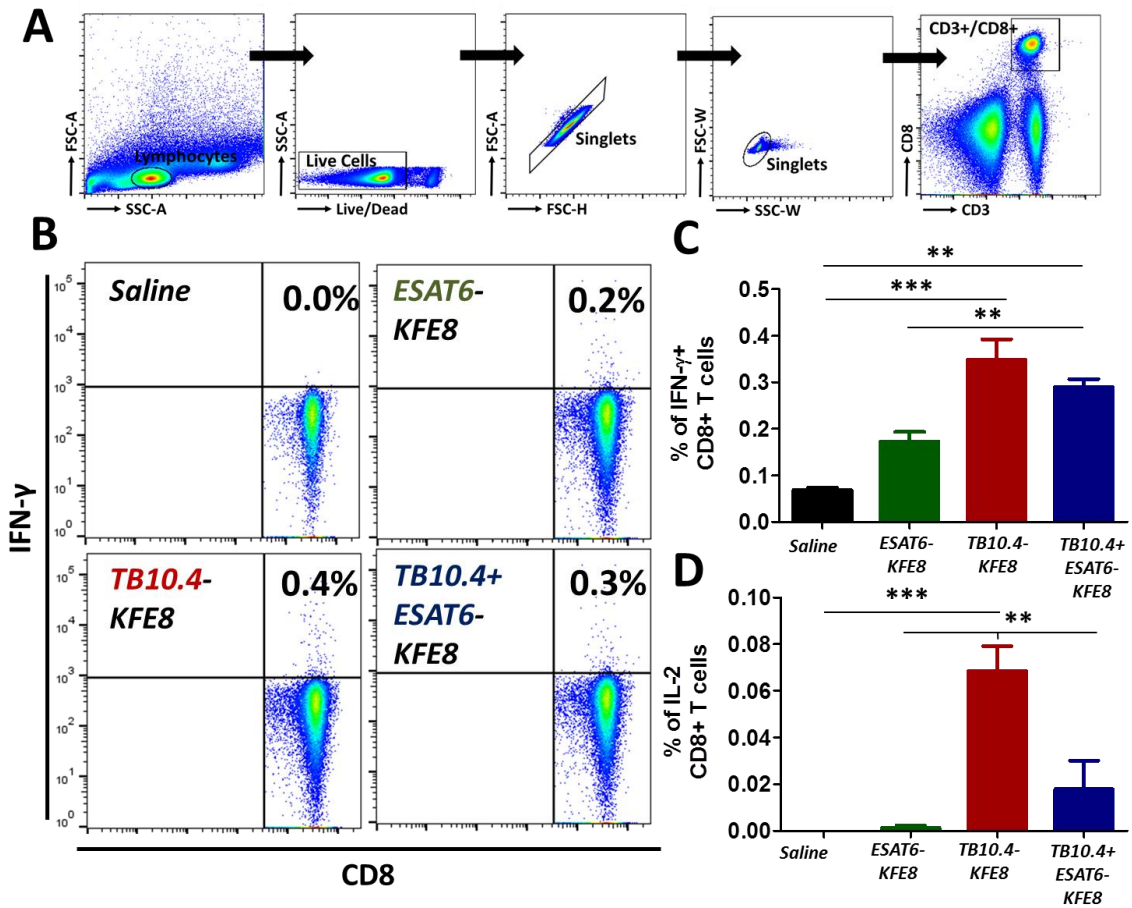

Figure 4.2 KFE8 nanofibers bearing dual MTB CD8+ elicit antigen specific immune responses

Typical gating strategy used for CD8+ T cells (A) Animal (n=4-5 per group) were inoculated in the footpad with two doses separated by 30 days. Popliteal and inguinal lymph nodes were removed and processed into single cells suspensions. Lymphocyte solutions were plates onto 96 well plates in duplicate and incubated with either TB10.4, ESAT-6 or both peptides for 6 hours. ICS was measured by flow cytometry. Representative flow plots for IFN-γ/CD8+ shown in (B). Mean percentage of cytokine positive cells ±SD from total CD8+CD3+ cells, for IFN-γ (C) and IL-2 (D). Statistical analysis by one-way ANOVA with multiple comparisons of means between all groups. ***=$p<0.001$, **$p<0.01$.

CD4+ T- CELL EPITOPES AND TLR2 AGONISTS INCREASE POLYFUNCTIONALITY

Multivalent nanofibers can be co-assembled with two or more peptide epitopes or immunomodulatory moieties. Although the supramolecular self-assembly has inherent activity as a self-adjuvant, inclusion of innate immune agonists has been show to enhance effector and memory CD8+ T cell responses specifically with peptide based vaccines. We therefore directly conjugated a TLR2 analogue linked through a Cysteine residue to the N-terminal residue of the self-assembling domain KFE8. We likewise synthesized the synthetic pan HLA-DR epitope PADRE CD4+ helper T cell sequence to the common self-assembling domain KFE8. Administration into mice elicited antigen specific responses although here the cytokine profile expression was altered such that single positive cells expressing TNF-α were significantly increased and the total overall numbers of IFN-γ expressing cells were increased with both the co-assembled PADRE nanofibers and the TLR2 agonist fibers (Figure 4.3A-C). Among the cytokine positive cells we saw a substantial number that were polyfunctional (cells that express IFN-γ along with TNF-α and or IL-2) from groups immunized with the PADRE epitope or TLR2 agonist (Figure 4.3D). TNF-α is an important cytokine for macrophage activation while IL-2 has a key role in driving a sustained T-cell response. The magnitude of the

polyfunctional T-cell response is hypothesized to be central in mediating protection against MTB and therefore an important factor for future TB vaccines.

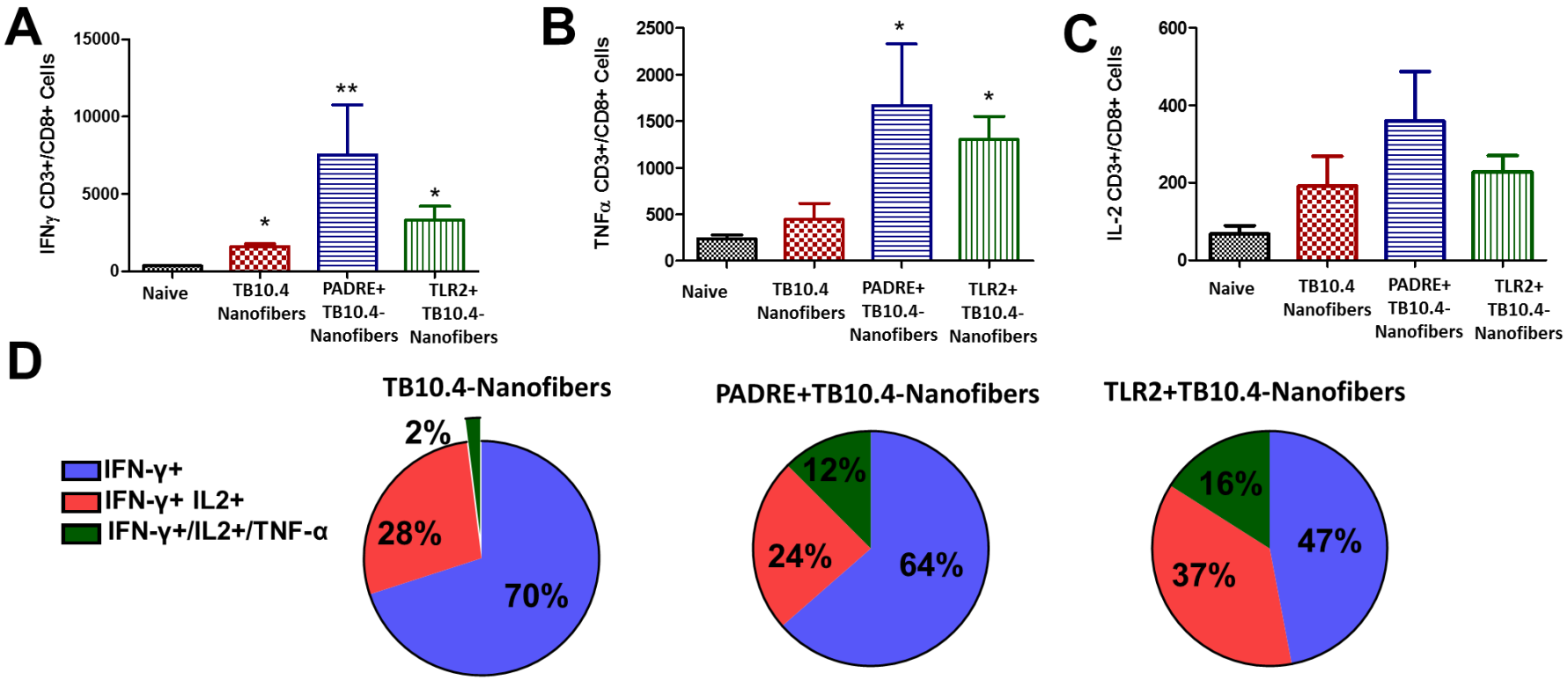
A
IFNγ CD3+/CD8+ Cells
15000
10000
5000
0
*
**
*
Naive
TB10.4 Nanofibers
PADRE+ TB10.4- Nanofibers
TLR2+ TB10.4- Nanofibers
B
TNFα CD3+/CD8+ Cells
2500
2000
1500
1000
500
0
*
*
Naive
TB10.4 Nanofibers
PADRE+ TB10.4- Nanofibers
TLR2+ TB10.4- Nanofibers
C
IL-2 CD3+/CD8+ Cells
600
400
200
0
Naive
TB10.4 Nanofibers
PADRE+ TB10.4- Nanofibers
TLR2+ TB10.4- Nanofibers
D
IFN-γ+
IFN-γ+ IL2+
IFN-γ+/IL2+/TNF-α
TB10.4-Nanofibers
2%
28%
70%
PADRE+TB10.4-Nanofibers
12%
24%
64%
TLR2+TB10.4-Nanofibers
16%
37%
47%

Figure 4.3 CD4+ T- cell epitopes and innate immune agonist co-assembled fibers increase polyfunctionality

The CD4+ epitope PADRE and TLR2 were conjugated separately to the N-terminus of the KFE8 self-assembling domain and co-assembled into single nanofiber formulations with the TB10.4 epitope. Mice (n=4-5 per group) were inoculated into the footpad with two doses separated by 30 days. 5 days later the draining inguinal and popliteal lymph nodes were excised and plated onto 96 well plates for ex vivo cytokine stimulation with the TB10.4 peptide. Cells were gated on lymphocytes-→ Live cells→ Singlelets (FSH v FSA; SSH v SSA; SSW v. FSW) → CD3+CD8+ cells. Total numbers of single positive cells for IFN-γ, TNF-α, or IL-2 (A, B, C). Inclusion of either the PADRE CD4+ epitope or the TLR2 agonist resulted in a 6 and 8 fold increase in the number of triple cytokine positive cells (D). *$p<0.05$, **$p<0.01$ by ANOVA with Tukey's post-hoc test for multiple group comparison.

MTB SPECIFIC CD4+ T- CELL CO-ASSEMBLED FIBERS STIMULATE ROBUST RECALL RESPONSES

CD4+ T cells are critical for controlled Mtb infection through Th1 cytokine expression and downstream macrophage activation. Patients with controlled Mtb infection or those with previous infections have both CD4+ and CD8+ T cells responsive to the Mtb secretory protein AG85B. We hypothesized our vaccine design may be improved with the inclusion of a predicted MHC class II epitope from the highly immunogenic protein AG85B connected via a short linker sequence to the self-assembling domain KFE8. AG85B co-assembled nanofiber hydrogels with the TB10.4 $_{(4-11)}$ antigen (TB-85B), the ESAT-6$_{(4-11)}$ antigen (E6-85B), or both CD8+ epitopes without AG85B (TB-E6) were administered to mice. We found that total IFN-γ expressing cells stimulated with the TB10.4 epitope were similar to the PADRE co-assembled fibers but that the single positive cells for TNF-α increased 25 fold (Figure 4.4C). Unexpectedly, when we stimulated lymphocytes with the AG85B epitope, both the TB-85B and E6-85B groups responded with significant expression of IFN-γ and IL-2 from CD8+ T cells

(Figure 4A & D). As a control to ensure that ex vivo peptide stimulation was antigen specific and a result of vaccination we also stimulated with alternative peptides than those included in the peptide vaccination. Lymphocytes isolated from mice vaccinated with TB-85B expressed high levels IFN-γ in response to stimulation with TB10.4, but not from the ESAT-6 peptide to which we used as a control (Figure 4.4B).

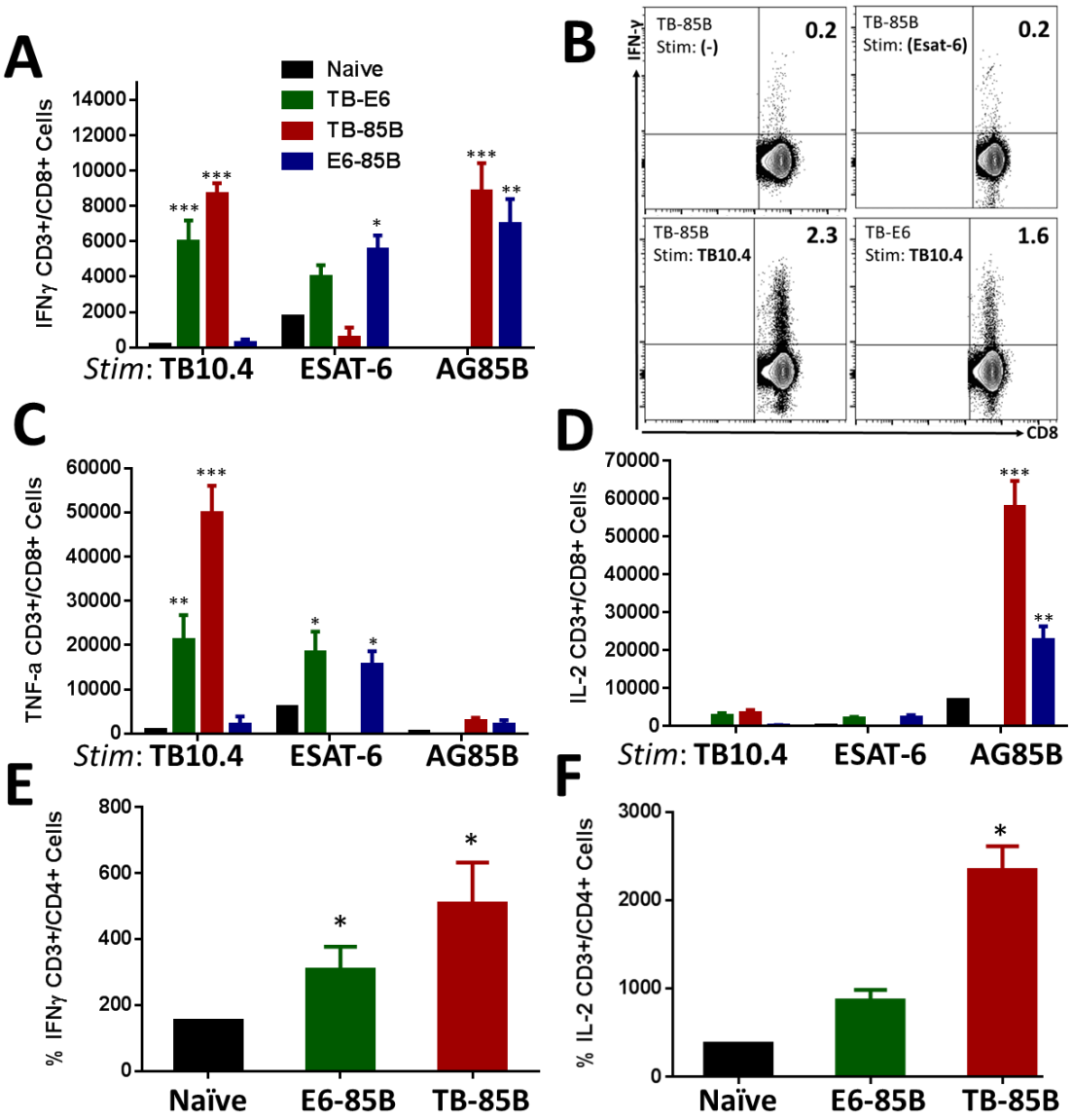

Figure 4.4 Mtb-specific CD4+ T- cell co-assembled fibers stimulate robust recall responses

M*tb* Antigen 85 complex B peptide was synthesized via the N-terminal of the KFE8 self-assembling domain. Mixtures of TB10.4 (TB) and ESAT-6 (E6) CD8+ epitopes previously shown to be immunogenic were co-assembled with AG85B (85B). Mice (n=5 per group) were inoculated into the footpad with two doses separated by 30 days. 5 days later the popliteal and inguinal nodes were removed and processed for ICS after stimulation with either the TB10.4, ESAT6 or AG85B peptides (X-axis; A, C, D). Panels A, C, and D are mean ± SD total cytokine positive cells for cytokines IFN-γ, TNF-α, and IL-2. Representative IFN-γ/CD8+ flow plots from lymph nodes gated on lymphocytes → Live cells → Singlets → CD3+CD8+ showing the effect of negative, Esat-6 or TB10.4 peptide stimulation from groups inoculated with TB10.4 co-assembled fibers (B). Total

mean CD4+ cytokine positive cells for IFN-γ & IL-2 expression were measured by ICS (E & F). ***=p<0.001, **=p<0.01 and *=p<0.05 by one or two way ANOVA with multiple comparison post-hoc tests for means across all groups.

AG85B POTENTIATES CENTRAL MEMORY CELL PROPAGATION AND ANTIBODY PRODUCTION

The development of central memory along with effector CD8+ T cells may be useful for assessing the degree to which a vaccine confers protection. Memory progenitor cells defined as CD62L+CD4+4+CD127^{high}KLRG1^{low}CD4+3^{low} [25] were found to be highest among those mice who received AG85B co-assembled nanofiber vaccines (Figure 4.5A). Interestingly, the percentages of effector CD8+ subsets CD62L-CD4+4+IL7R^{low}KLRG1^{high}CD4+3^{high} were comparable between single antigen nanofibers and the AG85B and TLR2 co-assembled vaccines (Figure 4.5B). Previously we have shown that humoral and cell-mediated responses were achievable with co-assembled nanofibers bearing CD8+ and CD4+ epitopes to malarial antigens and model antigens from chicken ovalbumin [8]. We evaluated all of the peptide epitopes used in this study for dual humoral responses and we found strong anti-AG85B titers circulating only in those mice vaccinated with co-assembled nanofibers containing this peptide epitope. Although we do not know what role anti-AG85B antibodies contribute to protection they may attenuate the infection severity or contribute to promotion of latent infection.

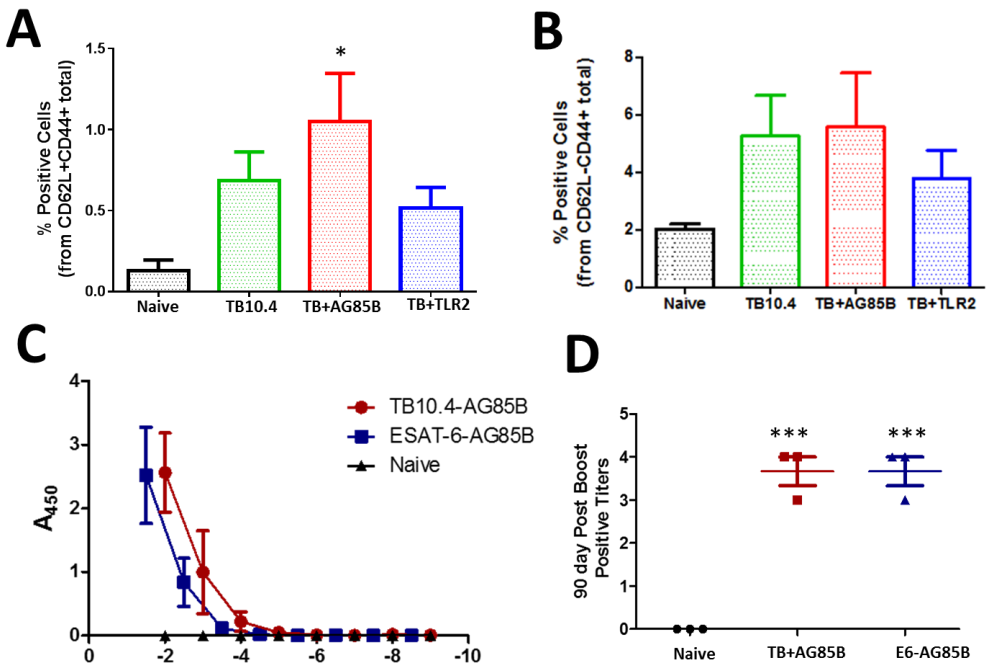

Figure 4.5 AG85B potentiates central memory cell propagation and antibody production

C57/B6 mice (N=3-5) were inoculated in the footpad with two doses of nanofiber vaccine separated by 30 days. Total mean percentages ±SD of all central memory phenotype CD62L+CD4+4+IL7R^{high}KLRG1^{low}CD4+3^{low} cells from CD3+CD8+CD62L+CD4+4+ population (A). Effector cell phenotype IL7R^{low}KLRG1^{high}CD4+3^{high} percentages from CD62L-CD4+4+ gate (B). Sera collected at time of sacrifice from intracardiac puncture was measured by ELISA against the AG85B peptide antigen. A450 is the raw absorbance values measured from our ELISA (C) with positive titers were determined from A450 values differentiated by 3xSD from control wells (D). ***=p<0.001, **p<0.01 by two-way ANOVA with post-hoc analysis for comparison between the means of route and treatment.

TLR2 AGONIST INCREASES THE FREQUENCY OF TB10.4 SPECIFIC CD8+ T-CELLS IN THE LUNGS

MTB is a pathogen that enters the respiratory mucosa via inhalation of infectious droplets. Mucosally delivered vaccines may confer a protective advantage against mucosal pathogens due to the somewhat compartmentalized nature of the mucosal immune system [26, 27]. Intranasal administration therefore may be an ideal route of

deliver for the next generation of TB vaccines [28]. To evaluate the importance of the route of administration we primed mice in either the footpad or intranasal followed by an intranasal boost on day 30. Lungs and mediastinal lymph nodes were excised and stimulated for cytokine expression. We found that not only did intranasal prime and boosting increase the proliferation and trafficking of TB10.4 CD8+ T cells present in the respiratory mucosa but that the addition of the TLR2 agonist was most effective for CD8+ T cell expansions when delivered in two doses intranasally (Figure 4.6A & B).

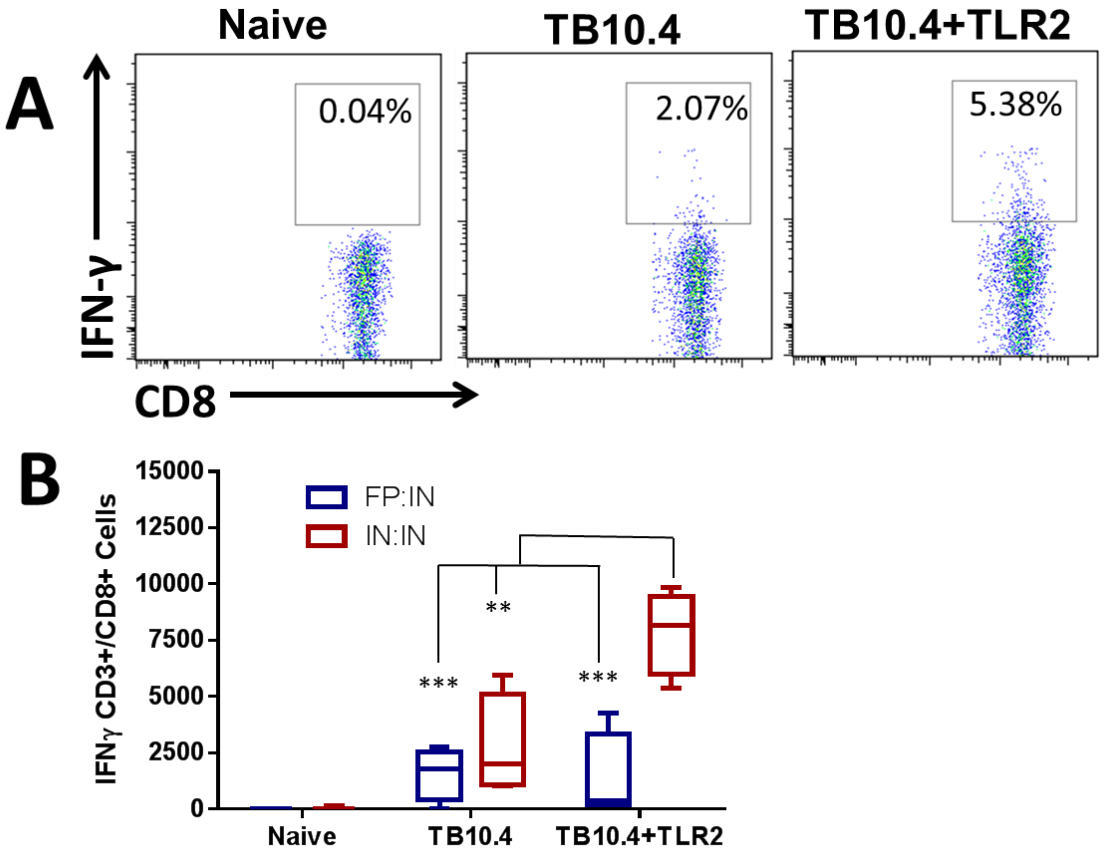

Figure 4.6 TLR2 agonist directs TB10.4 responsive cells to the lungs

(A) Representative flow plots showing IFN-γ expression from CD8+ T cells found in the lungs after intranasal vaccination. Lungs were excised and enzymatic digested in DNase I

and Collagenase D for 30 mins at 37C. Cell suspensions were seeded onto 96-well plates at 1E6 cells per well and stimulated with TB10.4 peptide for 6 hours. Histogram shows the difference in either footpad (FP) prime and intranasal (IN) boost compared to IN:IN prime and boost with respect to CD3+CD8+ IFNγ+ cells found in the lungs.

TLR2 NANOFIBERS INDUCE DC ACTIVATION AND MATURATION IN VITRO

The inclusion of innate immune agonist as adjuvants can improve antigen presentation and T lymphocyte priming leading to an enhanced immunogenicity. Rational vaccine design utilizing TLR4 analogue agonists such as MPLA are already approved for use in vaccines for HPV. The adjuvanticity of innate immune agonists with peptides alone is dependent on direct conjugation to the peptide antigen [29]. This is perhaps due to the co-delivery of the antigen and innate immune agonist simultaneously. We are currently exploring structural dependencies of TLR agonists on nanofiber scaffolds and how that correlates to improve immune responses. TLR agonists in vaccines are thought to promote the development of adaptive immunity through activation of DCs. To investigate whether nanofibers bearing a TLR2 agonist are able to interact with and stimulate DCs in a similar manner, we isolated CD11c+ cells from the spleen and found that TLR2 attached to the N-terminus of the KFE8 self-assembling nanofiber domain was able to activate cytokine expression and upregulation of co-stimulatory molecules on CD11c+ DCs. CD8+0, CD8+6 and MHC class II were all strongly upregulated after exposure to TLR2 nanofibers but not with LPS (Figure 4.6A). Interestingly, bare nanofibers had no effect on the upregulation of co-stimulatory molecules and MHC-ii, nor did it stimulate cytokine expression. We found similar but not identical cytokine profiles between LPS and TLR2 treatment groups (Figure 4.6B). Upregulation of IL-6, RANTES, MIP-1β, IL-1α and IL-1β was detected in the LPS treatment groups. Cytokines

expressed in both LPS and TLR2 treatments were generally lower in the TLR2 nanofiber groups, particularly with pro-inflammatory cytokines such as IL-1α, IL-1β, RANTES and MIP-1β. IL-12 which is important for macrophage activation and particularly favorable for a MTB vaccine or immunotherapy was upregulated in both LPS and TLR2 groups.

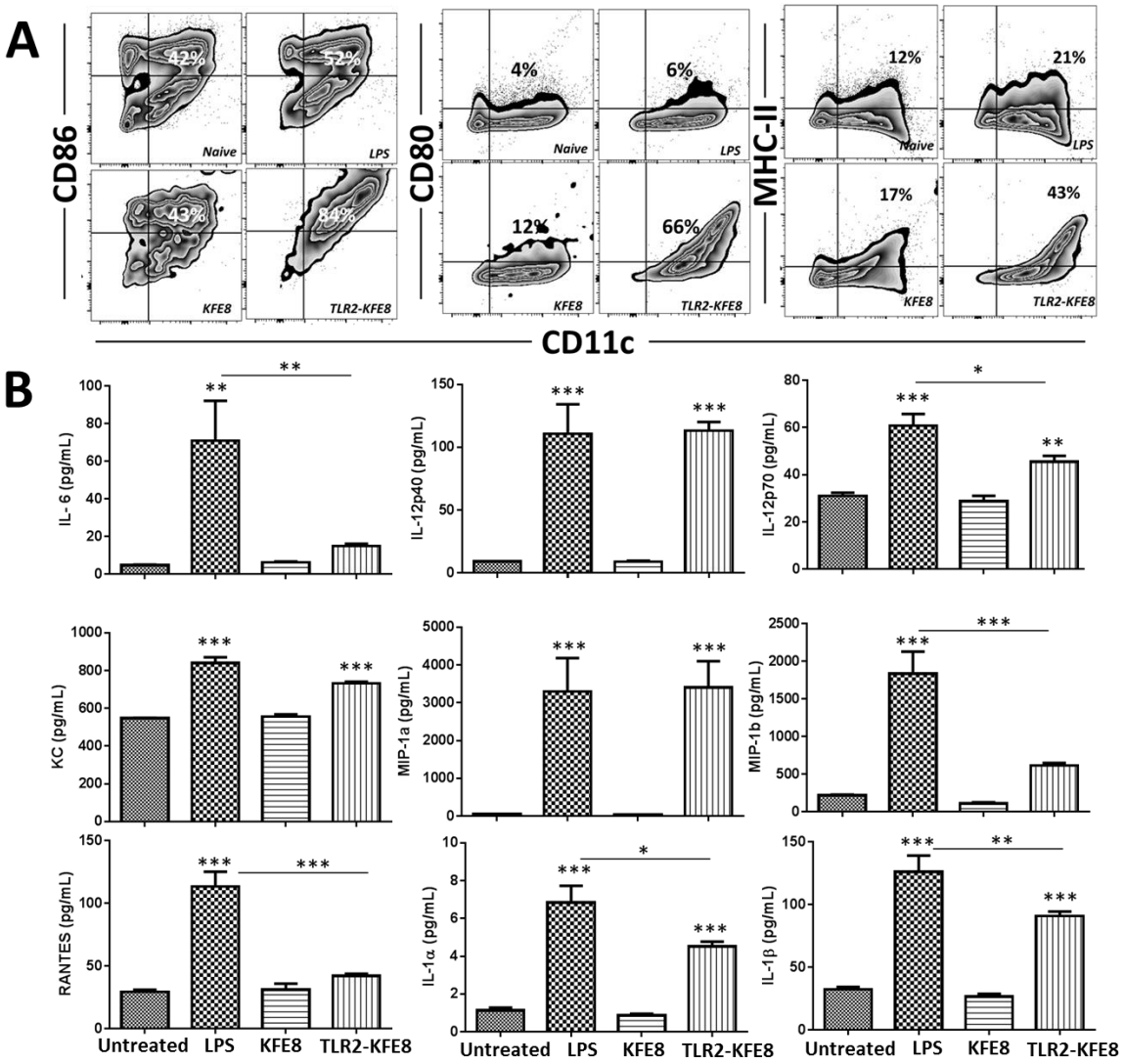

Figure 4.7 TLR2-KFE8 Nanofibers stimulate co-stimulatory molecule and cytokine expression on primary CD11c+ spleenocytes in vitro

Spleens from N=3 naïve C57/B6 were enzymatically digested and processed into single cell suspensions. After RBS lysis we isolated CD11c+ cells by magnetic positive selection and seeded at a density of 5E5 cells/well in duplicate onto 96 well plates. KFE8 and TLR2-KFE8 (TLR2) treatments were made the 24 hours prior and coated on wells in 100μL. LPS was added to cRPMI from frozen aliquots at 1μg/mL per well. Cells were incubated for 24 hours and then cells were stained for surface expression of co-stimulatory markers (A) while the supernatant was removed for cytokine bioplex (B).

.

PEPTIDE NANOFIBER VACCINES DECREASE BACTERIAL LOAD IN THE LUNGS

Strategies to improve the currently licensed vaccine BCG are urgently need. Therefore, we administered the nanofiber vaccines bearing peptide epitopes from TB10.4 and AG85B (TB-85B), or with TB10.4 and the TLR2 agonist (TB-TLR2) as a booster dose to BCG. Our hypothesis was that the enhanced secondary T cell response will function additively or even synergistically with BCG to provide enhanced control and elimination of MTB. To assess whether peptide nanofiber vaccines alone provide any level of protection we also vaccinated mice with two doses of peptide nanofibers. We challenged mice through low-dose infectious aerosol inhalation which is characteristic of naturally acquired infection and then enumerated the bacterial load in the total lungs and liver. BCG prime followed by boosting with peptide vaccines resulted in a full log decrease in bacterial loads in the lungs and represents improved protection and control of infection compared to BCG alone.

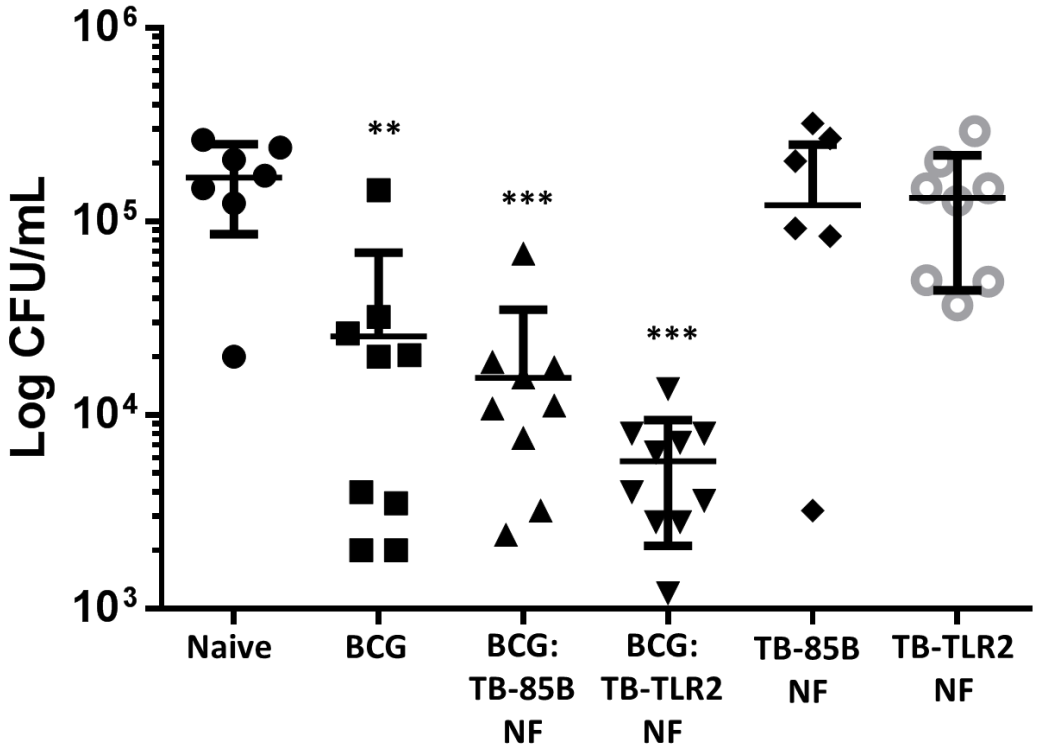

Figure 4.8 Peptide nanofiber vaccines enhance protection from Mtb aerosol challenge after BCG prime

Balb/C mice (N=8-10 per group) were aerosol challenged with 50 CFU H37Rv Mtb. Peptide nanofiber vaccinated groups were given two doses intranasally separated by 30 days, while BCG was administered i.p. with one dose (1E6 CFU). Mice vaccinated with peptide nanofibers as a booster dose in conjunction with BCG but not as a stand-alone vaccine significantly decreased bacterial loads in the lungs

Discussion

Nanofibrous materials are a basic platform that can serve as biomimetic scaffolds for tissue engineering [30, 31], regeneration [32, 33], or in our case antigen delivery and immune activation. Peptide self-assemblies used for inducing prophylactic immunity have been shown to elicit both humoral and cellular immune responses to model antigens from chicken ovalbumin, as well as humoral response to tumor associated antigens and in infectious disease such as malaria. Few vaccines are known or believed to elicit CD8+

cell mediated immunity and none are licensed on the basis of CD8+ T-cell activation. Vaccine design that activates CD8+ cell mediated immunity alone or in conjunction with a humoral component are essential for the development of a vaccine targeting intracellular pathogens as well as novel cancer immunotherapies.

Multifunctional or multivalent nanofibers are a novel platform for vaccine design due in large part to their modular nature and ease of synthesis. Multiple peptide antigens specific to a common pathogen, multiple pathogens, or combinations of the same peptide antigen that accommodates broad diversity across MHC class I haplotypes can be synthesized to a common self-assembling domain to form nanofiber scaffolds bearing combinations of biologically active ligands. Peptide epitopes are unfortunately risky for vaccination given that they only initiate a very specific immune response to one epitope compared to whole protein subunit vaccines which may carry numerous immunodominant epitopes and initiate multiple antigen specific T and B cells. Epitope selection is therefore the most critical step for peptide based vaccines and can be challenging for a pathogen such as Mtb which has nearly 4,000 gene products. Multiple studies using peptide libraries encompassing multiple immunogenic Mtb proteins, previous vaccine studies reporting on positive and negative protection data using subunit vaccines or peptide epitopes and the wide variety of bioinformatics and computational approaches to epitope prediction such as IED MHC prediction, SYFPEITH and EpiMer all contribute important epitope selection criteria for peptide based vaccine design.

CD4+ and CD8+ T cells are considered to be critical mediators of protection against Mtb and a number of previous preclinical and clinical studies have correlated TB10.4, ESAT-6 and AG85B antigen specific T-cells with protection to Mtb [9, 11, 12]. In this study we took a bottom-up approach to vaccine design that utilizes linear epitopes designed for presentation in MHC-I molecules to stimulate both CD8+ and CD4+ T cell activation and expansion. This materials based strategy offers several key advantages including ease of synthesis, low cost, and absence of microbial

contaminants. Using model antigens we have compared nanofiber vaccines to multiple peptide/adjuvant combinations and found that nanofiber vaccines with no extraneous adjuvants resulted in higher numbers of antigen specific CD8+ T cells in the absence of robust inflammatory conditions. The biocompatibility of peptides may contribute to the low levels of inflammation while the formation of supramolecular structures may provide the stimulus for an immune response.

Innate immune agonists are increasingly being used to prime the immune system when co-administered with a vaccine to increase the immunogenicity and efficacy of the vaccine. Monophosphorylipid A (MPLA) is currently the only TLR agonist included with licensed vaccines although several innate immune agonists are in various phases of clinical testing specifically in vaccines for Mtb [34]. TLR2 agonists such as MALP have been shown to increase antigen uptake and activation with dendritic cells as well as cross-presentation of peptides into MHC-I molecules [35, 36]. Cross presentation of exogenous antigen is required for subunit vaccines to stimulate a CD8+ T cell response. By co-assembling a TLR2 agonist with peptide epitopes into a single nanofiber scaffold, the TLR agonist and peptide are taken up together which is necessary for more efficient antigen cross presentation into MHC-I molecules. Coler and colleagues demonstrated that dual TLR4 and TLR9 agonists perform synergistically with ID93, a fusion vaccine of four Mtb proteins, to lower CFU loads in the lungs of mice [37]. CpG and Poly-IC are also effective TLR agonists currently used in several prospective Mtb subunit vaccines and are attractive co-stimulatory molecules for nanofiber vaccines due to their ability to electrostatically interact with positively charged amino acid side chains obviating the need to covalently bind the agonist to the peptide.

The route of immunization is particularly important when dealing with mucosal pathogens in which immune protection at the site of invasion often correlates with control and clearance or persistence and disease. Mucosal administered vaccines generally induce better mucosal immune responses leading to more efficient protection

[27, 38, 39]. In the respiratory mucosa, the propagation of T cell mediated immunity has been shown to be significantly more potent when vaccines are administered nasally or through aerosol against a multitude of bacteria including Mtb as well as viruses [26, 40-42]. Our findings with intranasal administration of peptide nanofiber vaccines also suggests that intranasally delivered vaccines may direct antigen specific T cell populations to the respiratory mucosa. Accumulation of T cells in the airway lumen is mediated in part by chemokines including MIP-1α, which was significantly expressed by DCs in vitro after stimulation with TLR2 bearing nanofibers.

Prolonged inflammation at the site of vaccination is generally inhibitory to establishing a protective immune response. Adjuvant induced inflammation can lead to the sequestration and dysfunction of antigen specific cells at the site of vaccination. TLR2 nanofibers stimulated DCs to express certain pro-inflammatory cytokines such as IL-1α and IL-1β, although at significantly lower levels than LPS treated DCs. IL-6, another pro-inflammatory pleotropic cytokine was not expressed in TLR2 treated cells and together may illustrate a more controlled inflammatory state representative of normal DC activation.

Repeated boosting with BCG is ineffective for prolonging and enhancing acquired immunity from BCG. Heterologous prime boost strategies with recombinant adenoviruses [43, 44], cationic liposomes [9], fusion proteins [45] , as well as peptides [46] have been shown to be an effective strategy for reinvigorating protective immunity to MTB after BCG prime. Peptide vaccines although shown to be effective for in vitro studies against MTB, may be most effective in vivo against a complex pathogen like MTB when used in conjunction with broadly antigenic vaccines such as BCG. Subunit vaccines are also suitable for immunocompromised individuals such as those with HIV and can prevent further reactivation of those with latent MTB infection.

Preclinical animal mouse models can be improved to better model the pattern of disease seen in humans [47]. Prophylactic vaccine studies in small animal models can not

completely prevent infection but can lower bacterial loads to subclinical levels compared to unvaccinated animals. Future studies will seek to evaluate a more human-like model of MTB infection and whether alternative peptides and TLR agonists are equally or more effective for controlling infection in conjunction with BCG.

Conclusion

In summary we have demonstrated that self-assembling peptides can serve as a multivalent and multifunctional vaccine platform. Nanofiber assemblies can elicit strong CD8+ T cell responses to two co-delivered peptide epitopes and the inclusion of CD4+ T cell help can augment the CD8+ T cell response. Additionally, TLR2 agonists co-assembled with CD8+ epitopes may be an effective strategy for inducing strong mucosal immunity and directing responding lymphocytes to the lungs. This strategy resulted in significantly lower bacterial loads in the lungs after BCG prime and low dose aerosol challenge with Mtb indicating that peptide vaccination can be an effective strategy even against complex pathogens such as Mtb. This work further supports the critical role of CD8+ T cell mediated protection and the necessity of front line defense at the site of pathogen entry. Future studies will also look into alternative materials designed for the delivery of peptide based vaccines to respiratory mucosa and to induce T cell responses in the lungs.

References

1. World Health Organization, *Global Tuberculosis Report*. 2015.

2. Al-Attiyah, R., et al., *Cytokine profiles in tuberculosis patients and healthy subjects in response to complex and single antigens of Mycobacterium tuberculosis.* FEMS Immunol Med Microbiol, 2006. **47**(2): p. 254-61.

3. Cooper, A.M., et al., *Disseminated tuberculosis in interferon gamma gene-disrupted mice.* J Exp Med, 1993. **178**(6): p. 2243-7.

4. Green, A.M., R. Difazio, and J.L. Flynn, *IFN-γ from CD4+ T cells is essential for host survival and enhances CD8+ T cell function during Mycobacterium tuberculosis infection.* J Immunol, 2013. **190**(1): p. 270-7.

5. Niu, H., et al., *Multi-Stage Tuberculosis Subunit Vaccine Candidate LT69 Provides High Protection against Mycobacterium tuberculosis Infection in Mice.* PLoS One, 2015. **10**(6): p. e0130641.

6. Chesson, C.B., et al., *Antigenic peptide nanofibers elicit adjuvant-free CD8+(+) T cell responses.* Vaccine, 2014. **32**(10): p. 1174-80.

7. Rudra, J.S., et al., *Modulating adaptive immune responses to peptide self-assemblies.* ACS Nano, 2012. **6**(2): p. 1557-64.

8. Rudra, J.S., et al., *Self-assembled peptide nanofibers raising durable antibody responses against a malaria epitope.* Biomaterials, 2012. **33**(27): p. 6476-84.

9. Elvang, T., et al., *CD4+ and CD8+ T cell responses to the M. tuberculosis Ag85B-TB10.4 promoted by adjuvanted subunit, adenovector or heterologous prime boost vaccination.* PLoS One, 2009. **4**(4): p. e5139.

10. Billeskov, R., et al., *Difference in TB10.4 T-cell epitope recognition following immunization with recombinant TB10.4, BCG or infection with Mycobacterium tuberculosis.* Eur J Immunol, 2010. **40**(5): p. 1342-54.

11. Dietrich, J., et al., *Exchanging ESAT6 with TB10.4 in an Ag85B fusion molecule-based tuberculosis subunit vaccine: efficient protection and ESAT6-based sensitive monitoring of vaccine efficacy.* J Immunol, 2005. **174**(10): p. 6332-9.

12. Shi, S. and A.J. Hickey, *PLGA microparticles in respirable sizes enhance an in vitro T cell response to recombinant Mycobacterium tuberculosis antigen TB10.4-Ag85B.* Pharm Res, 2010. **27**(2): p. 350-60.

13. Shi, S., et al., *Rational design of multiple TB antigens TB10.4 and TB10.4-Ag85B as subunit vaccine candidates against Mycobacterium tuberculosis.* Pharm Res, 2010. **27**(2): p. 224-34.

14. Devasundaram, S., A. Deenadayalan, and A. Raja, *In silico analysis of potential human T Cell antigens from Mycobacterium tuberculosis for the development of subunit vaccines against tuberculosis.* Immunol Invest, 2014. **43**(2): p. 137-59.

15. Khan, M.K., et al., *In silico predicted mycobacterial epitope elicits in vitro T-cell responses.* Mol Immunol, 2014. **61**(1): p. 16-22.

16. Kasturi, S.P., et al., *Programming the magnitude and persistence of antibody responses with innate immunity.* Nature, 2011. **470**(7335): p. 543-7.

17. Kamath, A.T., et al., *Protective anti-mycobacterial T cell responses through exquisite in vivo activation of vaccine-targeted dendritic cells.* Eur J Immunol, 2008. **38**(5): p. 1247-56.

18. Hamdy, S., et al., *Co-delivery of cancer-associated antigen and Toll-like receptor 4 ligand in PLGA nanoparticles induces potent CD8+ T cell-mediated anti-tumor immunity.* Vaccine, 2008. **26**(39): p. 5046-57.

19. Saiga, H., Y. Shimada, and K. Takeda, *Innate immune effectors in mycobacterial infection.* Clin Dev Immunol, 2011. **2011**: p. 347594.

20. Amaral, E.P., E.B. Lasunskaia, and M.R. D'Imperio-Lima, *Innate immunity in tuberculosis: how the sensing of mycobacteria and tissue damage modulates macrophage death.* Microbes Infect, 2016. **18**(1): p. 11-20.

21. Lindsey, D.R., S. Dhandayuthapani, and C. Jagannath, *Anti-tuberculosis immunity induced in mice by vaccination with Mycobacterium smegmatis over-expressing Antigen 85B is due to the increased influx of IFNgamma-positive CD4+ T cells into the lungs.* Tuberculosis (Edinb), 2009. **89 Suppl 1**: p. S46-8.

22. Mustafa, A.S., et al., *Identification and HLA restriction of naturally derived Th1-cell epitopes from the secreted Mycobacterium tuberculosis antigen 85B recognized by antigen-specific human CD4+(+) T-cell lines.* Infect Immun, 2000. **68**(7): p. 3933-40.

23. Kariyone, A., et al., *Immunogenicity of Peptide-25 of Ag85B in Th1 development: role of IFN-gamma.* Int Immunol, 2003. **15**(10): p. 1183-94.

24. Rudra, J.S., et al., *A self-assembling peptide acting as an immune adjuvant.* Proc Natl Acad Sci U S A, 2010. **107**(2): p. 622-7.

25. Caro-Gomez, E., et al., *Phenotype of the anti-Rickettsia CD8+(+) T cell response suggests cellular correlates of protection for the assessment of novel antigens.* Vaccine, 2014. **32**(39): p. 4960-7.

26. Li, A.V., et al., *Generation of effector memory T cell-based mucosal and systemic immunity with pulmonary nanoparticle vaccination.* Sci Transl Med, 2013. **5**(204): p. 204ra130.

27. Garg, R., et al., *Induction of mucosal immunity and protection by intranasal immunization with a respiratory syncytial virus subunit vaccine formulation.* J Gen Virol, 2014. **95**(Pt 2): p. 301-6.

28. Blazevic, A., et al., *Investigations of TB vaccine-induced mucosal protection in mice.* Microbes Infect, 2014. **16**(1): p. 73-9.

29. Zeng, W., et al., *Structural requirement for the agonist activity of the TLR2 ligand Pam2Cys.* Amino Acids, 2010. **39**(2): p. 471-80.

30. Nune, M., et al., *Self-assembling peptide nanofibrous scaffolds for tissue engineering: novel approaches and strategies for effective functional regeneration.* Curr Protein Pept Sci, 2013. **14**(1): p. 70-84.

31. Kumar, V.A., et al., *Highly angiogenic peptide nanofibers.* ACS Nano, 2015. **9**(1): p. 860-8.

32. Liao, S., et al., *Biomimetic electrospun nanofibers for tissue regeneration.* Biomed Mater, 2006. **1**(3): p. R45-53.

33. Martino, M.M., et al., *Engineering the growth factor microenvironment with fibronectin domains to promote wound and bone tissue healing.* Sci Transl Med, 2011. **3**(100): p. 100ra89.

34. Agger, E.M., *Novel adjuvant formulations for delivery of anti-tuberculosis vaccine candidates.* Adv Drug Deliv Rev, 2015.

35. Heit, A., et al., *Protective CD8+ T cell immunity triggered by CpG-protein conjugates competes with the efficacy of live vaccines.* J Immunol, 2005. **174**(7): p. 4373-80.

36. Oh, J.Z. and R.M. Kedl, *The capacity to induce cross-presentation dictates the success of a TLR7 agonist-conjugate vaccine for eliciting cellular immunity.* J Immunol, 2010. **185**(8): p. 4602-8.

37. Orr, M.T., et al., *A dual TLR agonist adjuvant enhances the immunogenicity and protective efficacy of the tuberculosis vaccine antigen ID93.* PLoS One, 2014. **9**(1): p. e83884.

38. Ninomiya, A., et al., *Intranasal administration of a synthetic peptide vaccine encapsulated in liposome together with an anti-CD4+0 antibody induces protective immunity against influenza A virus in mice.* Vaccine, 2002. **20**(25-26): p. 3123-9.

39. Stylianou, E., et al., *Mucosal delivery of antigen-coated nanoparticles to lungs confers protective immunity against tuberculosis infection in mice.* Eur J Immunol, 2014. **44**(2): p. 440-9.

40. Andersen, C.S., et al., *The combined CTA1-DD/ISCOMs vector is an effective intranasal adjuvant for boosting prior Mycobacterium bovis BCG immunity to Mycobacterium tuberculosis.* Infect Immun, 2007. **75**(1): p. 408-16.

41. Dietrich, J., et al., *Mucosal administration of Ag85B-ESAT-6 protects against infection with Mycobacterium tuberculosis and boosts prior bacillus Calmette-Guerin immunity.* J Immunol, 2006. **177**(9): p. 6353-60.

42. Tyne, A.S., et al., *TLR2-targeted secreted proteins from Mycobacterium tuberculosis are protective as powdered pulmonary vaccines.* Vaccine, 2013. **31**(40): p. 4322-9.

43. Magalhaes, I., et al., *rBCG induces strong antigen-specific T cell responses in rhesus macaques in a prime-boost setting with an adenovirus 35 tuberculosis vaccine vector.* PLoS One, 2008. **3**(11): p. e3790.

44. Rahman, S., et al., *Prime-boost vaccination with rBCG/rAd35 enhances CD8+(+) cytolytic T-cell responses in lesions from Mycobacterium tuberculosis-infected primates.* Mol Med, 2012. **18**: p. 647-58.

45. Lin, P.L., *The multistage vaccine H56 boosts the effects of BCG to protect cynomolgus macaques against active tuberculosis and reactivation of latent Mycobacterium tuberculosis infection*. 2012. p. 303-14.

46. Husain, A.A., et al., *Comparative evaluation of booster efficacies of BCG, Ag85B, and Ag85B peptides based vaccines to boost BCG induced immunity in BALB/c mice: a pilot study.* Clin Exp Vaccine Res, 2015. **4**(1): p. 83-7.

47. Calderon, V.E., et al., *A humanized mouse model of tuberculosis.* PLoS One, 2013. **8**(5): p. e63331.

Chapter 5 : PEPTIDE NANOFIBER-CACO3 COMPOSITE MICROPARTICLES AS INTRANASAL VACCINE DELIVERY VEHICLES

Partially reprinted from the publication "Peptide nanofiber–$CaCO_3$ composite microparticles as adjuvant-free oral vaccine delivery vehicles," J. D. Snook, C. B. Chesson, A. G. Peniche, S. M. Dann, A. Paulucci, I. V. Pinchuk and J. S. Rudra, J. Mater. Chem. B, 2016, Advance Article, DOI: 10.1039/C5TB01623A with rights as an author.

Introduction

It is estimated that 70% of human pathogens initiate infection via the mucosal surfaces [1]. The mucosal surfaces are in direct contact with the external environment and provide an entryway for pathogens to invade the host. Injected vaccines are often very poor at inducing mucosal immunity and local immunity in the mucosa is best induced by mucosal vaccination, which has the added advantage of being a needle and medical-waste free strategy [2]. The WHO estimates that unsafe healthcare injections accounted for 5% of HIV, 32% of hepatitis B and 40% of hepatitis C infections acquired in developing countries making mucosal vaccination a highly attractive alternative [3]. Mucosal vaccination also stimulates productive immune responses at distal sites via the interconnected mucosa-associated lymphoid tissue (MALT) and offers an avenue for mass vaccination programs in developing countries with high patient compliance,

eliminating the need for skilled personnel, and limiting the risk of infections due to needle reuse and medical waste [4, 5].

Developing mucosal vaccines is best described as challenging due to the numerous natural defense systems such as the thick mucus barrier that lines the mucosal surfaces. Many vaccines administered mucosally can be trapped within the mucus layer surrounding the epithelium where they are inactivated or degraded [6]. Vaccines administered directly to the nasopharynx must be protected from degradation, penetrate the mucus layer and have high affinity for the nasal epithelium. Despite these barriers the nasal mucosa does have attractive properties for vaccination such as a large surface area to interact with and uptake antigen and a highly vascularized surface. Mucosal associated lymphoid tissue (MALT) in the nasopharynx consists of mainly of organized lymphoid tissue, made up from the Adenoid and Tubal tonsils [1, 7]. At the sites of organized MALT, antigens are sampled by DCs, which are professional antigen presenting cells that stimulate T and B cell adaptive immune responses such as IgA induction or T cell activation [8].

Currently only two licensed vaccines for intranasal delivery exist, both of which are live attenuated Influenza vaccines, FluMist™ and the European Medicines Agency-approved Fluenz™. Live-attenuated vaccines are highly immunogenic but carry the risk of improper attenuation and cannot be administered to those with compromised immunity or children [6]. Subunit vaccines based on purified or recombinant peptide/protein antigens have better overall safety profiles, however they are poorly immunogenic and need to be co-administered with adjuvants for enhancing antibody and cellular immune responses [9, 10]. Bacterial toxins, such as cholera toxin (CT) and the heat-labile

enterotoxin (LT) of Escherichia coli are the most potent and extensively studied mucosal adjuvants available, but they are too toxic for clinical use [11, 12].

Polymeric micro/nano particle-based strategies are attractive for intranasal vaccination due to their ability to efficiently penetrate the mucus barrier and have the added advantage of protecting the antigen from proteases and other enzymes found in the mucus layer [1, 13, 14]. Intranasal vaccine delivery systems based on cationic polymers [15], chitosan nanoparticles [16, 17], liposomes [18], polymeric nanoparticles [19, 20] and microparticles [21] have been successfully developed and tested in small animal models. However, the widely adopted production-scale methodologies for fabrication of polymeric micro- and nanoparticles involve the use of organic solvents and cross-linkers, even low levels of exposure to which, could lead to toxic side effects [22]. Furthermore, In order to enhance the potency and penetration of the polymeric particles across the mucus barrier exogenous adjuvants are either encapsulated or chemically linked to the surface [4, 7]. To date the only PLGA and liposomal materials based strategies for mucosal vaccine formulations have progressed from animal models to clinical trials [23].

We previously reported an adjuvant-free vaccination platform based on self-assembling, β-sheet rich, peptide nanofibers, which induce robust humoral and cellular immune responses when linked to peptide or protein antigens [24-27]. Parenteral vaccination with peptide nanofibers has been shown to elicit protective immune responses in mouse models of malaria [27], cancer [28], and influenza [24]. However, the microenvironment and cellular populations of nasopharynx and respiratory mucosa differ significantly from peripheral lymph nodes and are therefore distinct as an inductive site for priming of acquired immune responses [1]. Based on the current understanding of

mucosal immunology, particulate antigens are highly effective at inducing mucosal immunity compared to soluble antigens and encapsulation strategies that render soluble nanofibers into particulate form would enhance their translocation across the mucus barrier and also protect them from the extracellular degradation [5].

Here, we report peptide nanofiber-CaCO3 composite microparticles as self-adjuvanting nasal vaccine delivery vehicles. Compared to polymeric microparticles, inorganic CaCO3- microparticles have unique advantages such as preparation in mild physiological buffers, biocompatibility, and biodegradability [29]. We synthesized peptide nanofiber-CaCO3 composite microparticles by precipitating CaCO3 in aqueous buffers containing self-assembling peptide nanofibers bearing the model antigenic peptide OVA (chicken egg ovalbumin 323-339) as well as TB antigens TB10.4 and AG85B described previously. The loading efficiency, size distribution, and morphology of the composite microparticles was characterized and their uptake by antigen-presenting cells (APCs) was investigated using in vitro bone marrow derived dendritic cell cultures (BMDCs). Our results indicate peptide nanofiber-CaCO3 composite microparticles are effective as self-adjuvanting oral and intranasal vaccine delivery vehicles for efficient induction of mucosal cell mediated responses. Intranasal delivery using a heterologous prime boost strategy between nanofibers and composite microparticles further augmented the CD8+ T cell response in the respiratory mucosa.

Materials and Methods

SYNTHESIS OF PEPTIDES AND OVA-KFE8/$CaCO_3$ COMPOSITE MICROPARTICLES

Peptides were synthesized by coupling OVA or (ISQAVHAAHAEINEAGR) or AG85B (FQDAYNAAGGHNAVF) to the N-terminus of the self-assembling peptide domain KFE8 (FKFEFKFE) via an amino acid linker (SGSG). CD8+ antigens SIIN (SIINFEKL) or TB10.4 (IMYNYPAML) were coupled to the C-terminus of KFE8 via an amino acid linker (GGAAY) using standard Fmoc Chemistry on a CS Bio-CS336X solid phase peptide synthesizer (CS Bio, CA). Rink Amide MBHA resin (Novabiochem, MA) was swelled in dry DMF for 1 h, and amino acids were double coupled using HBTU (O-(Benzotriazol-1-yl)-N,N,N′,N′-tetramethyluronium hexafluorophosphate) and HOBt (1-Hydroxybenzotriazole) chemistries. Peptides were cleaved from the resin using a 95% TFA/2.5% water/2.5% triisopropyl silane cocktail and precipitated in cold diethyl ether. The crude product was washed and purified by reverse-phase HPLC (C18 column) using Acetonitrile/H2O gradients (>90% purity) and peptide mass was confirmed by MALDI-TOF mass spectrometry using α-cyano-4-hydroxycinnamic acid matrix (Bruker Daltonics, MA). All peptides were lyophilized and stored at -20°C prior to use. Nanofiber/CaCO3 composite microparticles were synthesized by colloidal crystallization technique reported previously [29]. Briefly, KFE8 nanofibers were prepared by dissolving the peptide in sterile water (8 mM stock solution), stored overnight at 4°C, and diluted to working concentration of 2 mM using 0.33 M sterile calcium chloride (CaCl2). An equal volume of 0.33 M Na2CO3 was added under stirring (1000 rpm) and the mixture was stirred for additional 30 sec. The solution was allowed to stand for 30 min at RT and the precipitated nanofiber/CaCO3 composite microparticles were obtained by centrifugation at 4000 rpm for 5 min. The particles were washed three times with DI

water and dried under vacuum. For some studies composite microparticles were prepared using rhodamine-OVA-KFE8 nanofibers.

LOADING EFFICIENCY, SIZE DISTRIBUTION, AND RELEASE STUDIES

Loading efficiency of OVA-KFE8 nanofibers into CaCO3 microparticles was calculated by the measuring the fluorescent intensity of a solution of rhodamine-conjugated OVA-KFE8 nanofibers (stock) before microparticle synthesis against the fluorescent intensity of the supernatant (sup) after microparticle synthesis. The loading efficiency was evaluated as follows:

$$Le = \frac{Intensity(stock) - Intensity(\text{sup})}{Intensity(stock)} \times 100$$

To confirm that the nanofibers were not just bound to the microparticle surface, 1 mg of microparticles were washed multiple times with water and the release of rhodamine-OVA-KFE8 in the washes was calculated against an equal weight of microparticles treated with 0.5 M EDTA (100% release). The stability of the composite microparticles in acidic environment of the gut was investigated by a dissolution test where the microparticles were exposed to simulated gastric fluid (pH 1.2) compared to PBS (pH 7.5) for 90 minutes. The release of rhodamine-OVA-KFE8 over time was calculated using fluorescence measurements compared against an equal weight of microparticles treated with 0.5 M EDTA (100% release). Morphology of the microparticles after exposure to simulated gastric fluid was determined using scanning electron microscopy as discussed below. The size distribution was obtained using confocal laser microscopy to first image the particles, followed by using ImageJ (NIH) to measure the diameter of

the microparticles. 500 microparticles per batch were used to calculate the average diameter and size distribution range.

IN VITRO UPTAKE OF OVA-KFE8/$CaCO_3$ COMPOSITE MICROPARTICLES

To generate BMDCs, bone marrow was collected from the femurs of C57BL6 mice, suspended in RPMI-1640 medium (Invitrogen) supplemented with 10% heat-inactivated fetal bovine serum (HyClone), 1% penicillin-streptomycin, and 50 μM β-mercaptoethanol (Sigma Aldrich). Red blood cells were lysed using ACK buffer (Sigma Aldrich, MO) and cells were washed and re-suspended media supplemented with 50 ng/mL of granulocyte–macrophage colony-stimulating factor (GM-CSF). 106 cells/well were plated in six-well plates and cultured at 37°C for 7–9 days. Cells were fed on days 3, 5 and 7 with complete medium containing GM-CSF and on day 9, non-adherent cells were collected, washed and used for experiments. 50,000 cells/well were plated on cover slips in 6-well plates and primed with 50 ng/ml LPS for 18 hours and followed by 8-hour incubation with 100,000 composite microparticles (rhodamine-OVA-KFE loaded). The cover slips were gently removed, washed in media, and imaged using confocal microscopy (see below). To determine IL-1β production following microparticle uptake, culture media supernatant was collected and cytokine levels measured using mouse IL-1β ELISA Ready-SET-Go kit (eBioscience) as per protocols provided by the manufacturer. Cell surface markers Live/Dead (AmCyan), CD3 (PB), CD11b (PE), CD11c (PerCP-Cy5.5), CD8+0 (PE), CD8+6 (APC), and MHC-II (FITC) TNF-α (FITC) and IFN-γ (PE-Cy7) antibodies were purchased from BD Biosciences (San Jose, CA) and cell surface marker staining was performed according to standard protocol. Flow Cytometry was

performed using a BD LSR Fortessa and FlowJo software (Tree Star, OR) was used to analyze data.

MICROSCOPY

Peptide nanofibers were imaged using transmission electron microscopy and imaged on a JEM1400 TEM (JEOL) equipped with LaB6 electron gun and digital cameras. Stock solutions of 1 mM peptides were allowed to fibrillize in water overnight at room temperature, diluted in PBS to 0.3 mM and applied to 300 mesh copper grids with carbon support film (Quantifoil). The grids were negatively stained with 2% uranyl acetate and images were viewed and recorded with an Ultrascan 1000 camera (Gatan). OVA-KFE8/CaCO3 composite microparticles were imaged using a Nova NanoSEM 230 scanning electron microscope. Samples were sputtered with a 10 nm platinum-palladium coat to enhance the contrast and imaged using at an acceleration voltage of 7 kV.

ANIMALS AND IMMUNIZATIONS

All experiments were conducted under protocols approved by the Institutional Animal Care and Use Committee at the University of Texas Medical Branch. Female mice (C57BL/6, 6-8 weeks old) were purchased from Taconic Farms and allowed to acclimate for a week prior to vaccinations. Composite KFE8/CaCO3 and control microparticles were suspended in sterile PBS and OVA/TB KFE8 nanofibers were prepared for vaccination as described previously. Control mice received PBS or OVA peptide admixed with the gold standard mucosal adjuvant CTB. All mice received equal

moles of antigen whether encapsulated, bare fibers, or with CTB adjuvant. Nanofibers (200 μL of 2 mM formulation) or 13.5×106 OVA-KFE8/CaCO3 microparticles (200 μL of PBS) or 400 nmol of antigen admixed with 10 μg of CTB (200 μL of PBS). Mice were boosted on day 28 and sacrificed 5 days later. To account for batch-to-batch variation in nanofiber formation and microparticle synthesis, mice were vaccinated with two different synthetic preparations of nanofibers or microparticles with 3-4 mice per group per experiment.

EX VIVO CYTOKINE EXPRESSION

At the time of sacrifice lung tissue was harvested along with mediastinal and superficial cervical lymph nodes. Lung tissue was mechanically disrupted using a GentleMACS dissociator in PBS with 0.5mg/mL DNase I and 1.0mg/mL Collagenase D (Roche, USA). The tissue solution was allowed to incubate for 30 mins at 37C and then pushed through a 70μM cell strainer. The cell suspension was washed 2x in complete RMPI and then seeded onto 96 well plates at a concentration of 1E6 cells/well. Complete RMPI with and without 5μg/mL TB10.4 or SIIN peptide antigen was added to the cells and incubated for 1 hour at 37C. After one hour the media was replaced with the same media containing 1:1000 dilution of Brefaldin A to inhibit protein secretion. The cells incubated for 6 hours at 37C at which point they were washed twice and stained for intracellular cytokine expression as described previously. Flow cytometry was performed on a BD Biosciences LSR-II 18 color cytometer and analyzed using Flowjo analysis software V10 (Treestar, OR).

STATISTICAL ANALYSIS

All the experimental data were plotted using GraphPad Prism software and represented as mean ± SEM. Grubb's test was used to identify any statistical outliers and analysis was performed by ANOVA with Tukey's post hoc test. Significance was assigned at p values <0.05.

Results and Discussion

OVA-KFE8/$CaCO_3$ COMPOSITE MICROPARTICLE SYNTHESIS AND CHARACTERIZATION

Successful synthesis of OVA-KFE8/CaCO3 composite microparticles was achieved by dissolving OVA-KFE8 nanofibers in 0.33 M CaCl2 and an equal volume of 0.33 M Na2CO3 was added under stirring [30]. Precipitation of CaCO3 microparticles in the presence of OVA-KFE8 nanofibers led to the encapsulation of the nanofibers in the microparticle core (Fig. 5.1a). For visualization purposes rhodamine-OVA-KFE8 nanofibers were used. Confocal imaging of labeled nanofibers indicated gelatinous random aggregates, which were transformed into discrete fluorescent microparticles after precipitation, indicating loading of the fluorescent nanofiber within the CaCO3 matrix (Fig. 5.1b).

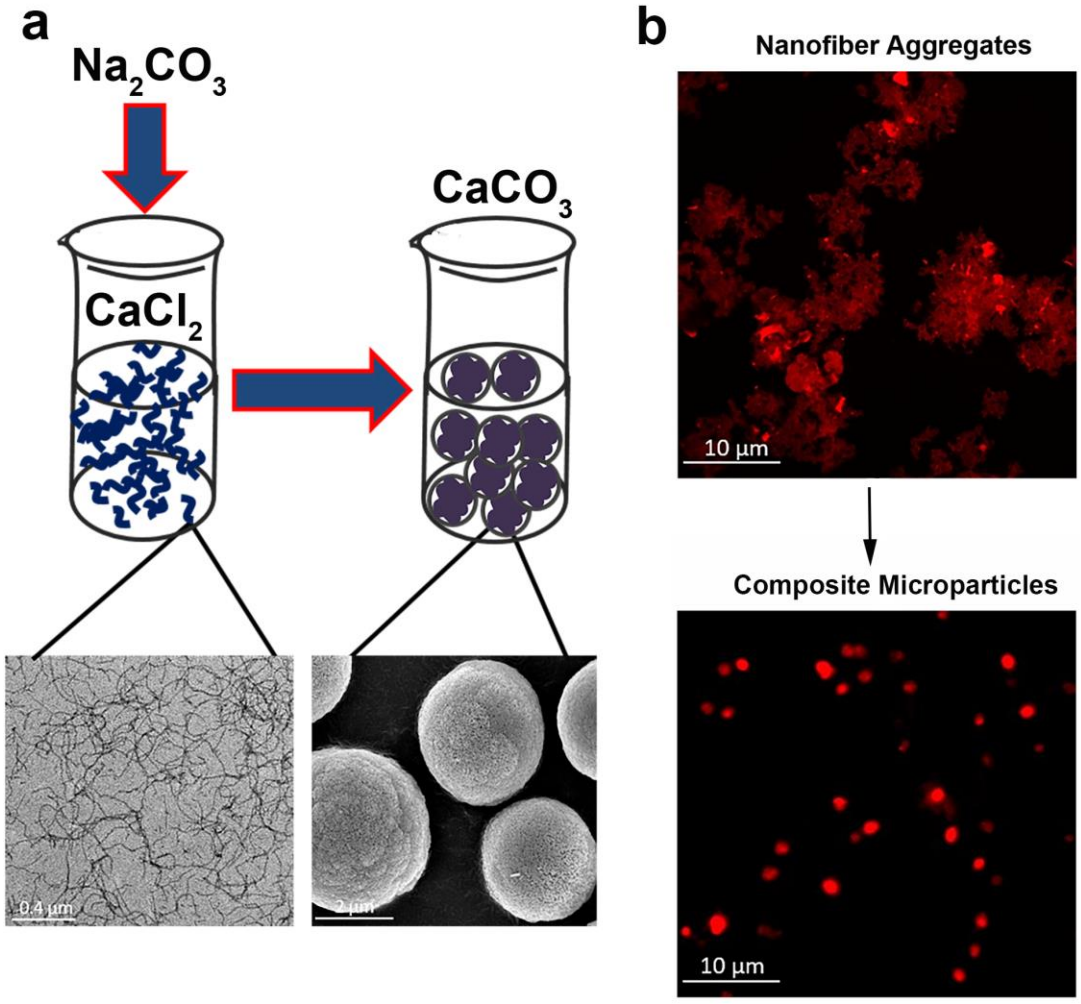

Figure 5.1. Composite microparticles encapsulate OVA-KFE8 nanofibers.

(a) Schematic depicting OVA-KFE8/$CaCO_3$ composite microparticle synthesis. OVA-KFE8 nanofibers were dissolved in 0.33 M $CaCl_2$ to which 0.33 M Na_2CO_3 solution was added under stirring. Precipitation of $CaCO_3$ resulted in encapsulation of OVA-KFE8 nanofibers within the $CaCO_3$ matrix. (b) Confocal microscopy images of OVA-KFE8 nanofibers and OVA-KFE8/$CaCO_3$ composite microparticles showing conversion from fibrous aggregates into discrete spherical microparticles.

The loading efficiency and morphology of the composite microparticles was found to be dependent on the concentration of nanofiber stock solution. Highest loading efficiency of ~72% was achieved when microparticles were synthesized using a 2 mM solution of OVA-KFE8 nanofibers (Fig. 5.2a). At higher concentrations OVA-KFE8 nanofibers formed viscous solutions, which prevented optimal stirring. To assess whether the nanofibers were uniformly distributed within the microparticle or were mostly surface bound, microparticles loaded with rhodamine-OVA-KFE8 nanofibers were washed in PBS, and leaching of the nanofibers was measured by fluorescence spectroscopy. To calculate percentage of loaded nanofibers released during serial washes, microparticles were dissolved in 0.5 M ethylenediaminetetraacetic acid (EDTA) leading to 100% release of the nanofibers [31]. Data indicated that only ~8% of the nanofibers leached out after the first wash and significantly decreased over serial washes and after 5 wash cycles ~15% of the OVA-KFE8 nanofibers were lost while ~85% were encapsulated within the $CaCO_3$ core (Fig. 5.2b) indicating that the bulk of the nanofibers were retained within the microparticles.

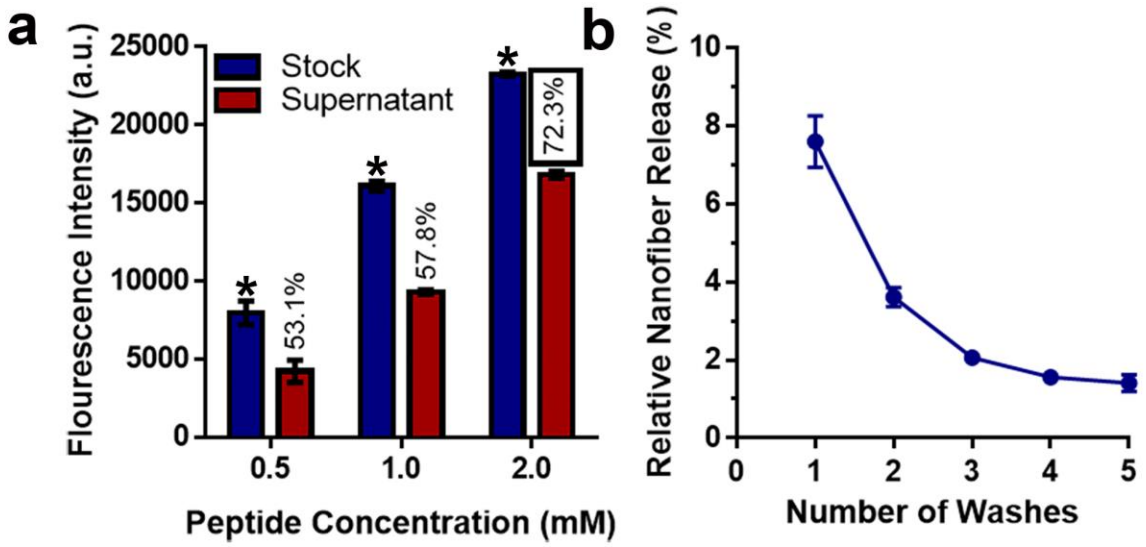

Figure 5.2. Microparticles efficiently encapsulate OVA-KFE8 nanofibers at 2mM

(a) Encapsulation efficiency of OVA-KFE8 nanofibers in $CaCO_3$ microparticles as a function of peptide nanofiber concentration. Highest nanofiber encapsulation ~72% was observed at 2 mM peptide concentration. (b) Figure showing loss of surface bound nanofibers from composite microparticles after serial washes. To calculate percentage of nanofibers released during serial washes, microparticles were dissolved in EDTA (100% release) and fluorescence intensity of supernatants was measured. Data indicated that ~8% of nanofibers are washed out and not bound within the microparticle core. *$p<0.05$ by ANOVA using Tukey post-hoc test.

Scanning electron microscopy revealed highly spherical structures and while subtle differences in surface morphology were evident between pure CaCO3 and OVA-KFE8/CaCO3 composite microparticles (Fig. 5.3a and 5.3b), gross differences in cross-sectional morphology were observed. Control microparticles had a highly porous interior (Fig. 5.3a) while the composite particles were dense and devoid of any porosity suggesting encapsulation of the nanofibers within the microparticle core (Fig. 5.3b). Mean diameter of control microparticles was found to be 3.5 μm (Fig. 5.3c), whereas the

composite microparticles had an average diameter of 2.2 μm (Fig. 5.3d), which is ideal for phagocytosis by APCs such as dendritic cells (DCs) and macrophages. Composite microparticles were also found to have a tighter size distribution profile compared to controls (Fig. 5.3d). In summary, our data suggest that OVA-KFE8/CaCO3 composite microparticles can be synthesized under mild physiological conditions with high yields and tight control over particle morphology and size distribution.

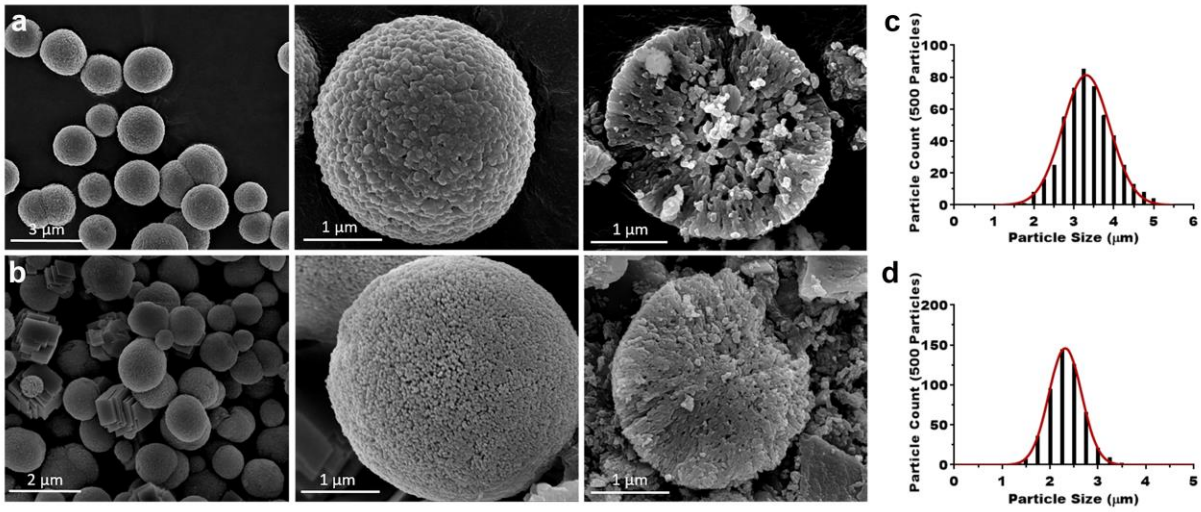

Figure 5.3. Composite microparticles have a more uniform density of range of particle size

(a) SEM micrographs of intact control $CaCO_3$ microparticles depicting spherical morphology and cross section showing a highly porous interior. (b) Composite microparticles are also spherical but have a denser surface and core suggesting nanofiber loading within the particle. (c) Size distribution of control $CaCO_3$ microparticles and (d) composite microparticles. Control microparticles had an average diameter of 3.5 μm whereas composite microparticles had an average diameter of 2.2 μm. Data shown is an average of 500 microparticles for each group.

UPTAKE OF COMPOSITE MICROPARTICLES BY BMDCS IN VITRO

Previous studies have demonstrated that peptide nanofibers are actively phagocytized by DCs and macrophages when injected into mice. Interestingly, only DCs exhibited increased expression of B7 co-stimulatory molecules CD8+0 and CD8+6 after

nanofiber uptake while expression of these molecules by macrophages remained unchanged. These molecules are critical for the induction of T cell proliferation/activity in response to the antigen presentation by APCs [32]. Therefore, we examined whether OVA-KFE8/CaCO3 composite microparticles could activate dendritic cells in vitro. To this end, BMDCs were incubated with composite microparticles and up-regulation of maturation markers CD8+0 and CD8+6 was determined using flow cytometry. Untreated or BMDCs incubated with OVA-KFE8 nanofibers were used as controls. Data indicated higher levels of CD8+0 and CD8+6 expression by BMDCs incubated in the presence of composite microparticles compared to OVA-KFE8 nanofibers or controls (Fig. 5.5 and 5.5b). Also, BMDCs incubated with OVA-KFE8 nanofibers had higher levels of CD8+0, and to a lesser extent CD8+6, compared to controls (Fig. 5.5a and 5.5b). Confocal microscopy indicated that OVA-KFE8/CaCO3 composite microparticles were efficiently phagocytized by BMDCs and had stellate morphology suggesting maturation (Fig. 5.5c).

Innate immune responses elicited by APCs in response to the stimulation of toll-like and nod-like pattern recognition receptor activation are critical for the chemo-attraction and regulation of effector immune responses [33]. It is not known whether self-assembling peptide nanofibers or inorganic minerals such as CaCO3 are capable of activating those innate immune receptors on APCs. However, particulates such as silica, asbestos, and aluminum salts have been shown to activate the NLRP3 inflammasome pathway leading to the production of the cytokine IL-1β, which supports the recruitment of pro-inflammatory immune cells. ELISA data indicated significantly higher levels of IL-1β in cultures of BMDCs treated with composite microparticles compared to OVA-KFE8 nanofibers or controls (Fig 5.5D). Although production of IL-1β is not direct

evidence of NLRP3 inflammasome activation, the data suggest that OVA-KFE8/CaCO3 composite microparticles, while improving the delivery of antigens to DCs, can also stimulate DCs to produce IL-1β, which is involved in the recruitment of the effector cells and induction of Th17 response, critical to the clearance of several mucosal pathogens [34, 35].

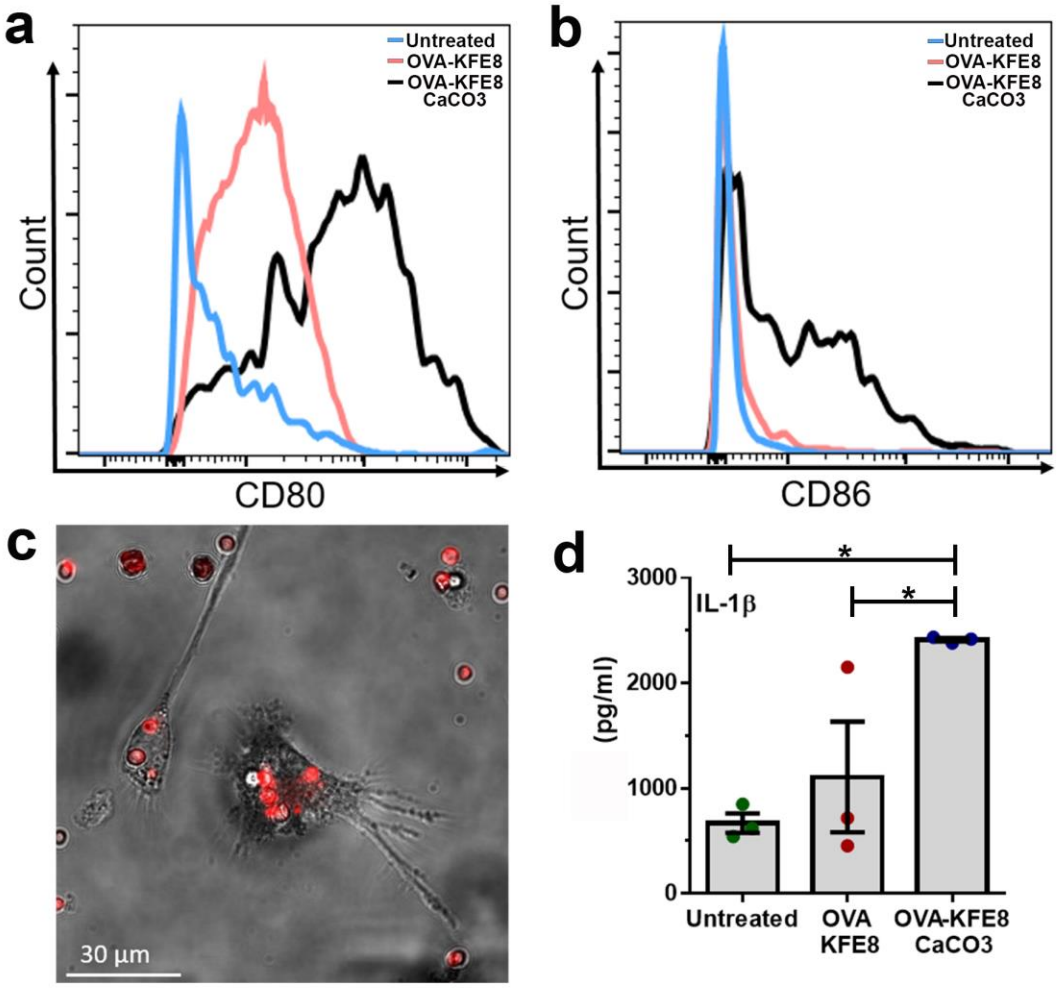

Figure 5.4. Composite microparticles are capable of activating DCs in vitro

Treatment of BMDCs with composite microparticles leads to DC maturation and production of pro-inflammatory cytokines. (a) Flow cytometry histograms of DC maturation markers (a) CD8+0 and (b) CD8+6 after 8 h incubation with composite microparticles showing significantly higher levels of co-stimulatory markers in DCs treated with microparticles compared to untreated or DCs treated with OVA-KFE8 nanofibers. (c) Confocal microscopy image showing phagocytosis of composite microparticles by BMDCs. (d) Treatment of BMDCs with composite microparticles leads to the production of cytokine IL-1β and significantly higher levels of IL-1β were detected in BMDC cultures treated with composite microparticles compared to OVA-KFE8 nanofibers or controls. *$p<0.05$ by ANOVA using Tukey post-hoc test.

INTRANASAL VACCINATION WITH OVA-KFE8/$CaCO_3$ COMPOSITE MICROPARTICLES

Lymphocytes the reside within the lungs and mediastinal lymph nodes provide the first line of defense against aerosolized pathogens that invade the body via the respiratory mucosa. The lungs contain a highly responsive immune repertoire and constantly are challenged with foreign particulates and pathogens in the air. Vaccination can induce immunity prior to exposure to pathogens and when mucosal immunity is desired it is favorable to vaccinate at the mucosa in which the pathogen is typically encountered. The respiratory mucosa may also benefit from the uniform size of composite microparticles leading to increased uptake across the respiratory mucosa and antigen cell activation. To evaluate immunogenicity of composite microparticle vaccines in the lungs we inoculate mice intranasally with two doses separated by 5 days (Figure 5.6A). We confirmed that microparticles encapsulating the model CD8+ epitope from chicken ovalbumin (SIIN) bearing nanofibers could elicit an expansion of CD8+ T cells comparable to other

mucosal adjuvants or SIIN nanofibers without encapsulation. Previously we have shown that intranasal administration of nanofibers bearing TB antigens was immunogenic and that the when both doses of the vaccine were given intranasally more antigen specific CD8+ T cells were localized in the lung parenchyma. Interestingly, when we inoculated mice such that they received SIIN composite microparticles followed by a booster vaccination of OVA nanofibers without encapsulation, the percentage of SIIN antigen specific CD8+ T-cells was higher in the lungs than two doses of SIIN nanofibers alone. Although not a true heterologous prime boost, this variation in the delivery vehicle may be a simple method for enhancing the magnitude of the immune response for either mucosal vaccinations or systemic.

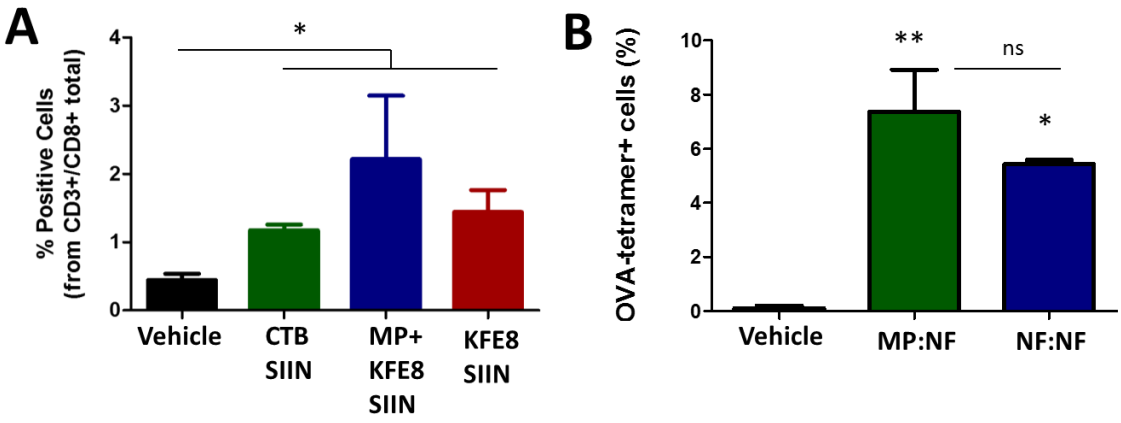

Figure 5.5 Intranasal delivery of composite microparticles enhances the magnitude of the cellular immune response.

Mice (n=5 per group) were intranasally inoculated with either cholera toxin-B/SIIN mixture, SIIN-KFE8 nanofibers or composite microparticles with two doses separated by 5 days. 3 days later lungs were excised and cells were seeded at a density of 1E6 cells/well in duplicate. Cells were stimulated for 6 hours with SIIN peptide and IFN-γ expression was measured by FACS (A). Robust expansion of SIIN-tetramer+ CD8+ T cells were seen with SIIN-KFE8 nanofiber intranasal inoculation with 2 doses separated by 30 days (B) which was increased in animals receiving intranasal heterologous prime (composite microparticles: MP) with SIIN-KFE8 boost (NF) Plots are mean expression from each individual animal ± SEM. *=$p<0.05$, **$p<0.01$ by ANOVA with Tukey's post-hoc test for multiple group comparison.

We have previously shown that intranasal administration with nanofibers bearing antigen epitopes from Mycobacterium *tuberculosis* were also capable of inducing robust CD8+ responses in the lungs when administered intranasally with two doses. Using a similar co-assembled nanofibers bearing Mtb epitopes from TB10.4 and AG85B we assessed the variation in order of delivery from the two modalities in a two dose series. We measured the response using ex vivo cytokine stimulation from isolated lung tissue. CD4+ and CD8+ T cells were equally recruited to the lung parenchyma after vaccination as compared to PBS inoculated mice (Figure 5.7C). We found that every combination or order of prime:boost vaccination resulted robust CD4+ and CD8+ cytokine secretion, although the mixed combinations including both composite microparticles and nanofibers were significantly enhanced. NF:MP mice elicited the highest CD8+ antigen specific cell expansion and both NF:MP and MP:NF mice were the only groups to have significantly increased TNF-α expression from CD4+ over controls. Our data suggests that peptide nanofibers whether encapsulated in microparticles are capable of eliciting a mucosal CD8+ immune response and directing lymphocytes to the lungs after vaccination. Further studies are needed to determine if intranasal administration with these two delivery methods results in any systemic immunity and how the nanofibers are sampled for antigen processing and presentation whether in the nasal mucosa or respiratory airways. We are also interested in the systemic immunity generated from parental inoculation with composite microparticles. Our current data suggests they are a valuable tool for mucosal delivery of antigen and can elicit strong mucosal cell mediated responses which we hypothesize will carry over to oral routes of administration.

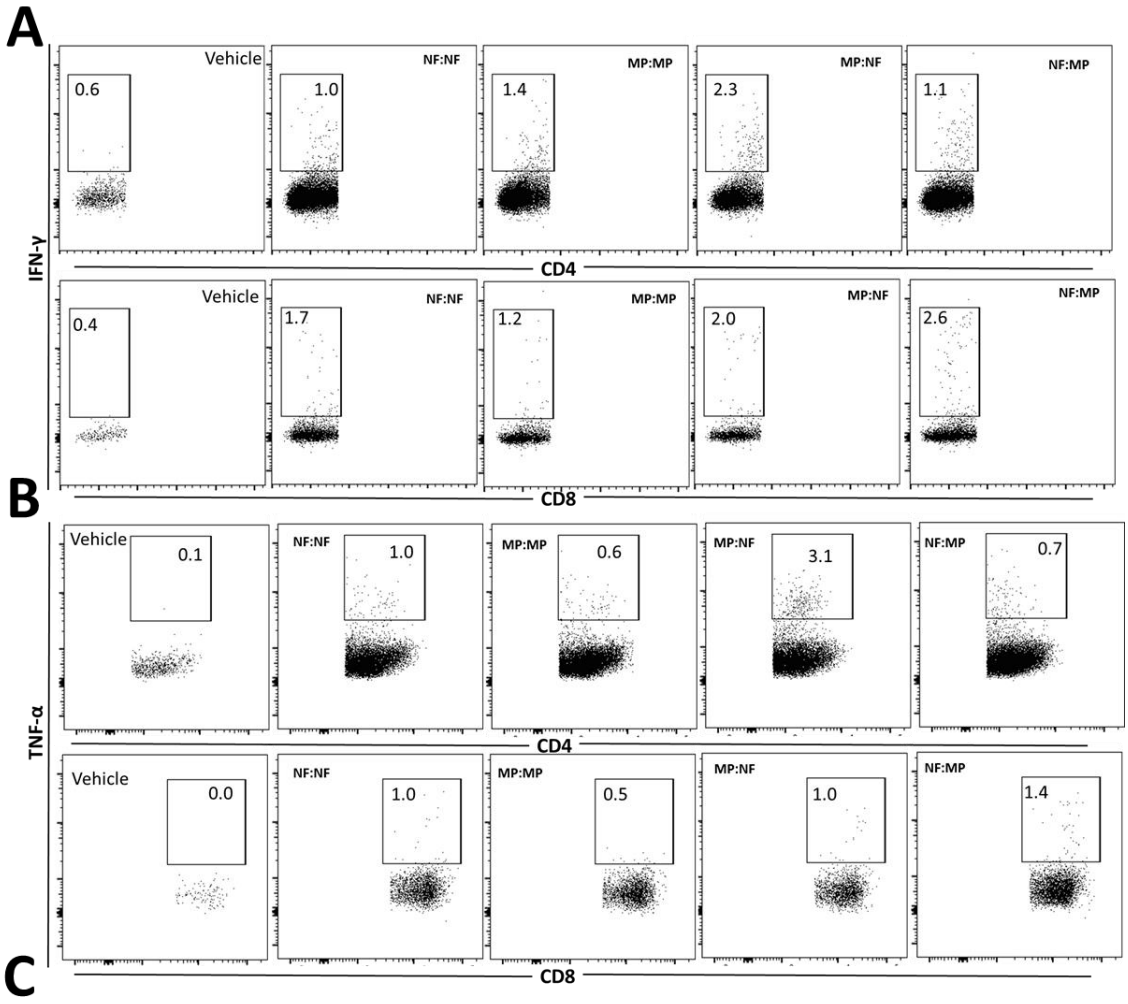
A
Vehicle
NF:NF
MP:MP
MP:NF
NF:MP
0.6
1.0
1.4
2.3
1.1
IFN-γ
CD4
0.4
1.7
1.2
2.0
2.6
CD8
B
0.1
1.0
0.6
3.1
0.7
TNF-α
0.0
0.5
1.0
1.4
C
Total CD4 Count
Total CD8 Count
Total IFN-γ Count [CD4+CD3+]
Total IFN-γ Count [CD8+CD3+]
Total TNF-α Count [CD4+CD3+]
Total TNF-α Count [CD8+CD3+]

Figure 5.7 Comparison of prime/boost combinations with composite microparticles containing antigen from M.*tuberculosis*.

Mice (N=4 per group) were inoculated intranasally with either nanofibers co-assembled with Mtb antigens TB10.4 and AG85B alone (NF) or encapsulated in microparticles (MP). Two doses separated by 30 days are depicted as [prime:boost] for the different modalities being compared. Flow plots are representative from lung tissue isolated 5 days after the last dose and stimulated with TB10.4 peptide. Intracellular staining for cytokines IFN-γ (A) and TNF-α (B) from CD3+CD4+ (top A and top B) or CD8+CD3+ (bottom A and bottom B) cell populations with % positive cells. Total cell counts in (C) are mean ± SD for total CD4+, CD8+, IFNγ+CD4+, IFNγ+CD8+, TNFα+CD4+, and TNFα+CD8+. ***=p<0.001, **p=<0.01 and *=p<0.05 as compared to vehicle control unless otherwise depicted by one-way ANOVA with multiple comparison post-hoc tests between means.

In this study, no exogenous adjuvants were incorporated into the composite microparticles to elicit cell mediated responses equivalent to those induced by CTB, a strong gold-standard mucosal adjuvant. Encapsulation of the nanofibers into CaCO3 microparticles not only protects the nanofibers but also ensures efficient delivery due to their uniform nanoscale size. Studies using synthetic carriers for mucosal vaccination have demonstrated that particles with hydrophobic or net positive surface charge are mucoadhesive due to interactions with the negatively charged mucus layer (48). Surface functionalization of hydrophobic PLGA microparticles with polyethylene glycol (PEG) chains has been shown to enhance their mucus penetrating properties (49). CaCO3 microparticles are intrinsically hydrophilic with a net neutral charge, which could enhance their translocation across the mucus barrier without further modification. Furthermore, they can be surface modified via simple adsorption with ligands specifically targeting receptors on mucosal DCs or other APCs including alveolar macrophages for targeted vaccine delivery.

We recently demonstrated that linking D amino acid self-assembling domains to antigens could enhance the potency of the humoral response to peptide nanofiber vaccines in mouse models (50). This strategy can be used to improve the mucosal and antibody responses elicited by the composite microparticles through encapsulation of peptide nanofibers bearing an all-D amino acid self-assembling domain. Although the all D-amino acid self-assembling domain was less efficient for cell mediated responses when delivered systemically, their inherent ability to resist enzymatic degradation in the harsh environment of the gastric mucosa may enhance their utility as a mucosal vaccine delivery system. The chemical versatility of self-assembling peptide nanofibers allows for covalent linkage of whole protein antigens and recent studies demonstrated that protein-bearing self-assembling peptide nanofibers are self-adjuvanting (31). This enables the development of composite microparticles loaded with protein-bearing nanofibers for enhancing the breath of protection and also covers broad population distributions. Furthermore, by controlling physical parameters such as agitation rate, mixing time, ionic strength, and temperature, $CaCO_3$ particle size and morphology can be manipulated (51). Future embodiments of the current work will investigate the oral route of delivery for peptide nanofibers to elicit cell mediated immune responses against enteric pathogens and what the role of particle size and stereochemistry plays in initiating robust adaptive immunity in the nasal and oral mucosa.

Conclusions

In summary, this study demonstrates the feasibility of peptide nanofiber-CaCO3 composite microparticles as oral vaccine delivery vehicles using the model antigen OVA as well as from peptide epitopes from Mycobacterium *tuberculosis*. We show that composite microparticles can be synthesized under mild physiological conditions with tight size distribution profile, spherical morphology, and high nanofiber loading efficiency. The composite microparticles are phagocytized by antigen presenting cells in vitro leading to the production of pro-inflammatory cytokines and upregulation of co-stimulatory molecules. Oral vaccination with peptide nanofiber-CaCO3 composite microparticles leads to the production of robust cell mediated responses with given alone but was enhanced using a quasi-heterologous prime boost model. Composite microparticles offer an advantageous platform for inducing mucosal immunity.

ACKNOWLEDGEMENTS

This study was supported by funds from the Sealy Center for Vaccine Development, and the Department of Pharmacology and Toxicology, UTMB (J.S.R). TEM studies were conducted at the Sealy Center for Structural Biology Cryo-electron Microscopy core lab and we thank Dr. Misha Sherman and Michael Woodson for assistance with imaging. Flow cytometry was conducted at the Flow Cytometry and Cell Sorting Facility at UTMB and we thank Mark Griffin for his expertise.

References

1. Woodrow, K.A., K.M. Bennett, and D.D. Lo, *Mucosal vaccine design and delivery.* Annu Rev Biomed Eng, 2012. **14**: p. 17-46.
2. Neutra, M.R. and P.A. Kozlowski, *Mucosal vaccines: the promise and the challenge.* Nat Rev Immunol, 2006. **6**(2): p. 148-58.
3. Pépin, J., et al., *Evolution of the Global Burden of Viral Infections from Unsafe Medical Injections, 2000–2010*, in *PLoS One*, D. Paraskevis, Editor. 2014: San Francisco, USA.
4. Fujkuyama, Y., et al., *Novel vaccine development strategies for inducing mucosal immunity.* Expert Rev Vaccines, 2012. **11**(3): p. 367-79.
5. Zhu, Q. and J.A. Berzofsky, *Oral vaccines: Directed safe passage to the front line of defense*, in *Gut Microbes*. 2013. p. 246-52.
6. Shakya, A.K., et al., *Mucosal vaccine delivery: Current state and a pediatric perspective.* Journal of Controlled Release.
7. Devriendt, B., B.G. De Geest, and E. Cox, *Designing oral vaccines targeting intestinal dendritic cells.* Expert Opin Drug Deliv, 2011. **8**(4): p. 467-83.
8. Mabbott, N.A., et al., *Microfold (M) cells: important immunosurveillance posts in the intestinal epithelium.* Mucosal Immunol, 2013. **6**(4): p. 666-77.
9. Black, M., et al., *Advances in the design and delivery of peptide subunit vaccines with a focus on toll-like receptor agonists.* Expert Rev Vaccines, 2010. **9**(2): p. 157-73.
10. O'Hagan, D.T. and E. De Gregorio, *The path to a successful vaccine adjuvant--'the long and winding road'.* Drug Discov Today, 2009. **14**(11-12): p. 541-51.

11. Lewis, D.J., et al., *Transient facial nerve paralysis (Bell's palsy) following intranasal delivery of a genetically detoxified mutant of Escherichia coli heat labile toxin.* PLoS One, 2009. **4**(9): p. e6999.

12. Lawson, L.B., E.B. Norton, and J.D. Clements, *Defending the mucosa: adjuvant and carrier formulations for mucosal immunity.* Curr Opin Immunol, 2011. **23**(3): p. 414-20.

13. Ensign, L.M., R. Cone, and J. Hanes, *Oral drug delivery with polymeric nanoparticles: the gastrointestinal mucus barriers.* Adv Drug Deliv Rev, 2012. **64**(6): p. 557-70.

14. McNeela, E.A. and E.C. Lavelle, *Recent advances in microparticle and nanoparticle delivery vehicles for mucosal vaccination.* Curr Top Microbiol Immunol, 2012. **354**: p. 75-99.

15. Li, M., et al., *Intranasal Vaccination against HIV-1 with Adenoviral Vector-Based Nanocomplex Using Synthetic TLR-4 Agonist Peptide as Adjuvant.* Mol Pharm, 2016.

16. van der Lubben, I.M., et al., *Chitosan for mucosal vaccination.* Adv Drug Deliv Rev, 2001. **52**(2): p. 139-44.

17. Xu, J.H., et al., *Mucosal immunization with PsaA protein, using chitosan as a delivery system, increases protection against acute otitis media and invasive infection by Streptococcus pneumoniae.* Scand J Immunol, 2015. **81**(3): p. 177-85.

18. Takagi, A., et al., *Highly efficient antiviral CD8+ T-cell induction by peptides coupled to the surfaces of liposomes.* Clin Vaccine Immunol, 2009. **16**(10): p. 1383-92.

19. Stano, A., et al., *PPS nanoparticles as versatile delivery system to induce systemic and broad mucosal immunity after intranasal administration.* Vaccine, 2011. **29**(4): p. 804-12.

20. Dwivedi, V., et al., *PLGA nanoparticle entrapped killed porcine reproductive and respiratory syndrome virus vaccine helps in viral clearance in pigs.* Vet Microbiol, 2013. **166**(1-2): p. 47-58.

21. Puras, G., et al., *Encapsulation of Abeta(1-15) in PLGA microparticles enhances serum antibody response in mice immunized by subcutaneous and intranasal routes.* Eur J Pharm Sci, 2011. **44**(3): p. 200-6.

22. Dixit, K., R.B. Athawale, and S. Singh, *Quality control of residual solvent content in polymeric microparticles.* J Microencapsul, 2015. **32**(2): p. 107-22.

23. Climent, N., et al., *Loading dendritic cells with PLA-p24 nanoparticles or MVA expressing HIV genes induces HIV-1-specific T cell responses.* Vaccine, 2014. **32**(47): p. 6266-76.

24. Chesson, C.B., et al., *Antigenic peptide nanofibers elicit adjuvant-free CD8+(+) T cell responses.* Vaccine, 2014. **32**(10): p. 1174-80.

25. Rudra, J.S., et al., *A self-assembling peptide acting as an immune adjuvant.* Proc Natl Acad Sci U S A, 2010. **107**(2): p. 622-7.

26. Rudra, J.S., et al., *Modulating adaptive immune responses to peptide self-assemblies.* ACS Nano, 2012. **6**(2): p. 1557-64.

27. Rudra, J.S., et al., *Self-assembled peptide nanofibers raising durable antibody responses against a malaria epitope.* Biomaterials, 2012. **33**(27): p. 6476-84.

28. Figdor, C.G., *A totally synthetic, self-assembling, adjuvant-free MUC1 glycopeptide vaccine for cancer therapy.* Biomaterials, 2012. **134**(21): p. 8730-3.

29. Volodkin, D., *CaCO(3) templated micro-beads and -capsules for bioapplications.* Adv Colloid Interface Sci, 2014. **207**: p. 306-24.

30. Parakhonskiy, B.V., A. Haase, and R. Antolini, *Sub-micrometer vaterite containers: synthesis, substance loading, and release.* Angew Chem Int Ed Engl, 2012. **51**(5): p. 1195-7.

31. Petrov, A.I., D.V. Volodkin, and G.B. Sukhorukov, *Protein-calcium carbonate coprecipitation: a tool for protein encapsulation.* Biotechnol Prog, 2005. **21**(3): p. 918-25.

32. Merrill, J.T., *The functional maturation of M cells is dramatically reduced in the Peyer's patches of aged mice.* Clin Immunol, 2013. **6**(5): p. 1027-37.

33. Frosali, S., et al., *How the Intricate Interaction among Toll-Like Receptors, Microbiota, and Intestinal Immunity Can Influence Gastrointestinal Pathology*. J Immunol Res, 2015. **2015**: p. 489821.

34. Krishna, S. and L.S. Miller, *Innate and adaptive immune responses against Staphylococcus aureus skin infections.* Semin Immunopathol, 2012. **34**(2): p. 261-80.

35. Lina, T.T., et al., *CagA-dependent downregulation of B7-H2 expression on gastric mucosa and inhibition of Th17 responses during Helicobacter pylori infection.* J Immunol, 2013. **191**(7): p. 3838-46.

Chapter 6 General Discussion

Vaccines for many diseases which currently have no vaccine, or one with limited efficacy, require novel approaches to design a successful candidate. The current movement in vaccine design is towards recombinant subunit, chimeric viral with limited replication or virus like and nanoparticle based vaccines. Many of these are safer alternatives to inactivated or live-attenuated whole cell pathogens but may suffer from poor expression vectors, bacterial contamination or high-cost of manufacturing. Our approach using individual peptide epitope bearing nanofibers confers many attractive advantages for vaccine design. Peptides are low-cost and easily synthesized, and the modular nature of our system allows for straightforward exchange of the peptides making it easily adaptable to another pathogen. The major drawback of this type of vaccine is the very specific nature of the immune response we are creating. Comparatively, viral chimeras and protein subunit vaccines create broader antigenic responses that result in more comprehensive immunity that may translate toward more complete protection.

The specific nature of the immune response we are creating with peptide epitopes is particularly advantageous when the goal is to target perhaps a very unique sequence. Cancer is one such situation where this type of immunotherapy could be incredibly valuable. Tumor associated antigens are inherently self-antigens but they can be altered in a number of ways such as through mutations. Mutated epitopes can be recognized by antigen specific T-cells as foreign. In relation to cancer, peptide based vaccines can be used to induce an immune response to mutated self-epitopes presented on the tumor or cancerous cell. This particular situation would require a very specific immune response and one in which the vaccine could be easily personalized to the specific patient. More

encompassing immune responses with mutated-self recombinant proteins that may result in tolerance or regulatory T-cell expansion after being recognized as a self-antigen and thus have negligible or negative effects on tumor burden.

The work from this project has several important contributions to biomaterial based vaccines that may lead to clinical application of this platform. We are the first to show how this platform may be used to elicit antigen specific CD8+ T-cell responses from nanofibers bearing one or more peptide epitopes. The importance of this cannot be understated. Live-attenuated vaccines that invade intracellularly can produce a cellular immune response but many new subunit vaccines function through humoral or antibody based immunity. Targeted cellular immunity may work in conjunction with the original immune response from a licensed vaccine to enhance immunity and protection. Further, peptide based vaccines that incorporate several epitopes broaden the applicability of this platform while still maintaining a high degree of specificity from selected antigens.

Beyond inducing CD8+ T-cell expansion from peptide epitopes our data supports that the inclusion of immunomodulatory ligands and CD4+ T-cell epitopes may be effective strategies to create distinctive cellular phenotypes or enhance antigen specific T-cell proliferation. TLR agonists co-assembled into single nanofiber scaffolds resulted in poly-functional CD8+ T-cells, which enhanced the protective capacity of the BCG vaccine when administered as a booster dose. The importance of T-cell poly-functionality is debatable for many diseases and may even have detrimental effects for some. In these cases perhaps a TLR-2 agonist may not be appropriate. Future studies will include other TLR agonists that are easily conjugated to or associate with our nanofiber platform.

Manipulating the stereochemistry of the fibril forming domain gives us another variable that impacts the immune response. Fibril forming domains from 'D' amino acids further enhanced the resulting antibody titer while the proliferation of antigen specific T-cells was maximized using 'L' amino acids. We are currently investigating the immune responses to mixtures of stereoisomers within the same peptide or within common domains and what the impact of these structural variations are on the immune response. From our research it is unclear about what drives the differential adaptive immune response based solely on absolute configuration, however it is possible that this variable may be instrumental for directing the path of immunity given the antigen.

Perhaps the most important aspect of this platform is that we found it to be very effective for mucosal delivery. Mucosal vaccines are important for providing front line defense against mucosally invasive pathogens. Microparticle encapsulation of nanofiber scaffolds is an efficient delivery method for both aerosol and oral routes. The composite microparticle protects the nanofibers from degradation in the gastric mucosa and may even facilitate the uptake of antigen in the intestinal lumen. There is a number of enteric pathogens for which a vaccine is desperately needed and in many cases the question is focused on antigen delivery. Microparticle encapsulation of an already effective nanofiber vaccine platform may also be a viable solution to enteric pathogens, not only as a vaccine but perhaps an immunostimulatory therapy as well, although the combined net effect of a successful mucosal delivery system with an effective vaccine platform that stimulates cellular immunity through peptide epitopes may have its best application in gastric, colon, or lung cancer.

The real challenge with applying this technology to cancer is developing faster tools for tumor associated antigen identification and then turnaround into a viable immunostimulatory agent. Mass spectrometry methods are among the best tools for current identification of HLA class-I restricted peptides found among cancer cells. Incorporating these peptides into an immunostimulatory therapy could then drive the effective induction of tumor reactive cytotoxic lymphocytes. The broad applicability of this type of platform certainly does not limited to it cancer, but the narrow immunological range per formulation favors it. It is not currently known how many epitopes or immunostimulatory ligands we can actually incorporate into a single fibril domain nor do we know the proper molar ranges for optimal CD8+ T-cell induction. Clearly much more research is needed on this unique and formidable strategy for the induction of CD8+ T lymphocytes.

Vitae

Charles Brent Chesson was born in New Bern, North Carolina to parents, Thomas Bradford and Nan Gardner Chesson. Brent began his career in research at the University of North Carolina under the direction of Dr. Joanna Kreuger through an NSF Nanosure research program where he researched the physical properties of ionic liquids. He also served as a teaching aid for multiple chemistry courses and laboratory sections while pursuing his degree. While at the University of Texas Medical Branch Brent had worked twice as in an intern for the World Health Organization where he completed research on numerous vaccine related projects. He is completed his dissertation research under the direction of Dr. Jai S Rudra in the department of Pharmacology and Toxicology.

Education

B.S. Chemistry, December 2002, North Carolina State University, North Carolina

B.S. Microbiology, May 2011, University of North Carolina – Charlotte, North Carolina

Master of Public Health, December 2015, University of Texas Medical Branch, Texas

This manuscript was typed by Charles Brent Chesson.